THIN LAYER CHROMATOGRAPHY – FLAME IONIZATION DETECTION

ANALYSIS OF IN-SITU PETROLEUM BIODEGRADATION

A Thesis

by

FRANK L. STEPHENS

Submitted to the Office of Graduate Studies of
Texas A&M University
in partial fulfillment of the requirements for the degree of

MASTER OF SCIENCE

August 2004

Major Subject: Civil Engineering

THIN LAYER CHROMATOGRAPHY – FLAME IONIZATION DETECTION

ANALYSIS OF IN-SITU PETROLEUM BIODEGRADATION

A Thesis

by

FRANK L. STEPHENS

Submitted to Texas A&M University
in partial fulfillment of the requirements
for the degree of

MASTER OF SCIENCE

Approved as to style and content by:

James S. Bonner (Chair of Committee)	Robin L. Autenrieth (Member)
K. C. Donnelly (Member)	Paul N. Roschke (Head of Department)

August 2004

Major Subject: Civil Engineering

ABSTRACT

Thin Layer Chromatography – Flame Ionization Detection

Analysis of In-Situ Petroleum Biodegradation.

(August 2004)

Frank L. Stephens, B.S., Texas A&M University

Chair of Advisory Committee: Dr. James S. Bonner

This research was initiated after a 100-year flood caused an oil spill on the San Jacinto River (Houston, Texas) in October of 1994. After the floodwaters subsided the released petroleum floating on the water was deposited on the surrounding lands. The petroleum spill was used as an opportunity to research intrinsic petroleum biodegradation in a 9-acre petroleum impacted estuarine wetland. The first phase of this research (Phase I) began in December 1994, approximately 1.5 months after the spill of opportunity and involved the study and quantification of *in-situ* petroleum biodegradation. The second phase of the research (Phase II) began in March 1996 with a controlled oil release to study and evaluate the success of two bioremediation treatments versus natural biodegradation. The study of *in-situ* petroleum hydrocarbon degradation and the evaluation of bioremediation amendments were successfully quantified using GC-MS analytical techniques. However, the GC-MS technique is limited to the analyses of hydrocarbon compounds, a disadvantage that precludes the overall characterization of petroleum degradation.

The research presented here details an analytical technique that was used to provide a full characterization of temporal petroleum biodegradation. This technique uses thin layer chromatography coupled with flame ionization detection (TLC-FID) to characterize the saturate and aromatic (hydrocarbon) fractions and the resin and asphaltene (non-hydrocarbon, polar) fractions. Other analysis techniques, such as

HPLC-SARA analysis, are available for the full characterization of the four petroleum fractions. However, these techniques do not lend themselves well to the application of large sample set analysis.

A significant advantage of the TLC-FID analysis to other petroleum analysis techniques is the ability to analyze several samples concurrently and quickly with relative ease and few resources. For the purposes of the Phase I and Phase II research the TLC-FID analysis method was evaluated, refined and applied to quantify the temporal biodegradation and bioremediation of petroleum. While the TLC-FID analysis produces a full characterization, it cannot supplant the GC-MS analysis for petroleum bioremediation research. However, it can be used in conjunction with the GC-MS to expand the knowledge of petroleum bioremediation and remediation strategies.

DEDICATION

For my parents who have given me the opportunity and ambition to pursue a Masters Degree. To my friend, my dear wife, and my sunshine, Danica C. Mueller whose support and encouragement have helped me achieve this milestone in my life. To God for the will and perseverance to overcome life's obstacles to complete this work.

ACKNOWLEDGMENTS

To Dr. James S. Bonner for the vision and dedication to the project that made this opportunity possible. I appreciate the enthusiasm you projected during the hard times and the good times.

To Dr. Robin L. Autenrieth, and K.C. Donnelly for the patience and opportunity they have given me to finish the work I started long ago. I also greatly appreciate the dedication they bring to the classroom and thoroughly enjoyed every class.

To Dr. Cheryl Page for her support and time which helped make this possible. I will always have one more idea up my sleeve Cheryl, thanks for your patience, time, and understanding getting everything together.

To Dr. Tom McDonald for his help and insights developing the laboratory analyses and overcoming research obstacles. Thank you for always bringing your smile and upbeat spirit whenever there was a room full of downtrodden graduate students.

For the members of the San Jacinto River Research group, namely, Marc Mills, Mark Simon, Salvador Aldrett, Jason Leik, Jim Sweeney, Daniele La Riviera, Jon Schwantes, Yolanda Mills, Cord Harris, Hari Paudel and the rest of the group. I appreciate all of the wonderful memories we have of the interesting and always exciting work we performed.

To Dr. Peter Keating for his understanding and fairness supporting my efforts to engage this long overdue task.

To the Texas General Land Office for their funding and Robin Jamail, Director of Research & Development, for her support of our efforts.

TABLE OF CONTENTS

Page

ABSTRACT iii

DEDICATION v

ACKNOWLEDGMENTS vi

TABLE OF CONTENTS vii

LIST OF FIGURES x

LIST OF TABLES xi

CHAPTER I INTRODUCTION 1
Background 1
Research Objectives 4

CHAPTER II METHOD DEVELOPMENT OF THE TLC-FID ANALYSIS FOR LARGE SCALE PETROLEUM BIOREMEDIATION FIELD STUDIES 5
Overview 5
Introduction 5
Methods 8
TLC-FID QA-QC Analysis 8
Experimental Samples 8
TLC-FID Chromarod Drying, Chromarod Orientation, and Scan Speed 9
TLC-FID Chromarod Mass Loading 10
Monitoring Instrument Error 10
Monitoring Method Error 11
Monitoring Procedural Error 11
Shewhart Control Charts 11
Repeatability 12
Petroleum Analytical Techniques 12
TLC-FID Procedure 12
Total Extracted Materials (TEM) Procedure 13
TPH Open Column Chromatography Procedure 14
HPLC – SARA Procedure 14

Page

Results 14
TLC-FID QAQC Analysis 14
TLC-FID Chromarod Drying, Chromarod Orientation, and Scan Speed 15
TLC-FID Chromarod Mass Loading 17
Monitoring Instrument Error 19
Monitoring Method Error 20
Monitoring Procedural Error 22
Comparison of TLC-FID and Other Petroleum Analysis Techniques 23
Conclusions 25

CHAPTER III APPLICATION OF THE TLC-FID ANALYSIS FOR PETROLEUM BIOREMEDIATION FIELD STUDIES 28
Overview 28
Introduction 28
Methods 33
Site Description 33
Phase I (Natural Attenuation after an Actual Oil Spill) 33
Phase II (Bioremediation of a Controlled Oil Release) 34
Collection, Extraction, and Analysis of Field Samples 37
Statistical Analysis 37
Results 38
Phase I Natural Attenuation Study 38
Phase I Fraction Percentages 38
Phase I TEM Concentrations 40
Phase I TLC-FID Fraction Concentrations 42
Phase I Hopane-Normalized Fraction Concentrations 44
Phase I Asphaltene-Normalized Fraction Concentrations 46
Phase II Bioremediation Study 48
Phase II Fraction Percentages 49
Phase II TEM Concentrations 54
Phase II TLC-FID Fraction Concentrations 56
Phase II Hopane Normalized Fraction Concentrations 61
Phase II Asphaltene Normalized Fraction Concentrations 67
Conclusions 72

Page

CHAPTER IV SUMMARY AND CONCLUSIONS 75

REFERENCES 77

APPENDIX A 81

VITA 107

LIST OF FIGURES

Page

Figure 2.1 Representative Chromatograms of Chromarod Mass Loading.....18
Figure 3.1 Diagram of the Phase I San Jacinto Wetland Research Facility.....35
Figure 3.2 Diagram of the Phase II San Jacinto Wetland Research Facility.....36
Figure 3.3 Phase I Fraction Percent TLC-FID Data.....39
Figure 3.4 Phase I TEM Data.....41
Figure 3.5 Phase I Fraction Concentration TLC-FID Data.....43
Figure 3.6 Phase I Hopane Normalized Fraction Concentration TLC-FID Data.....45
Figure 3.7 Phase I Asphaltene Normalized Fraction Concentration TLC-FID Data.....47
Figure 3.8 Phase II Fraction Percent TLC-FID Saturate Data.....50
Figure 3.9 Phase II Fraction Percent TLC-FID Aromatic Data.....51
Figure 3.10 Phase II Fraction Percent TLC-FID Resin Data.....52
Figure 3.11 Phase II Fraction Percent TLC-FID Asphaltene Data.....53
Figure 3.12 Phase II TEM Data.....55
Figure 3.13 Phase II Fraction Concentration TLC-FID Saturate Data.....57
Figure 3.14 Phase II Fraction Concentration TLC-FID Aromatic Data.....58
Figure 3.15 Phase II Fraction Concentration TLC-FID Resin Data.....59
Figure 3.16 Phase II Fraction Concentration TLC-FID Asphaltene Data.....60
Figure 3.17 Phase II Hopane Normalized TLC-FID Saturate Data.....62
Figure 3.18 Phase II Hopane Normalized TLC-FID Aromatic Data.....63
Figure 3.19 Phase II Hopane Normalized TLC-FID Resin Data.....64
Figure 3.20 Phase II Hopane Normalized TLC-FID Asphaltene Data.....65
Figure 3.21 Phase II Asphaltene Normalized TLC-FID Saturate Data.....69
Figure 3.22 Phase II Asphaltene Normalized TLC-FID Aromatic Data.....70
Figure 3.23 Phase II Asphaltene Normalized TLC-FID Resin Data.....71

LIST OF TABLES

Page

Table 2.1 QA-QC Results for Drying Procedure, Rod Orientation, and Scan Speed. 16
Table 2.2 QA-QC Monitoring Results for Instrument Error 19
Table 2.3 QA-QC Monitoring Results for Method Error 21
Table 2.4 QA-QC Results for Sample Replicates 23
Table 2.5 Percent Fractions of Bonny Light LCS-P by Different Analyses 24

CHAPTER I

INTRODUCTION

Petroleum is a highly complex mixture of hydrocarbons and non-hydrocarbon compounds. When released into the environment, these compounds are affected by environmental exposure, thus altering their chemical state. What results over the duration of environmental exposure is a very complex mixture of organic molecules. Consequently, there are several techniques to measure and characterize petroleum released into the environment. Each of these techniques has its advantages, disadvantages and limitations. Through time, trial and error, and improvements in technology, some of the disadvantages and limitations have been overcome and new techniques have been developed. However, when it comes to understanding the fate of petroleum in the environment, in particular reference to biodegradation, gaps in our knowledge still exist.

BACKGROUND

When crude oil or petroleum products are released into the environment they are immediately subjected to a wide variety of weathering and degradation processes. Weathering processes are numerous and can include, but are not limited to, evaporation, photochemical oxidation, dissolution, dispersion, emulsification, microbial degradation and sediment particulate adsorption (Atlas, 1995; Cerniglia, 1984; Leahy and Colwell, 1990; Payne and McNabb, 1984). These processes act directly on the oil and alter the physical-chemical composition of the oil. However, the rate and extent of any of these processes, specifically microbial degradation, are highly dependent on environmental factors and crude oil composition (Leahy and Colwell, 1990; Prince, 1993; Westlake et al., 1974).

Environmental factors like temperature, dissolved oxygen and nutrient availability influence the weathering processes of the oil and play a key role in the

---

The style and format of this thesis follows that of Marine Pollution Bulletin.

success of petroleum bioremediation efforts. (Atlas and Bartha, 1972; Cerniglia, 1984; Leahy and Colwell, 1990). Left alone, oil spills that make landfall will degrade through numerous weathering processes. Of these weathering processes, research has demonstrated that in favorable conditions, the significant pathway of oil removal is intrinsic microbial degradation (biodegradation). Bioremediation is an oil spill response technique that enhances environmental conditions to further encourage biodegradation of oil through the addition of amendments (either nutrient or microbial). It is considered the least intrusive and most environmentally-friendly response technique for sensitive ecosystems (Atlas, 1995; Bragg et al., 1994; Leahy and Colwell, 1990; Prince, 1993; Pritchard et al., 1992; Swanell et al., 1997).

In addition to evaluating environmental parameters, the chemical state of the petroleum at the time of remediation can also have an impact on remedial success. Petroleum products are a complex mixture of compounds that vary greatly in their composition, but can be classified by their relative content of paraffinic (saturate) and aromatic hydrocarbons, and non-hydrocarbon polar (resin and asphaltene) compounds. The specific composition of these petroleum compounds in a spilled petroleum product can have an effect on remedial efforts as portions of these compounds are degraded relatively quickly and easily, while other portions are more recalcitrant and will persist for many years (Prince, 1993; Atlas, 1981).

Petroleum bioremediation research conducted over the last three decades has yielded a side benefit of improved laboratory techniques to quantify and evaluate the fate of catastrophic petroleum spills in the environment (Mills et al., 1999; Prince, 1993; Swanell et al., 1999; Venosa et al., 1996). Currently the most widely accepted analytical technique used to evaluate petroleum biodegradation is Gas Chromatography coupled with Mass Spectrometry (GC-MS) analysis of key (or target) petroleum analytes (Prince, 1993; Venosa et al., 1996; Swanell et al., 1999). To complement a GC-MS petroleum analysis, other less sophisticated techniques can be considered, such as open column chromatography (referred to as total petroleum hydrocarbon, or TPH, in this paper), and high performance liquid chromatography (HPLC) saturate, aromatic, resin, asphaltene

(SARA) analysis. However these techniques are not widely popular because they can be elaborate, labor intensive, time consuming, and qualitative results are not easily reproducible (Cavanagh et al., 1995; Goto et al., 1994; Ray et al., 1981; Selucky et al., 1985).

A technique that is gaining prominence in the quantitative and qualitative analysis of petroleum is the Thin Layer Chromatography, Flame Ionization Detection (TLC-FID) analysis (Cavanagh et al., 1995; Goto et al., 1994; Ishihara et al., 1995; Venkateswaran et al., 1995). The TLC-FID technique is already widely applied in the biology, medicine, petrochemical and the pharmaceutical industries (Ackman, 1981; Karlsen and Larter, 1991; Ray et al., 1981; Selucky et al., 1985). The method utilizes a process of chromatography based on the component polarity of petroleum compounds and the ionization energy of organics quantified with a FID. The TLC-FID technique overcomes some of the limitations of other petroleum analyses and has proven to be a rapid, convenient, and reliable semi-quantitative characterization technique for petroleum compounds (Cavanagh et al., 1995; Cebolla et al., 1998; Goto et al., 1994; Ray et al., 1981; Selucky, 1985; Vela et al., 1998). The TLC-FID can produce quantitative measurements of each of the four petroleum fractions that make up the hydrocarbon and polar petroleum fractions.

RESEARCH OBJECTIVES

It is proposed that in addition to providing a full degradation characterization that complements a GC-MS biodegradation analysis, the TLC-FID analysis can be used to quickly determine the biodegradation potential of a catastrophic spill prior to remedial action. Monitoring the composition the four petroleum fractions over the course of a remedial effort also provides a complete characterization of remedial efforts that can impact the long term remedial strategies. Thus, the objectives of this research involve:

- Development of quality assurance and quality control (QA-QC) procedures for the TLC-FID analysis utilizing existing field samples,
- comparison of the TLC-FID analysis to other petroleum analyses, and
- application of the TLC-FID analysis to sediment sample sets from two field petroleum bioremediation studies.

CHAPTER II
METHOD DEVELOPMENT OF THE TLC-FID ANALYSIS FOR LARGE SCALE PETROLEUM BIODEGRADATION FIELD STUDIES

OVERVIEW

Traditional methods used to monitor catastrophic petroleum spills often do not present a full characterization of petroleum compounds. Effective monitoring or studies of catastrophic petroleum spills require the collection of large sets of samples. Although there are techniques available to perform full characterizations, they do not lend themselves well to the analysis of large sample sets. One such method is HPLC-SARA analysis where all four fractions of petroleum can be quantified. With regards to large sample set analysis, the drawback of this method is the tedious and time-consuming effort involved to analyze samples. Thin layer chromatography (TLC), coupled with flame ionization detection (FID) is a method that can also characterize and quantify all four fractions of petroleum quickly and with greater ease. These advantages lend themselves well to the analysis of large sample sets.

The TLC-FID research presented here briefly compares the TLC-FID analysis to the HPLC-SARA analysis. This research also presents the methods developed for quality control and quality assurance protocols used for, and results of, the analysis of large sample sets from two petroleum bioremediation field studies.

INTRODUCTION

Breaking down the composition of petroleum can be a daunting task considering that estimates on the number of crude oil compounds indicate hundreds of thousands of complex molecular compound mixtures (Prince, 1993). Although petroleum is mainly comprised of carbon and hydrogen, the diversity of compounds arises from an almost infinite number of combinations that these elements can form. Grouping these compounds by general properties makes their characterization and quantification more manageable. The most general classification of petroleum is by structural sub-groups,

hydrocarbons and non-hydrocarbon (polar) materials. A more specific chemical classification scheme identifies groups within this general framework. This classification includes the saturate fraction (saturated hydrocarbons), aromatic fraction (unsaturated hydrocarbons), and resin and asphaltenes fractions (polar materials) (Atlas, 1981; Leahy and Colwell, 1990).

Conventional methods of measuring oil released into the environment include total extractable material analysis (TEM), open column chromatography for "total petroleum hydrocarbon" analysis (TPH), high performance liquid chromatography (HPLC) for SARA analysis, and gas chromatography coupled with flame ionization or mass spectrometry (GC-FID, GC-MS) for specific target analyte analysis.

These conventional methods, although useful, have their limitations. Besides the time and costs, the largest limitation of conventional methods is the inability to characterize the non-hydrocarbon (i.e. polar) fractions of oil. The most widely used conventional methods (TPH and GC-MS/FID) cannot effectively quantify polar non-hydrocarbon materials from collected samples. To achieve a full characterization of petroleum compounds the HPLC-SARA analysis is often applied. However, this technique is often described as tedious and time consuming, which are unfavorable characteristics for the analysis of large sample sets (Cavanagh et al., 1995; Goto et al., 1994; Ray et al., 1981; Selucky et al., 1985). The Thin Layer Chromatography, Flame Ionization Detector (TLC-FID) method is not limited in this manner. It has the advantage of characterizing the major hydrocarbon and non-hydrocarbon components of petroleum.

The TLC-FID method is a derivative of planar chromatography that has been developed into an easily applied, effective, and efficient petroleum compound analysis technique. The method is a process of exposing silica adsorbent rods (chromarods) to three different solvents of increasing polarity, thus creating chromatographic separations. The chromarods have a thin silica adsorbent layer that has been sintered on with a non-organic binder; the chromarod dimensions are 0.9 mm. in diameter and 15 cm in length (Iatron, 1995). Chromatography of the petroleum is based on the component polarity of

the petroleum compounds and the increasing strength of the solvent bath in each elutriation chamber. The FID hydrogen flame ionizes the organic components separated on the surface of the chromarods. The ions generated are charged both negatively and positively, creating ion currents between the oppositely charged burner and detector (Iatron, 1995). These ion currents are measured proportional to the mass of components ionized in the flame and a response is recorded (Iatron, 1995).

The TLC-FID output produces data that characterize the FID-generated chromatograms. These data include retention times, peak areas, peak heights, peak widths, and the relative percentages of the total peak area for each identified peak. The resolved peaks represent the relative concentration of petroleum compounds that are soluble in the different solvents: a) saturates in hexane, b) aromatics in toluene, and c) resins in a 95:5 (vol:vol) dichloromethane-methanol mixture. Asphaltenes are quantified as those compounds detected at the point of origin on the chromarods. It is understood that the asphaltene compounds are the heaviest polar compounds not soluble in the extraction solvents, and consequently are not eluted on the chromarods.

Several studies have been performed to refine the application of the TLC-FID technique for petroleum analysis. Ray et al. (1981) was one of the first to develop methods to apply the TLC-FID technique to petroleum analysis. Karlsen and Larter (1991) performed a comprehensive analysis of the TLC-FID operating parameters with several crude oils and identified recommended operation ranges. Bharati et al. (1993) demonstrated the relation of TLC-FID variability due to the varying API gravity of over 30 crude oils. Cebolla et al. (1998) analyzed a suite of polynuclear aromatic hydrocarbons (PAH) compounds to determine the effects of FID scan speed versus sample evaporation. Vela et al. (1998) analyzed a variety of heavy molecular weight petroleum products to demonstrate calibration techniques.

The TLC-FID technique can prove valuable in providing information regarding biodegradation losses of oil as it analyzes all four fractions of oil, and relatively rapid assessments of large sample sets can be determined. The objectives for the research presented in this chapter include:

- Using large sample sets from two field petroleum studies, conduct the needed quality assurance and quality control (QA-QC) protocols for the TLC-FID technique when evaluating oil biodegradation, and
- compare the TLC-FID analysis to the HPLC-SARA analysis.

METHODS

TLC-FID QA-QC Analysis

As the large sets of field samples were collected temporally, the sample analyses QA-QC was also performed temporally. Two different laboratory control standards (LCSs) were prepared to provide long term temporal method error and repeatability QA-QC data. The first LCS was a synthetic blend (LCS-S) used to monitor instrument error. The second LCS was a petroleum based standard (LCS-P) that had the same relative API gravity as the spilled oil and was used to monitor method error. Ten chromarods are available on each tray for sample analysis, one sample per chromarod. For the purposes of this research, four of the ten chromarods on each tray were used for QA-QC and the remaining 6 chromarods were used for samples. Real time QA-QC of the TLC-FID sample analysis for the two field studies was monitored using Shewhart control charts to monitor three types of error: a) instrument error, b) method error, and c) procedural error. Method repeatability was evaluated using a relative standard deviation (%RSD) analysis of the two LCSs.

Experimental Samples

The LCS-S consisted of a mix of a saturate compound (C_{17} heptadecane), a light molecular weight aromatic compound (1-phenyl-tridecane), a mix of 4 heavier PAH compounds (anthracene, dibenzothiophene, fluorene, and phenanthrene), and a resin compound (3-pentadecyl-phenol), all dissolved in dichloromethane (DCM). For the Phase I study, these compounds were mixed in the following ratios; 15 % Saturate, 20% Light Aromatic, 15% Heavy Aromatic, and 50 % Resins. For the Phase II study, these compounds were mixed in the following ratios; 20% Saturate, 20% Light Aromatic, 15%

Heavy Aromatic, and 45 % Resins. The LCS-S was used for the QA-QC of the field sample extract analysis.

Based on research presented by Bharati et al. (1993) which demonstrated the relationship of the TLC-FID analysis to the API gravity of an oil, the LCS-P (Bonny Light crude oil, API-36) was chosen as a representative petroleum to the petroleum spilled in the field (Arabian Light crude oil, API–34.5). The LCS-P was used for the QA-QC of the field sample extract analysis. The results of the 49 LCS-P replicates were used for the TLC method comparisons and alternate petroleum analytical technique comparisons.

As part of the QA-QC, individual field sample extracts were replicated on each ten chromarod tray. The samples were collected from two wetland field studies of *in-situ* petroleum bioremediation. The first set of data were generated from a spill of opportunity study (Phase I), where sediment samples were collected 11 times over a 343-day period. Six sample replicates were collected at each sampling event. A total of 66 sample extracts were analyzed over ten analysis events, producing ten QA-QC event replicates. The second study (Phase II) focused on the evaluation of bioremediation amendments on a controlled oil release. The sediment samples were collected ten times over a 140-day period. Six sample replicates for each of three treatments and three unoiled controls were collected on each sampling event. A total of 210 sample extracts were analyzed over 39 analysis events, producing 39 QA-QC event replicates. Further details of both studies are presented in Chapter III of this thesis, with additional information provided in Mills et al. (2003) and Mills et al. (2004).

TLC-FID Chromarod Drying, Chromarod Orientation, and Scan Speed

These three issues were investigated by analyzing the LCS-P simultaneously under three different conditions to determine the appropriate TLC-FID procedures for this research. Chromarod drying is a key step in the TLC procedure that stops the chromatography of a solvent by drying the chromarod, i.e. evaporating the solvent. This step has not been readily discussed in the literature reviewed and the standard

recommended method is to dry the chromarods in a low heat oven. This method was investigated to determine any effects of this procedure and determine an acceptable alternate method.

Literature reviews suggested that improved FID responses have been noted when the TLC chromarods are turned so that the sample spot faces the FID flame (Bharati et al., 1993; Karlsen and Larter, 1991). This procedure was investigated to determine any impacts to the TLC-FID procedures for this research.

Several successful bioremediation TLC-FID studies have been performed with the scan speed used in this research (30 sec/rod), however some uncertainty exists with regards to the FID scan speeds and sample volatilization (Ishihara et al., 1995; Karlsen and Larter, 1991; Venkateswaran et al., 1995). This procedure was investigated to determine any impacts to the TLC-FID procedures for this research. The results of these analyses are presented in the results section.

TLC-FID Chromarod Mass Loading

To standardize the analyzed sample response over the course of the analysis period, a specific chromarod mass loading (8-10 mg/ml TEM) was determined that provided unique and clear peak separation. The results of this analysis are presented in the results section. Based on this approach the relative percent peak areas were used to quantify petroleum concentrations.

Monitoring Instrument Error

Instrument errors were identified as varying instrument conditions, such as variable hydrogen/air flow rates, fouled chromarods, or fouled detectors, which could affect the sample analysis results. Instrument errors were monitored using the LCS-S that modeled the component fractions of petroleum and did not degrade over the course of the study. The results were charted on a Shewhart Control chart to monitor QAQC (Appendix A).

Monitoring Method Error

Method errors were identified as non-user related conditions that affected the sample analysis method, such as ambient temperature and humidity. Effects from method errors were monitored using the LCS-P. It was hypothesized that errors experienced by the LCS-P would be relative to the effects experienced by the Arabian Light Crude oil sample extracts. The results were charted on a Shewhart Control chart to monitor QAQC (Appendix A).

Monitoring Procedural Error

Procedural errors were identified as varying user conditions that affected the sample analysis results, including poor sample spotting and poor tray handling. Procedural errors were monitored by replicating one sample extract three times on each tray of ten rods. The results were charted on a Shewhart Control chart to monitor QAQC (Appendix A).

Shewhart Control Charts

Shewhart control charts were used to identify any significant deviations from the average results. Deviations were identified as results that exceeded warning and action limits, set at 2 and 3 standard deviations respectively, above and below each average condition. When an LCS exceeded the action limits once, sample analysis continued, but efforts were made to minimize all forms of errors. When an LCS exceeded the action limits consecutively, then sample analysis stopped and analysis conditions were reevaluated before more samples were analyzed. For all action limit exceedances the associated LCSs and sample data were reviewed and compared and if deemed necessary, the sample results were discarded and reanalyzed.

Repeatability

For the temporal analysis of these large sample sets, the determination of method repeatability was evaluated using the relative standard deviation (%RSD) analysis given by the equation:

$$\%RSD = \frac{(100St - Dev.)}{Avg.}. \qquad (2.1)$$

Where St-Dev. is the respective LCS standard deviation and Avg. is the respective average fraction percentage of the temporal LCSs. A %RSD of 5% (95% confidence interval), was considered acceptable for LCS sample sets of ten or less and 10% (90% confidence interval) for LCS sample sets greater than 10.

Petroleum Analytical Procedures

As the TLC-FID technique is not yet widely applied to the analysis of petroleum biodegradation, it is important to understand how the results compare and contrast to other commonly-used analysis techniques. The TLC-FID protocols and brief summaries of these other petroleum analytical protocols used in this research are outlined as follows.

TLC-FID Procedure

Specific details of the TLC-FID protocol that was used for the analysis of field samples are outlined as follows. The TLC-FID instrument used for this research was an Iatroscan MK-5, (Iatron Laboratories, Tokyo, Japan). Extract all samples with dichloromethane (DCM) using standard Soxhlet procedures (see Chapter III for more details). Adjust extracts to yield an extract concentration between 8 and 10 mg/ml TEM. Pass the chromarods through the FID hydrogen flame twice to clean and dry them before samples are applied. Line one side of the hexane and the toluene solvent chambers with filter paper to aid in the elution of the solvents on the chromarod. Apply a 1µl aliquot of the concentration-adjusted extract to the origin point of each chromarod with a micropipette. Place the rack of ten chromarods in the first (hexane) solvent chamber for

a 30-minute elution period or until the saturate hydrocarbons gas at low pressure. Place the chromarods in the second (toluene) filter lined solvent chamber to elute for 15 minutes or until the aromatic fraction moves 5 cm up the chromarod. Remove the tray from the solvent chamber and dry again with low-pressure nitrogen. Place the rack in the last solvent chamber to elute in a 95:5 dichloromethane:methanol solution for 2.5 minutes to separate the resins from the asphaltenes. Do not leave the rack in this solvent chamber for longer than 2.5 minutes as this solvent elutes rapidly. Remove the tray from the solvent chamber and dry again with low-pressure nitrogen. The asphaltenes are left stationary at the sample application point of the chromarod. Store the chromarods in a desiccant chamber when possible. When the chromarods have passed through all the solvent chambers and are dry, place the rack with ten chromarods in the Iatroscan MK-5 automated FID system for analysis. Set the scan speed to 30 seconds per chromarod; maintain the hydrogen flow rate at 160 ml/min and the airflow rate at 2 L/min. All the solvents used were of pesticide grade or better quality.

Total Extracted Materials (TEM) Procedure

The TEM procedure is a gravimetric measurement of the gross organic compounds and some inorganic species (e.g., sulfur) soluble in hot dichloromethane. For a field sediment sample, this can include petroleum hydrocarbons, petroleum polar compounds, and any biological organic compounds that may be found in a sediment sample such as plant waxes, etc. The TEM protocol is detailed as follows. After sample extraction with dichloromethane, concentrate each sample extract to a known volume. From the extract, add a 100-*u*l aliquot to a tared glass fiber filter. Allow the DCM solvent to evaporate in a clean and dry location; weigh the filter again to determine the residual organic mass. Use the weights and known volumes to determine the TEM in each sample.

TPH Open Column Chromatography Procedure

The TPH procedure is a chromatography protocol that allows for separation and quantification of the saturate and aromatic fractions from the rest of the oil. The polar compounds are not recovered from the column. The chromatography protocol includes building a silica-alumina fractionation column and eluting it with various solvents (n-pentane and a 1:1 pentane-DCM solution). The elutriates are collected, concentrated and the elutriate concentrations are determined for the relative "total-saturate petroleum hydrocarbons" (TsPH) and the "total-aromatic petroleum hydrocarbons" (TarPH). These two values combined give the TPH of a petroleum extract. These methods and procedures are discussed in more detail in Mills et al. (1999).

HPLC – SARA Procedure

The saturate, aromatic, resin, asphaltene (SARA) fractionation by HPLC analysis is a patented process that was contracted to an outside laboratory (Houston Advanced Research Center, Houston, TX). The process uses YMC Amino columns for fractionation and four solvents for compound separation and is summarized as follows. An aliquot of a petroleum sample extract is first eluted through both columns with hexane. The resins and asphaltenes are retained in the first column and the aromatics are retained in the second column. The saturated fraction is collected first from the first column. Then the second column is back flushed with a chloroform-hexane mixture to elute the resins and then back-flushed with a methanol-acetone-chloroform mixture to elute the asphaltenes. The first column is then back-flushed with chloroform to elute the aromatics.

RESULTS

TLC-FID QA-QC Analysis

Of the ten chromarods available on each tray, four of them were used for QA-QC purposes. The remaining 6 chromarods were used for sample extracts. Real time QA-QC of the TLC-FID sample analysis for the two field studies was monitored using

Shewhart control charts to monitor three types of error: a) instrument error, b) method error, and c) procedural error. Method repeatability was evaluated using a relative standard deviation (%RSD) analysis of the two LCSs and comparing the standard deviations of one sample extract replicated on each tray of ten chromarods.

TLC-FID Chromarod Drying, Chromarod Orientation, and Scan Speed

The results for these brief investigations are presented in Table 2.1. The three different sets of results characterize the investigations where 1) the sample chromarods were dried in a low heat oven versus drying with low pressure nitrogen, 2) the chromarods were oriented with the sample facing the flames versus a random orientation of the chromarods (both dried with low pressure nitrogen), 3) all samples were analyzed at the 30 sec/rod scan speed to identify any appreciable fraction degradation. The values presented in Table 2.1 for the "Low Pressure Nitrogen (n=49)" and "Random Orientation (n=49)" are the relative fraction percentages for the LCS-P replicate results for the Phase I and Phase II study. The results for the "Low Heat Oven (n=10)" and "Facing Flame (n=10)" are separate analyses that were performed during the method development. The high %RSD values observed in the small percentage fractions are due to the low values of the averages more so than high standard deviations.

Literature reviews have characterized the fraction composition of the Bonny Light LCS-P as 60% saturates, 30% aromatics, 9% resins, and 1% asphaltenes (Goto et al., 1994; Venkateswaran et al., 1995). In the literature review to determine methods applied in this research, the most common procedure described for drying chromarods between solvent baths was to dry them in a low heat oven. This procedure was further investigated by drying the saturate hydrocarbon rich LCS-P in a low heat oven versus drying with low pressure nitrogen. From the reduced saturate fraction percentages observed in the results for the Low Heat Oven analysis presented in Table 2.1 it is evident that drying the chromarods in a low heat oven volatilized the saturate compounds of the LCS-P. Therefore the procedure for drying the chromarods between solvent baths was modified to dry the chromarods with low pressure nitrogen gas.

Table 2.1 QA-QC Results for Drying Procedure, Rod Orientation, and Scan Speed.

Drying Procedure	Low Heat Oven (n=10)			Low Pressure Nitrogen (n=49)		
LCS-P	Avg. %	St-Dev	%RSD	Avg. %	St-Dev	%RSD
Saturate	44.4	1.65	3.7	59.0	1.93	3.3
Aromatic	29.9	7.80	10.2	28.3	1.23	4.3
Resin	24.0	2.45	10.2	11.1	1.30	11.7
Asphaltene	3.0	1.47	49.2	1.6	1.16	74.1
Rod Orientation	Facing Flame (n=10)			Random Orientation (n=49)		
LCS-P	Avg. %	St-Dev	%RSD	Avg. %	St-Dev	%RSD
Saturate	57.0	1.99	3.5	59.0	1.93	3.3
Aromatic	28.6	1.23	4.3	28.3	1.23	4.3
Resin	12.6	0.69	5.5	11.1	1.30	11.7
Asphaltene	1.8	1.92	104.7	1.6	1.16	74.1

Once an effective method of drying the chromarods was determined, orienting the chromarods to face the FID flame was also tested by analyzing two different trays of ten chromarods, one with samples oriented towards the flame and the other with samples oriented randomly. No significant differences were observed in the results presented in Table 2.1 to suggest changing this procedure.

Karlsen and Larter (1991) performed an analysis with various crude oils that indicated loss of volatile components at high scan speeds (10-40 sec/rod) and improved FID responses for scan speeds approaching 60 seconds. This hypothesis was tested by analyzing the saturate hydrocarbon rich LCS-P at the 30 sec/rod scan speed to determine if there was a significant loss of the volatile saturate fraction. The results presented in Table 2.1 were all scanned at the 30 sec/rod scan speed, and except for the samples dried in a low heat oven, there was no appreciable volatilization of the volatile saturate fraction observed. Thus, no modifications were made to this procedure.

TLC-FID Chromarod Mass Loading

To standardize the sample response over the course of the analysis period, a specific chromarod mass loading was determined that provided unique and clear peak separation. Increasing concentrations of the LCS-P were loaded on the chromarods to determine an effective mass loading concentration for analysis of the field samples. Three representative chromatograms (Figure 2.1) that show the chromarod mass loading with the LCS-P at a high concentration (Graph A) of 30 mg/ml TEM; an acceptable concentration (Graph B) of 8 mg/ml TEM, and a low concentration (Graph C) of 5 mg/ml TEM. The vertical scale is relative to the peak heights while the horizontal scale is relative to the chromarod length where time 0 minutes is the top of the rod and time 0.5 minutes is the base of the rod, where the samples are spotted. The vertical scale of Graph A is twice as great as the vertical scale of Graph B and C to present the data clearly. The four peaks shown on the three graphs represent the four fractions of petroleum: saturates, aromatics, resins, and asphaltenes. Graph A shows that the chromarod is overloaded and fraction peaks are not well separated. Graph B shows good fraction separation and qualitatively good fraction detection. Graph C shows good fraction separation, but qualitatively the fraction detection appears poor. These results demonstrate that the clearest TLC separation occurred at an approximate sample extract concentration of 8 mg/ml TEM per chromarod. Therefore prior to analysis, each sample extract was adjusted to a TEM concentration of 8 to 10 mg/ml TEM.

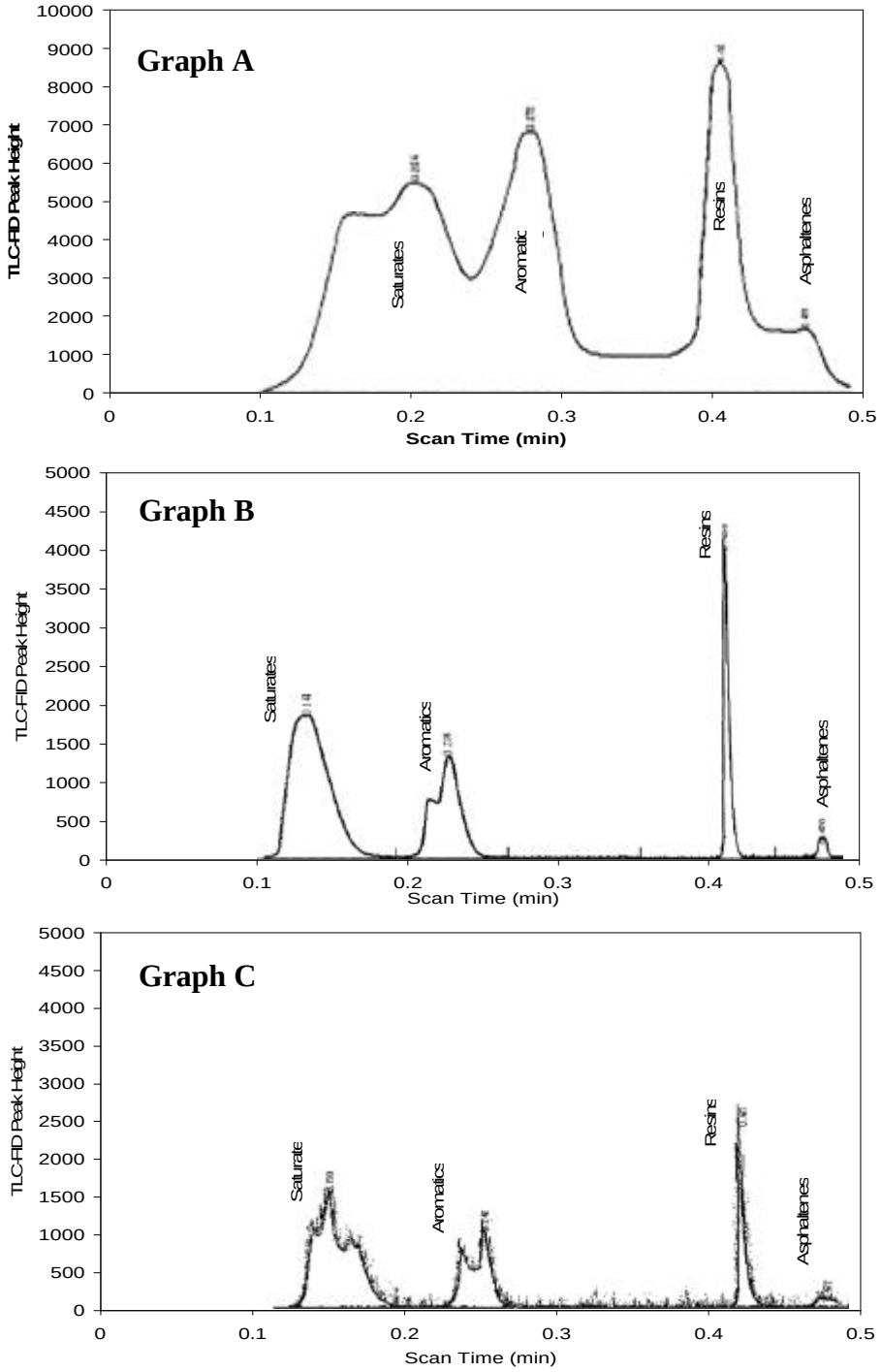

Figure 2.1 Representative Chromatograms of Chromarod Mass Loading. Three representative chromatograms showing fraction separation and FID response for different mass loads: A) 30 ug TEM, poor fraction separation, B) 8 ug TEM showing good fraction separation, and C) 5 ug TEM, showing good fraction separation, but a noisy response.

Monitoring Instrument Error

While no significant errors were observed during the sample analysis, instrument errors could occur if the FID oxygen or hydrogen flow rates varied, the chromarods were fouled, or the FID was fouled. This type of error was monitored with the Shewhart control chart and was indicated by repeated warning limit exceedances of the LCS-S or a measurable component degradation of the LCS-S fractions over time.

To monitor this type of error, the LCS-S was spotted on one chromarod of each ten chromarod tray. Repeatability of these results confirmed that the identified errors were controlled and minimized. The QA-QC results of the LCS-S relative fraction percentages for the ten Phase I study replicates and 39 Phase II study replicates are presented in Table 2.2. The Shewhart control chart numbers presented in Table 2.2 indicate the number of exceedances above (+) or below (-) the set limits respectively; the actual Shewhart control charts are presented in Appendix A.

Table 2.2 QA-QC Monitoring Results for Instrument Error.

Phase I Study	Shewhart Control Chart		Replicates, n=10		
LCS-S	Warning	Action	Avg. %	St-Dev	%RSD
Saturate	0	0	15.7	0.63	4.0
Light Aromatic	0	0	18.8	0.32	1.7
Heavy Aromatic	0	0	12.9	0.59	4.1
Resin	+1	0	52.5	0.84	1.6
Phase II Study	Shewhart Control Chart		Replicates, n=39		
LCS-S	Warning	Action	Avg. %	St-Dev	%RSD
Saturate	+2*	0	20.0	0.63	3.5
Light Aromatic	0	0	19.5	0.32	1.6
Heavy Aromatic	-2*	0	15.8	0.59	3.2
Resin	-2*	0	44.5	0.84	2.6

* - indicates non consecutive occurrences

For the Phase I Shewhart control monitoring, there was only one warning level exceedance that was below the action limit. Overall the %RSDs for Phase I was below the 5% limit set for sample sets less than 10. For the Phase II Shewhart control monitoring, there were several warning level exceedances but none that were consecutive or exceeded the action limits. The %RSD for Phase II was also below the 10% limit set for sample sets greater than 10.

Monitoring Method Error

Poor sample replication and poor fraction separation were observed when the ambient atmospheric humidity and temperature conditions in the laboratory exceeded approximately 60% relative humidity and 21 degrees Celsius. Based on observations made during preliminary trials, it was hypothesized that the relative humidity of the laboratory directly affected the chromatographic quality of the chromarods. This hypothesis is based on the observations that the chromarods provided improved fraction separation when the analyses were performed in dry ambient conditions. The assumption of this hypothesis is that in humid conditions the chromarods draw water from the air and saturate the silica pore space. To minimize this problem the laboratory conditions were constantly monitored with a thermohygrometer and samples were not analyzed when the ambient laboratory conditions described above were exceeded significantly. Additional precautions included a) storage of chromarods in a desiccant chamber when not in use, b) blank scan of chromarods in the FID twice prior to sample analysis, and c) lining solvent chambers with filter paper to saturate the chamber space with solvent vapors. Storing the chromarods in a desiccant chamber kept them dry and scanning the chromarods in the FID cleaned and removed moisture from them. The solvent chambers were lined with filter paper to wick and evaporate solvent to create a solvent saturated environment inside the chambers.

To monitor method error, the LCS-P (Bonny Light crude) was spotted on one chromarod of each ten-rod tray. The variability of these replicates was monitored with a Shewhart chart over the course of the project. Repeatability of these results confirmed that the identified errors were controlled and minimized. The QA-QC results of the ten Phase I LCS-P replicates and 39 Phase II LCS-P replicates are presented in Table 2.3. The Shewhart control chart numbers presented in Table 2.3 indicate the number of exceedances above (+) or below (-) the set limits respectively; the Shewhart control charts are presented in Appendix A.

Table 2.3 QA-QC Monitoring Results for Method Error.

Phase I Study	Shewhart Control Chart		Replicates, n=10		
LCS-P	Warning	Action	Avg. %	St-Dev	%RSD
Saturate	0	0	60.4	0.63	1.8
Aromatic	0	0	27.7	0.69	2.5
Resin	0	0	10.9	0.59	5.4
Asphaltene	0	0	0.9	0.22	24.2
Phase II Study	Shewhart Control Chart		Replicates, n=39		
LCS-P	Warning	Action	Avg. %	St-Dev	%RSD
Saturate	-1	-1	58.6	1.93	3.3
Aromatic	+1	0	28.5	1.28	4.5
Resin	+2*	+2*	11.2	1.44	12.9
Asphaltene	+1	+1	1.7	1.23	72.1

* - indicates non consecutive occurrences

For the Phase I Shewhart control monitoring, there were no warning level exceedances. The %RSD for the Phase I saturate, aromatic, and resin fractions of the LCS-P were below or close to the 5% limit set for sample sets less than 10. The high %RSD for the Phase I LCS-P asphaltene fraction is due to the low values of the average percent area and not due to high deviations in the data. For the Phase II Shewhart

control monitoring there were several warning level and action level exceedances but none of them occurred consecutively. The %RSDs for the Phase II LCS-P saturate, and aromatic fractions were also below the 10% limit set for sample sets greater than 10. Like the Phase I %RSD for the asphaltene fraction, the Phase II %RSD is higher than the 10% limit. This is attributed to the low values of the average percent area for the asphaltene fraction.

Monitoring Procedural Error

Poor sample replication of the saturate and aromatic fractions was observed when the 1-ul sample extract was not consistently spotted on the chromarods. For consistent sample replication the sample extract should be spotted on the chromarod in one location and should be no larger than 1-2 mm in diameter. The QA-QC results of the ten Phase I replicates and 39 Phase II replicates are presented in Table 2.4. The Shewhart control chart numbers presented in Table 2.4 indicate the number of exceedances above (+) or below (-) the set limits respectively; the Shewhart control charts are presented in Appendix A.

To monitor this type of error, one field sample extract was replicated on three chromarods on each ten-chromarod tray. Procedure errors were identified by poor and unequal fraction separation between the three replicates. The variability of these replicates was monitored by tracking the average standard deviation of the replicate results on a Shewhart chart over the course of the analysis period. Consistency of the analysis was determined acceptable because the average standard deviations remained low.

Table 2.4 QA-QC Results for Sample Replicates.

Phase I	Shewhart Control Chart		Replicates, n=10
Sample Replicates	Warning	Action	Avg. St-Dev
Saturate	0	0	1.1
Aromatic	0	0	1.0
Resin	0	0	1.4
Asphaltene	+1	0	1.5
Phase II	Shewhart Control Chart		Replicates, n=39
Sample Replicates	Warning	Action	Avg. St-Dev
Saturate	+2*	0	0.9
Aromatic	+1	0	1.5
Resin	+2*	0	2.7
Asphaltene	+2*	0	2.2

* - indicates non consecutive occurrences

Comparison of TLC-FID and Other Petroleum Analysis Techniques

In an effort to compare TLC-FID results with established analytical procedures for petroleum characterization, the Bonny Light crude oil used for the LCS-P was also characterized by TPH and HPLC-SARA analyses. Three replicates were performed for the packed column TPH Bonny Light analysis and a 10-ml aliquot of the Bonny Light was sent to an outside laboratory for HPLC-SARA analysis. The TLC-FID and TPH analyses were performed in Texas A&M University laboratories. The Bonny Light LCS-P QAQC replicate results (n=49 replicates) were used for the basis of the TLC-FID comparisons. A GC-MS analysis was not performed on the Bonny Light for comparison purposes as it quantifies specific petroleum analytes and the techniques compared here quantify the gross relative fractions of petroleum compounds.

The results of these analyses were evaluated by two methods: 1) a quantitative comparison of the relative gravimetric fraction percentages determined by each analysis, and 2) a comparison of the ratio of saturate-to-aromatic fractions as determined by each analysis. Table 2.5 shows the relative quantified gravimetric fractions of the LCS-P determined by all three methods and the saturate-to-aromatic fraction ratios.

Table 2.5 Percent Fractions of the Bonny Light LCS-P by Different Analyses.

Bonny Light	TPH		HPLC-SARA		TLC-FID	
% Saturates	47	Ratio	61	Ratio	58.6	Ratio
% Aromatics	20	2.35-1	26	2.34-1	28.5	2.1-1
% Resins	33*		5		11.2	
% Asphaltenes	- na -		8		1.60	

* - unresolved fractions characterized as polar compounds

The HPLC-SARA analysis characterized the LCS-P fraction makeup similar to the TLC-FID analysis, while the hydrocarbon fractions characterized by the TPH analysis were significantly lower. The remaining 33% unquantified TPH fraction is considered unrecovered from the column and characterized as polar compounds. The saturate-to-aromatic ratios are similar for the TPH and HPLC-SARA analyses, but lower for the TLC-FID analysis.

CONCLUSIONS

The TLC-FID ability to analyze ten samples (ten chromarods per tray) at the same time is a significant laboratory advantage that allows samples and QA-QC LCSs to be analyzed concurrently. It also provides the flexibility to analyze large sets of samples relatively quickly. In general, from the start of the TLC procedure to the end of the FID analysis, ten samples can be analyzed in under two hours. In addition, the TLC-FID analysis does not require large volumes of solvents for chromatography. The TLC-FID solvent baths each require approximately 100 ml of solvent for analysis.

The method analysis of the TLC-FID application provided an acceptable method for drying chromarods between solvent baths, dismissed questions regarding the chromarod orientation relative to the FID, and demonstrated that the 30 sec/rod scan speed was acceptable for this petroleum study. In addition an acceptable mass loading was determined for clear fraction separation. Overall these results were applied to the TLC-FID procedures used for the analysis of the sample extracts of the two petroleum biodegradation studies discussed further in Chapter III of this thesis.

The QA-QC methods presented here were applied to the analysis of the field sample extracts to establish effective protocols for the successful application of the TLC-FID analysis. Several procedures were investigated for this specific research and several types of potential errors and means to monitor them were identified. Two of these error types, instrument error and method error were monitored using two different laboratory control standards (LCSs). The acceptable %RSD numbers determined for the LCS-S and LCS-P confirmed that these types of errors were minimized and controlled. The low %RSD numbers also demonstrate the success of using Shewhart control charts to monitor the analysis QA-QC. In addition to using two representative LCSs, field sample extracts were also used for the third, most common type of error, procedural or user related errors. These types of error were also shown to be controlled over the analysis period. Together these QA-QC results demonstrate that without internal sample references and with effective protocols in place, the TLC-FID analysis is suitable for large field sample set analyses.

The results of the petroleum analytical methods comparison demonstrate that the HPLC-SARA and TLC-FID analysis had similar characterizations of the Bonny Light. However, the TPH analysis revealed very different characterizations of the Bonny Light. Although the HPLC-SARA analysis was similar to the TLC-FID and the TPH analysis was not, these two methods (HPLC-SARA and TPH) demonstrated similar saturate-to-aromatic ratios. These results are more indicative of the differences between the TLC-FID and these methods.

While the HPLC-SARA analysis yields similar characterizations as compared to the TLC-FID analysis, the HPLC-SARA procedure is regarded as time consuming and inadequate for large sample sets. Another disadvantage of the HPLC-SARA method not readily demonstrated here is the difficulty of quantifying compounds that may remain in the HPLC column after the fractions are extracted (Goto et al., 1994; Pollard et al., 1992).

Although an industry standard, the open-column-chromatography TPH analysis did not demonstrate a similar characterization of the Bonny Light petroleum as compared to the TLC-FID analysis. Most notable is the reduced hydrocarbon fraction for the TPH analysis. It is hypothesized that significant portions of the hydrocarbon fraction are lost to volatilization due to the significant amount of processing and exposure that the sample is subjected to before and after loading it onto the column (Douglas et al., 1991). Also, because a significant portion of the sample cannot be recovered from the packed column, it is difficult to reliably quantify the losses (Pollard et al., 1992). This TPH method also requires significant user skill and time to build the columns, prepare the samples, and collect the elutriates, which makes it inadequate for large sample sets. Reproducibility of results has also been identified as a disadvantage given that each column is dependent on the user skill for consistent column construction.

Although not compared to the TLC-FID, GC-MS analysis of petroleum products is unique in that it can quantify specific petroleum compounds. This proves beneficial for "fingerprinting" oils and for the determination of petroleum bioremediation; however this can also prove to be a limitation of the analysis. The GC-MS can only measure a specific range of the hydrocarbons, quantitative recovery of non-hydrocarbon and nonvolatile components from the GC column is rarely achieved (Goto et al., 1994). This leaves a significant portion of the sample undetected. It is for this reason that the GC-MS analysis is not used for compositional characterizations of petroleum.

The TLC-FID cannot quantify compound specific characteristics (like the GC-MS), but it does have the capability to quantify gross petroleum fraction characteristics. Used together, a GC-MS analysis and the TLC-FID analysis can produce a complete picture of *in-situ* petroleum degradation. The field application of the TLC-FID analysis presented in Chapter III of this thesis will demonstrate the capability to identify petroleum biodegradation and quantify the gross compositional losses.

CHAPTER III

APPLICATION OF THE TLC-FID ANALYSIS FOR PETROLEUM BIOREMEDIATION FIELD STUDIES

OVERVIEW

The characterization and evaluation of petroleum bioremediation is largely performed with a GC-MS analysis of target hydrocarbon compounds. Although this type of characterization has significant benefits, it can be an incomplete characterization as heavy molecular weight compounds cannot be quantified with the GC-MS. These compounds were once thought recalcitrant, but recent research indicates otherwise. The TLC-FID technique provides the capability to achieve gross characterizations of the four petroleum fractions (saturates, aromatics, resins, and asphaltenes). This technology coupled with a GC-MS analysis can provide a more complete characterization of petroleum bioremediation.

The TLC-FID research presented here reviews the applicability of the TLC-FID to evaluate the temporal variations of the four petroleum fractions due to *in-situ* biodegradation. The specific objectives include the evaluation of the TLC-FID analysis to identify and quantify natural attenuation of a wetland following a catastrophic petroleum spill in an estuarine wetland; and the evaluation of the TLC-FID analysis to quantify differences between petroleum bioremediation amendments on a simulated petroleum spill in an estuarine wetland.

INTRODUCTION

The National Research Council (NRC) estimates that 12 percent of the 11.0 million tons of petroleum produced worldwide (per day) are discharged in various ways into the Earth's oceans (NRC, 2003). Large catastrophic petroleum spills occurring in the open sea eventually disperse through various mechanisms in a relatively short time period. Open sea spill response typically consists of physical collection methods including skimming, adsorbing, and vacuuming the petroleum from the water surface

(NRC, 2003; Prince et al., 1999). Of particular concern are petroleum spills that occur in coastal environments, which can have devastating ecological and economic impacts. Oil spills that make landfall in tidal marshes and rocky beaches often require physical collection or other more aggressive measures including power washing the petroleum back into the water for ease of collection, and burning the oil (Prince et al., 1999). However, these types of clean-up methods can be destructive, ineffective, and damaging to these sensitive ecosystems (DeLuane et al., 1990; Prince et al., 1999; Swanell et al., 1997).

Bioremediation of oil spills is considered the least intrusive and most environmentally friendly response technique for sensitive ecosystems (Atlas, 1995; Bragg et al., 1994; Leahy and Colwell, 1990; Prince, 1993; Pritchard et al., 1992; Swanell et al., 1997). Research has demonstrated that catastrophic petroleum spills can overwhelm and shutdown a natural ecosystem's ability to degrade petroleum by limiting essential ingredients necessary for microbial biodegradation of the petroleum (Lee and DeMora, 1999, Leahy and Colwell, 1990; Bragg et al., 1994; Pritchard et al., 1992). Most bioremediation research performed today seeks to make adjustments to the carbon-nitrogen-phosphorus ratios found after a catastrophic petroleum spill reaches land. Nitrogen and phosphorus amendments in the form of oleophilic fertilizers are added to stimulate the microbial biodegradation of petroleum (Atlas and Bartha, 1972; Bragg et al., 1994; Fedorak and Westlake, 1981; Leahy and Colwell, 1990; Pritchard et al., 1992;).

The key to successfully evaluating petroleum bioremediation is characterizing the biological degradation of the spilled product. The discovery of a "conservative reference" inherent to petroleum, readily detectable with a GC-MS, and assumed to be non-biodegradable, made the GC-MS analysis the preferred method of evaluating petroleum biodegradation (Butler et al., 1991; Prince, 1993; Wang and Fingas, 1995; Venosa et al., 1996). Target analytes measured with a GC-MS are normalized to the conservative biomarker (reference) compound 17α, 21β(H)-hopane (hopane) in order to quantify compositional losses of the petroleum due to biotic and abiotic activity. It is

assumed that hopane is not biodegradable in the timeframe of most experiments or monitoring periods.

However the GC-MS analysis does have quantitative limitations. The GC-MS technique can only measure a specific range of hydrocarbons, representing as little as 10 percent of the petroleum compounds present in a crude oil. Quantitative recovery of non-hydrocarbon and nonvolatile (high boiling point, high molecular weight) components from the GC column is rarely achieved (Goto et al., 1994; Pollard et al., 1992). Consequently, a significant portion of the sample is left undetected.

Petroleum products are a complex mixture of compounds that vary greatly in their composition, which can have an effect on remedial efforts as portions of these compounds degraded relatively quickly, while other portions are recalcitrant and will persist for many years (Prince, 1993; Atlas, 1981). Westlake et al. (1974) demonstrated that the qualitative composition of the four petroleum fractions directly influences the overall biodegradability of the oil. Possibly the most important fraction with regards to oil biodegradability is the saturate fraction, as it is the most susceptible to microbial activity (Jobson et al., 1974; Atlas, 1995). This can be key for monitoring the microbial degradation of the polar fractions, which are often considered recalcitrant (Prince, 1993). Research has demonstrated that hydrocarbon compounds can serve as catalyst for the degradation of polar compounds; i.e. they can be oxidized in the presence of hydrocarbons that serve as growth substrates (Atlas and Cerniglia, 1995; Dutta and Harayama, 2000; Lee and Levy, 1991; Westlake et. al., 1974). These conclusions suggest that oils with a high hydrocarbon-to-polar ratio have a greater biodegradation potential than oils with a low hydrocarbon-to-polar ratio.

A technique that is gaining prominence for the rapid characterization of the four petroleum fractions is Thin Layer Chromatography, Flame Ionization Detection (TLC-FID) analysis (Cavanagh et al., 1995; Goto et al., 1994; Ishihara et al., 1995; Venkateswaran et al., 1995). The TLC-FID is already widely applied in the bioscience, medicine, and petrochemical industries, and has proven to be a rapid, convenient, and reliable characterization technique for petroleum compounds (Cavanagh et al., 1995;

Cebolla et al., 1998; Goto et al., 1994; Ray et al., 1981; Selucky, 1985; Vela et al., 1998).

Recent TLC-FID biodegradation studies have largely consisted of laboratory microcosm and mesocosm research. Goto et al. (1994) demonstrated the application of the TLC-FID to quantitatively evaluate the oil-degrading capabilities of marine microorganisms in a shake flask study. Cavanagh et al. (1995) performed a qualitative TLC-FID analysis to demonstrate microbial degradation of low-molecular-weight hydrocarbons also in a shake flask study. Ishihara et al. (1995) used the TLC-FID analysis to evaluate the oil-degrading capabilities of a marine microorganism consortium in a mesocosm study. Venkateswaran et al. (1995) used the TLC-FID analysis to qualitatively demonstrate the microbial degradation of resin compounds in a shake flask study. Pollard et al. (1992) used the TLC-FID method as a screening tool to quantify the potential biotreatability or inherent recalcitrance of hydrocarbon waste mixtures at petroleum and creosote contaminated sites. However, there have been no field study research projects for the application of the TLC-FID to large scale *in-situ* temporal petroleum degradation studies.

For the research presented in this chapter, the TLC-FID analysis was applied to monitor the temporal degradation of Arabian Light crude oil in two *in-situ* field studies of petroleum biodegradation in an estuarine wetland. In the first study (Phase I), petroleum-contaminated samples were collected temporally after a catastrophic spill of opportunity where intrinsic biodegradation was characterized. In the second study (Phase II), petroleum-contaminated samples were collected temporally from a controlled oil spill to evaluate petroleum bioremediation treatments. In both studies, GC-MS analysis of specific petroleum analytes determined that biodegradation was the significant pathway of petroleum reduction (Mills et al., 2003; Mills et al., 2004).

To measure temporal changes in the petroleum composition, the TLC-FID analyses of the samples are presented as relative concentrations of the four major petroleum fractions: a) saturate, b) aromatic, c) resin, and d) asphaltene. In addition, three other data analyses of the TLC-FID results were performed to determine the best

approach for applying the TLC-FID to large scale *in-situ* bioremediation studies. The four data analyses used to evaluate the TLC-FID results are described as follows:

1. Temporal comparison of the relative compositional changes of the petroleum by analyzing the fraction percentage results. The fraction percentage data were determined by quantifying the relative percent of the peak areas for each sample.
2. Temporal comparison of the TLC-FID fraction concentrations. The fraction concentration data were determined by multiplying the fraction percentages with the respective TEM concentrations to yield a fraction concentration. It was hypothesized that these TLC-FID data results represent gross petroleum degradation activity including biotic and abiotic degradation.
3. Temporal comparison of the TLC-FID fraction concentrations normalized to the GC-MS resolved hopane biomarker. These concentrations were determined by dividing the TEM concentration with the hopane concentration (as determined by GC-MS analysis) and then multiplying this modified TEM value with the TLC-FID fraction percent values. It was hypothesized that this analysis would demonstrate a lower biodegradation rate, longer half-lives, and higher model correlation coefficients than the non-normalized data.
4. Temporal comparison of the TLC-FID fraction concentrations normalized to the TLC-FID asphaltene fraction concentrations. It was hypothesized that this analysis would be analogous to the hopane-normalized analysis.

METHODS

Site Description

Sediment samples for this research were collected from the San Jacinto Wetland Research Facility (SJWRF), near Houston Texas. The SJWRF was constructed after a catastrophic oil spill on the San Jacinto River in 1994. The spill was the result of a 100-year flood that ruptured several submerged pipelines releasing gasoline (64,000 bbls), home heating oil (146,000 bbls), and Arabian Light crude oil (196,000 bbls) (Snyder, 1996; Mills et al., 2003). The released products ignited and the fire consumed the majority of the gasoline and fuel oil. The site, established by the Texas General Land Office and Texas A&M University, is situated in a wetland cove and was designated for a long-term research program to study oil spill remediation strategies. To conduct the research, 21 plots (5 meter by 5 meter) were constructed. An elevated scaffold system above each plot was built to avoid physically impacting the plots during the experiments. Details of the SJWRF and its history can be found elsewhere (Harris et al., 1999; Mueller et al., 1999; Townsend et al, 2000). Sediment samples from the first two research phases were analyzed for the research presented in this thesis.

Phase I (Natural Attenuation after an Actual Oil Spill)

The initial objective of the SJWRF research program was to monitor the natural attenuation (intrinsic remediation) of petroleum after the catastrophic release during the 1994 flood. The samples for this Phase I study were collected over a 343-day period. The sediment samples were collected 11 times; because it was a spill of opportunity, the first samples were collected 44 days after the initial spill. Additional samples were collected on Days 63, 70, 77, 84, 108, 129, 157, 203, 232, and 387 and six sample replicates were collected at each sampling event. The layout of the sample areas is shown on Figure 3.1. Results of accompanying nutrient, toxicity, and ecological studies for Phase I can be found elsewhere (Harris et al., 1999; Mueller et al., 1999; Wood et al., 1997).

Phase II (Bioremediation of a Controlled Oil Release)

The second phase of research at the SJWRF involved a petroleum bioremediation study. Arabian Light crude oil was artificially weathered to simulate oil spill conditions and applied to the wetland research plots in a controlled manner. The petroleum bioremediation treatments for this study included a no-action oiled control (O-C), an inorganic nutrient (diammonium phosphate) amendment (O-N), and the same inorganic nutrient plus an alternate electron acceptor (nitrate) amendment (O-NN). It was hypothesized that these amendments would increase the rate and extent of biodegradation of the weathered crude oil applied to the research plots. Each treatment had six replicate plots, in addition to three unoiled control plots as shown in Figure 3.2. After oil application (Day -4), sediment samples were collected on the first day of amendment application (Day 0). Additional samples were collected on days 8, 15, 29, 57, 70, 85, 113, 126 and 140. Six sample replicates were collected for each of three treatments and three unoiled controls were collected at each sampling event.

Results of accompanying toxicological and microbiological studies for Phase II can be found in Mueller et al. (2003) and Townsend et al. (2000), respectively. Subsequent research efforts at the site include a bioaugmentation experiment (Simon et al., 1999), a shoreline cleaner study (Bizzell et al., 1999), a redox dynamics study (LaRiviere et al., 2003), and a chemically-dispersed oil experiment (Page et al., 2002).

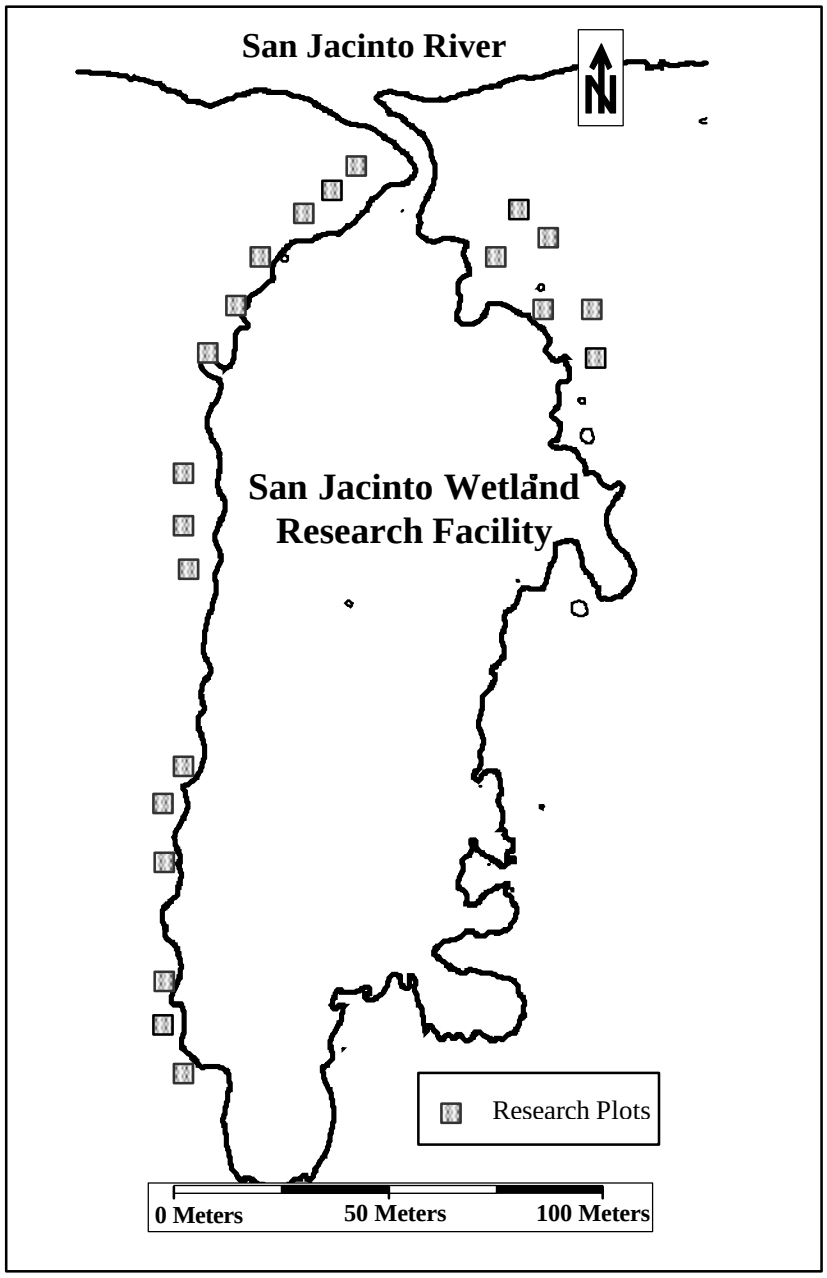

Figure 3.1 Diagram of the Phase I San Jacinto Wetland Research Facility. For Phase I the research plots were built in the areas that visually had the highest oil impact.

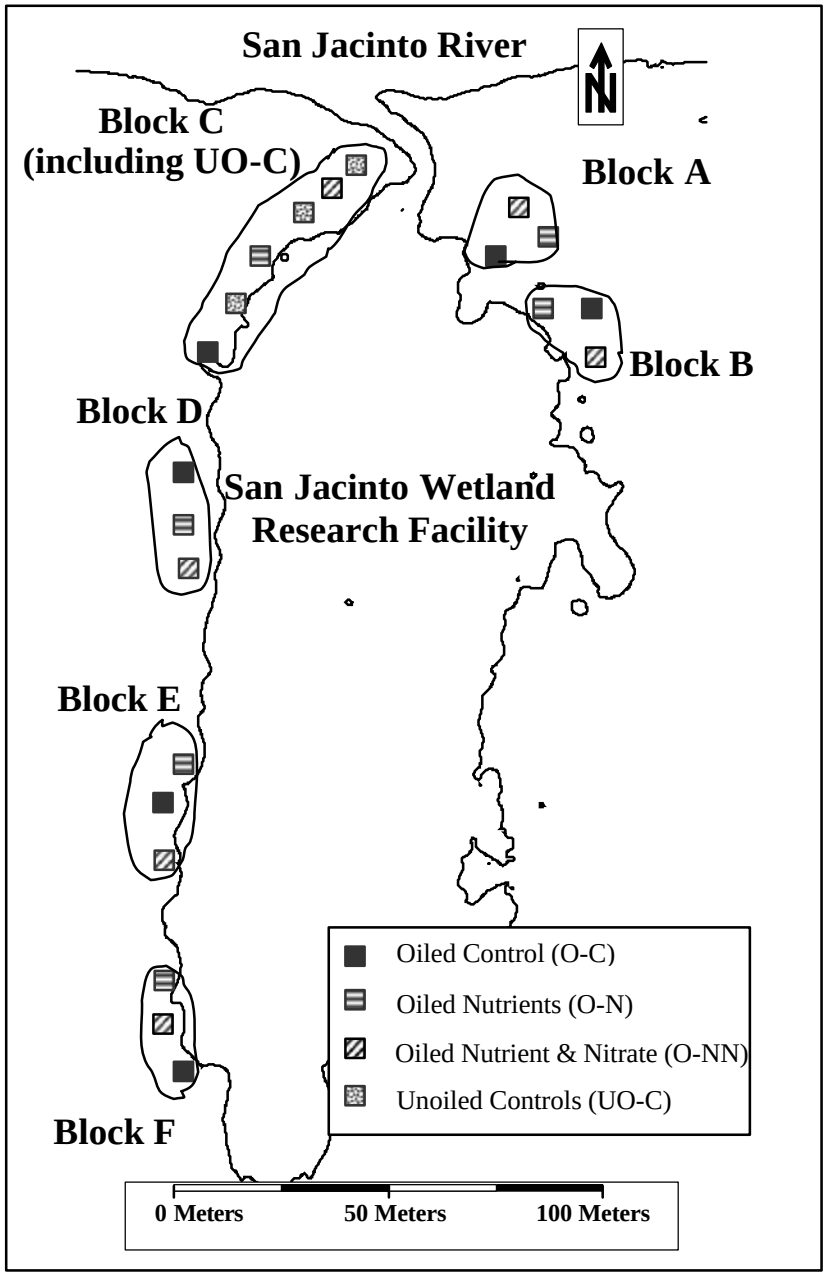

Figure 3.2 Diagram of the Phase II San Jacinto Wetland Research Facility. For Phase II equal amounts of oil (6 gallons) were evenly applied to the respective plots prior to the application of treatments.

Collection, Extraction, and Analysis of Field Samples

In both the Phase I and Phase II studies, three replicate samples were collected from each research plot with a 5-cm diameter stainless steel core sampler to an approximate depth of 10 cm. Once the sediment core samples were removed from the plots they were split into 0-5 cm and 5-10 cm depths and homogenized with their respective plot replicates. The samples were chilled on ice for transport to Texas A&M University in College Station, Texas. The samples remained refrigerated in the laboratory at 4 degrees Centigrade until they were processed for analysis. Only sediment extracts from the 0-5 cm splits were used for the TLC-FID study.

All laboratory preparations, extractions, and analyses of the samples followed the procedures detailed by Mills et al. (1999). A brief overview is as follows. When the samples arrived at the laboratory, sediments were again homogenized before an aliquot was prepared for the petroleum chemistry analyses. Each aliquot was frozen at –20 ^{o}C and then freeze-dried. The dried samples were extracted for 24 hours with DCM using standard Soxhlet procedures, and the extracts were reconstituted to a known volume. More details of the sample preparation procedures are presented in Mills et al. (1999). The details of the TLC-FID analysis are presented in Chapter II (Methods section) of this thesis.

Statistical Analysis

For each field study first-order non-linear regression models were generated. The models followed the procedure that Venosa et al. (1996) proposed when evaluating hopane normalized petroleum biodegradation in a sandy beach bioremediation study. The first order model for petroleum hydrocarbon biodegradation proposed the following biodegradation relationship over time:

$$C_i = C_O e^{-kt}. \qquad (3.1)$$

Where C*i* is the petroleum concentration at time t, Co is the concentration at time zero, and k is the first order biodegradation rate constant. The nonlinear regressions were completed using the Microsoft Excel software application. For Phase II, to compare and

evaluate the bioremediation treatments, the data were transformed into a linear form using the first-order biodegradation rate constants from the models. In its linear form a single factor ANOVA analysis, using a 95% confidence level, was performed to determine significant differences between treatment models.

RESULTS

Phase I Natural Attenuation Study

For the Phase I field study, these analyses and model results are shown in Figures 3.3 through 3.7. Each datum point represents the mean of the sample replicates, with error bars indicating one standard deviation. The curves represent the first-order regression models (eq-3.1) for each respective component fraction. The Co values represent the predicted initial fraction concentration at Day 0 for both Phase I and Phase II; the k value represents the model rate constant. The ($t_{1/2}$) values represent the predicted half-lives of the fraction concentrations. The correlation coefficients (R^2) represent a measure of the model fit; an R^2 of 1.0 indicates a perfect fit of the model to the data. An R^2 value greater than 0.65 was considered a "good fit" for the field data first order models.

Phase I Fraction Percentages

Figure 3.3 presents the temporal fraction percentage characteristics of the petroleum. The data show that on the first day of sampling, 44 days after the catastrophic spill and subsequent fire, the Arabian light crude oil can still be characterized as hydrocarbon- rich, made up of approximately 45% saturates, 25% aromatics, 25% resins, and 5% asphaltenes. By the final sampling event (Day 387), the residual oil was changed significantly and primarily consisted of polar compounds (19% saturates, 9% aromatics, 51% resins, and 21% asphaltene).

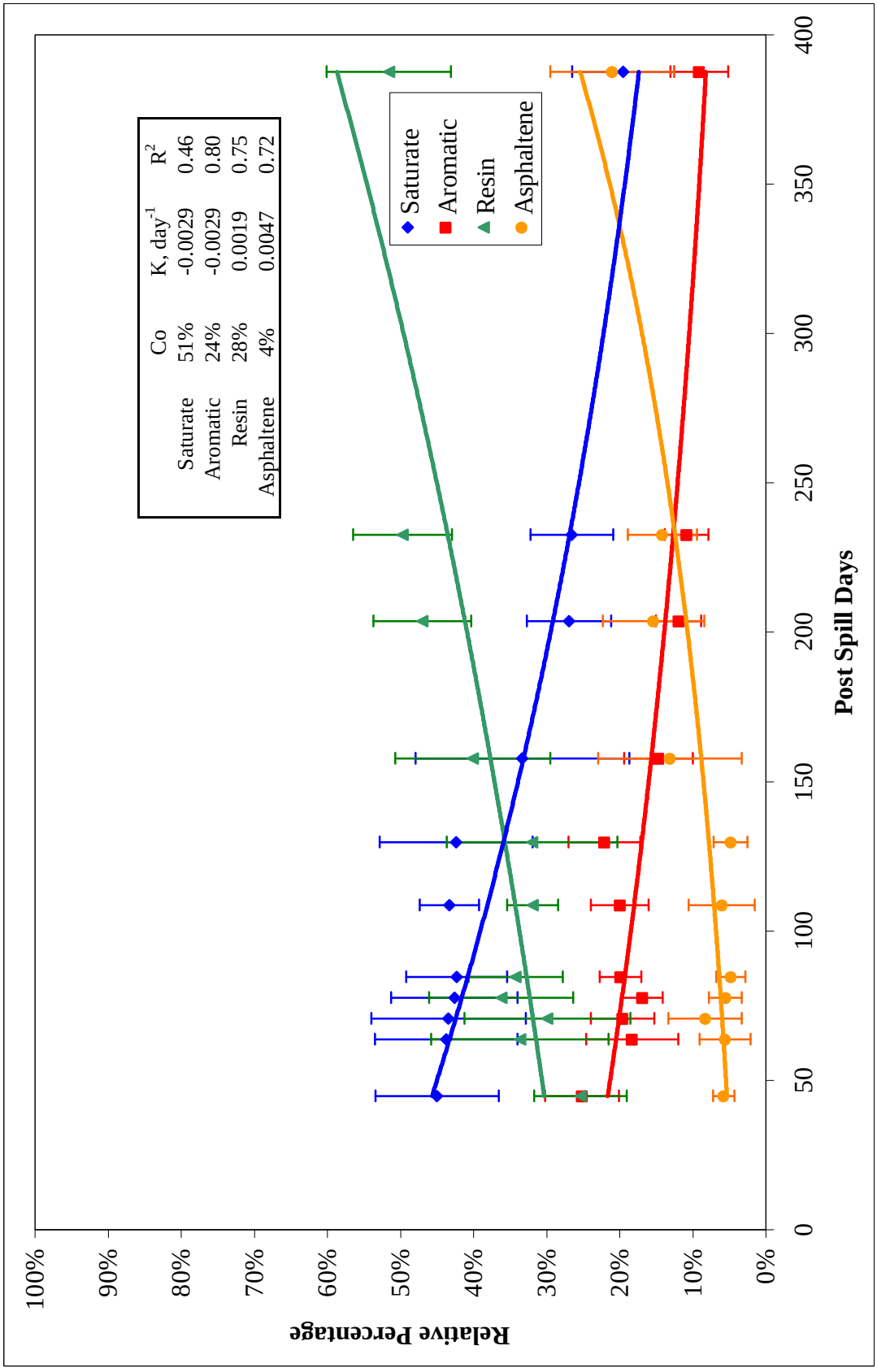

Figure 3.3 Phase I Fraction Percent TLC-FID Data. Shows the gross temporal variations of the saturate, aromatic, resin, and asphaltene fractions. The data points represent the respective average percent values and the lines represent the respective models. Error bars represent one standard deviation.

These temporal fraction changes indicate a 67% (average) reduction of the hydrocarbon fractions and a 68% (average) increase of the polar fractions. This observed pattern of simultaneous hydrocarbon fraction reduction and polar fraction increase is indicative of the biotic losses associated with the biodegradation of the more susceptible hydrocarbon compounds (Atlas and Bartha, 1972; Leahy and Colwell, 1990; Westlake et al., 1974).

The regression model results presented on Figure 3.3 show that the R^2 coefficient indicates a good fit, except for the saturate fraction. The reduction rate coefficients for the saturate and aromatic hydrocarbons were equal, suggesting no preferential degradation of either fraction. The significant polars enrichment observed in this data is not a direct representation of significant polars concentration enrichment; rather it is an effect of the 100 percent data analysis.

Phase I TEM Concentrations

The temporal TEM concentrations presented in Figure 3.4 demonstrate the high variability of the data. Although the regression model data suggest an overall temporal TEM concentration reduction, the R^2 coefficients indicates a poor fit of the model. The variability of the data is largely due to the spatial heterogeneity of the petroleum deposits after the catastrophic spill and the random sampling scheme subsequently employed. As this was a spill of opportunity it is difficult to quantify the indigenous TEM or background petroleum characteristics as this river area has been exposed to prior petroleum releases. Bowden (1986) indicated that high plant production can promote nitrogen-rich organic soils in tidal marshes, which may contribute to the sustained high TEM concentrations through the monitoring period.

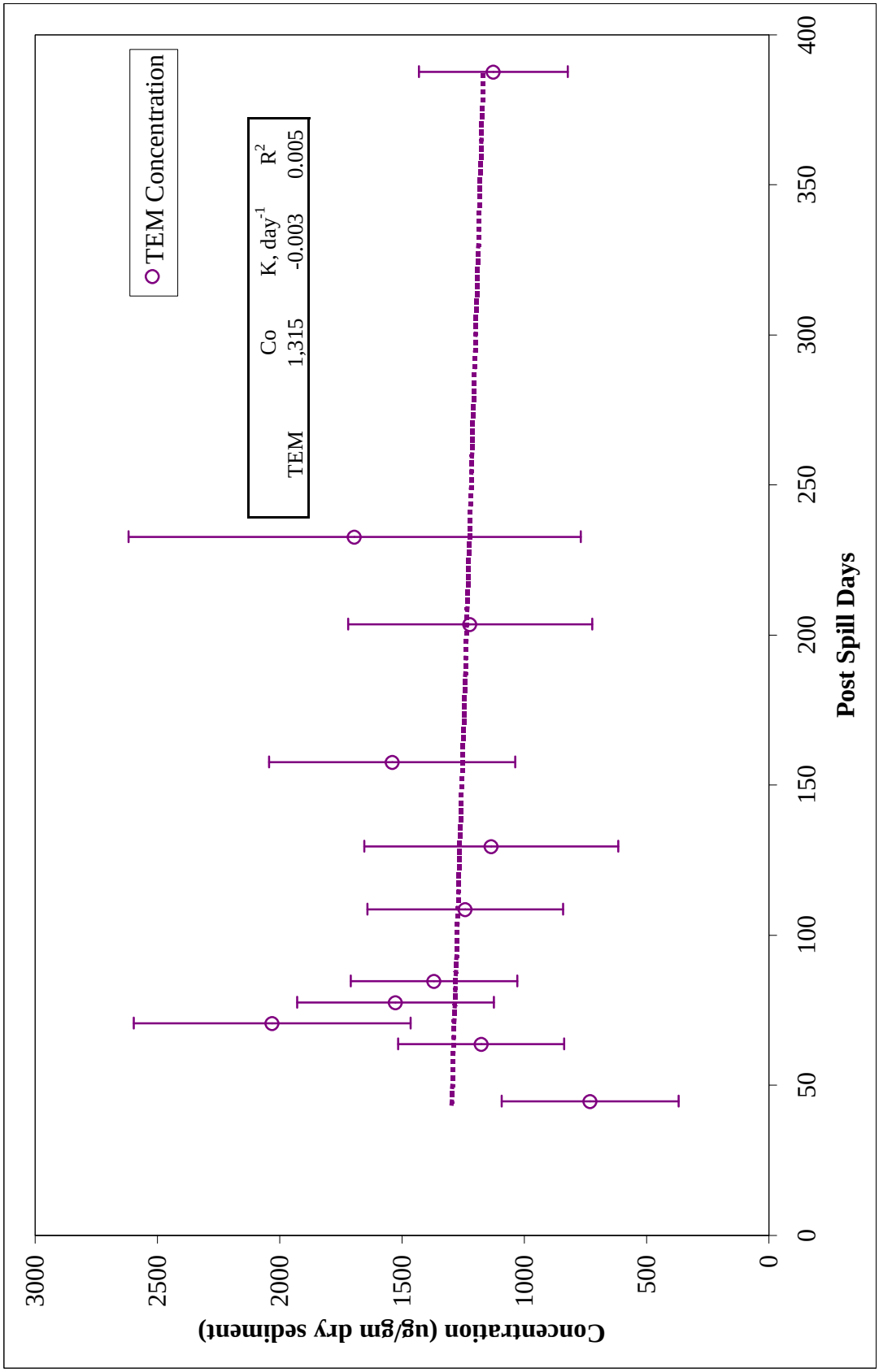

Figure 3.4 Phase I TEM Data. Shows the gross temporal variations of the TEM concentrations. The data points represent the respective average values and the line represents the respective model. Error bars represent one standard deviation.

Phase I TLC-FID Fraction Concentrations

The fraction concentrations results presented in Figure 3.5 quantify the total (biotic and abiotic) temporal changes of the petroleum. The data show an average 67% reduction of the hydrocarbon concentrations and an average 74% increase of the polar concentrations. The modeled rate constants for all the fractions are comparable to those determined for the fraction percent data (Figure 3.3). Despite the high TEM variability, ANOVA analysis of the Day 44 and the Day 387 fraction concentrations did show a significant difference for each component fraction. The R^2 coefficients indicate weak correlations between the data and the models, largely due to the variable TEM data.

The saturate and aromatic fraction concentrations were reduced by 69% and 70%, respectively. The half-lives predicted from the regression models were approximately 231 days for the saturate fraction and 224 days for the aromatic fraction. The rates of reduction, the rate constants, and the half-lives determined for the two hydrocarbon fractions were similar to each other, supporting the conclusion suggested by the fraction percent results: during the monitoring period there was no preferential degradation of either hydrocarbon fraction.

The polars data indicate a 48% and 81% concentration increase of the resin and asphaltene fractions, respectively. These are significant increases when compared to the level of hydrocarbon concentration reductions. The enrichment rate constant for the resin fraction was almost half the rate of the hydrocarbon reductions while the asphaltene rate constant was almost 1.5 times greater than that of the hydrocarbon reduction rates.

While it is not clear what the observed polar trends indicate, other conclusions can be confirmed by the fraction concentration results. By the time the study started, there was no preferential degradation of either hydrocarbon fraction. The reduction of the hydrocarbon fraction and the increase of the polars fraction suggest that the major process of hydrocarbon removal was biotic activity.

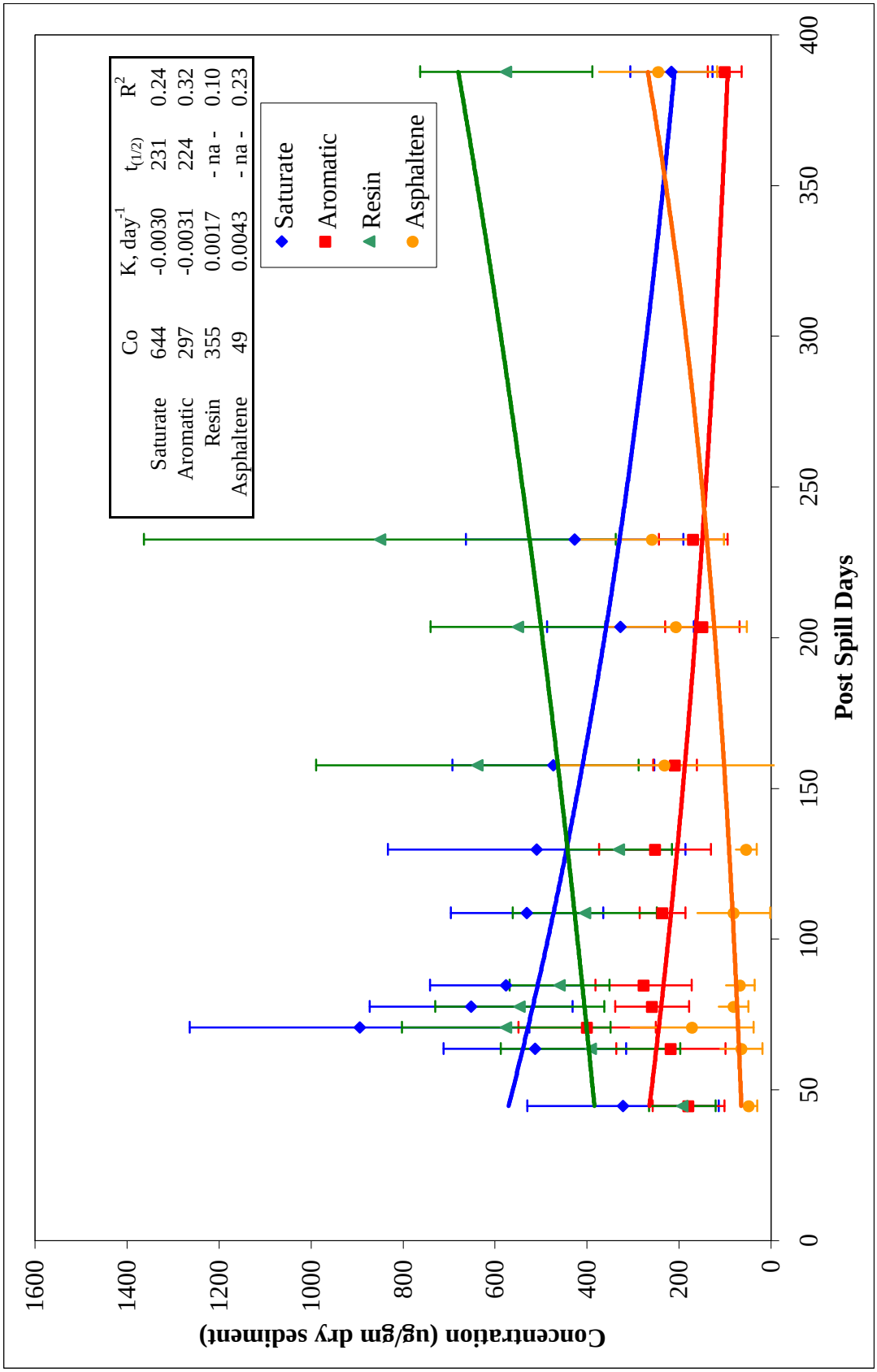

Figure 3.5 Phase I Fraction Concentration TLC-FID Data. Shows the gross temporal variations of the saturate, aromatic, resin, and asphaltene fractions. The data points represent the respective average values and the lines represent the respective models. Error bars represent one standard deviation.

Fraction-specific abiotic or biotic activity cannot be differentiated from this data analysis. However, it is hypothesized that gross abiotic activity will affect all four fraction concentrations with the same rate of mass removal. Therefore, the effects of gross abiotic activity would be more evident in this analysis, where all four fraction concentrations would demonstrate equal rates of concentration reduction. Gross abiotic reductions were not the major process of removal as the fraction concentration results did not demonstrate an equal concentration reduction of all four fractions equally. Where this hypothesis fails is the occurrence of fraction-specific abiotic reductions. For the purposes of this study it was assumed that fraction-specific abiotic reductions were negligible.

Phase I Hopane-Normalized Fraction Concentrations

The GC-MS analysis by Mills et al. (2003) concluded that normalizing the data to hopane identified significant biodegradation (90% reductions) of specific saturate and aromatic hydrocarbon analytes. Similarly, a hopane normalization strategy was performed with the TLC-FID data.

Figure 3.6 presents the hopane-normalized concentration data for all four fractions. The data indicate an average 79% reduction of the hydrocarbon concentrations and an average 60% increase of the polar concentrations. The modeled rate constants for all the fractions are slightly higher, but comparable to those determined for the fraction concentration data (Figure 3.2). ANOVA analysis of the initial (Day 44) and final (Day 387) concentrations revealed significant differences for all four fractions except the resin fraction. The R^2 coefficients indicate weak correlations between the data and the models.

The saturate and aromatic fraction concentrations were reduced by 77% and 80% respectively, with predicted half lives of 182 days and 169 days, respectively. The hopane normalized predicted half-lives are shorter than the non-normalized half-lives. The rates of reduction, the rate constants, and the half-lives determined for the two

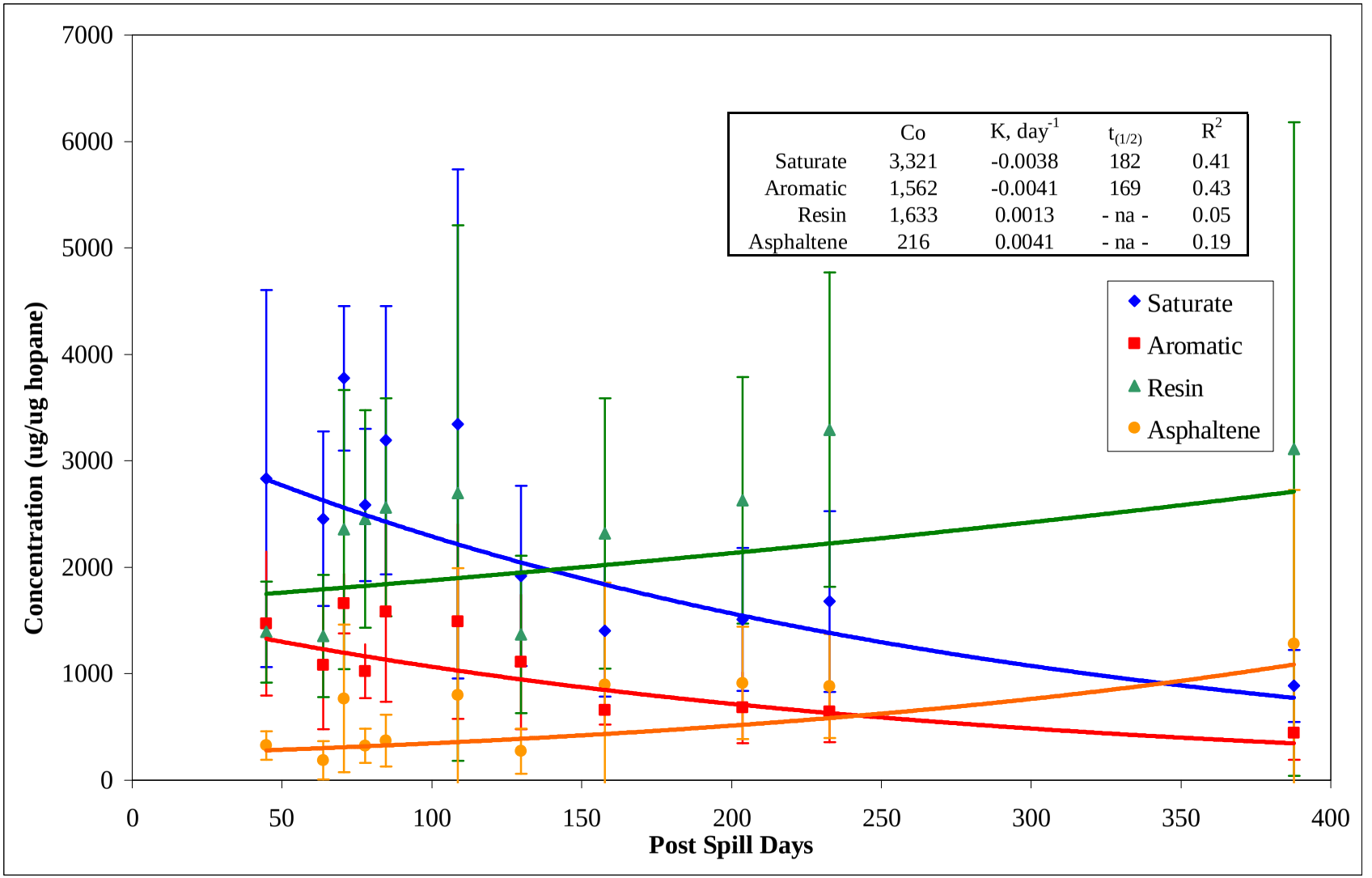

Figure 3.6 Phase I Hopane Normalized Fraction Concentration TLC-FID Data. Shows the gross temporal variations of the saturate, aromatic, resin, and asphaltene fractions. The data points represent the respective average values and the lines represent the respective models. Error bars represent one standard deviation.

hydrocarbon fractions were similar to each other, again supporting the conclusion that there was no preferential degradation of either hydrocarbon fraction during the monitoring period.

The polars results indicated positive enrichment rates comparable to the non-normalized polars data. The polars experienced a 48% and 81% concentration increase for the resin and asphaltene fractions, respectively. Assuming that hopane normalization eliminates the abiotic reduction effects, the hopane-normalized data for the polar fractions indicate that there is a biological enrichment of these compounds.

It was assumed that normalizing the data with hopane would account for abiotic activity. Based on this assumption it was hypothesized that decreased degradation rates, increased half-lives, and increased R^2 coefficients would be observed in the hopane normalized data. The hypothesis is not supported as only higher R^2 coefficients were observed but, temporal rates were higher and half-lives shorter than the non-normalized results.

Phase I Asphaltene-Normalized Fraction Concentrations

Hopane normalization to identify biotic and abiotic degradation is based on the assumption that hopane is not biodegradable in the timeframe of the experiment. Analogously, the asphaltenes represents the most recalcitrant fraction of petroleum compounds. So, fraction concentration data were normalized with the asphaltene fraction and the results are presented in Figure 3.7. The R^2 coefficients indicate weak correlations between the data and the models.

ANOVA analysis of the beginning (Day 44) and final (Day 387) concentrations revealed a significant difference for the hydrocarbons and resin concentrations. The data presented in Figure 3.7 show similar reductions in the two hydrocarbon concentrations (94% each) and a 65% reduction of the resin concentration. The predicted half lives for the saturate and aromatic fractions were 95 and 94 days, respectively. The biodegradation rate constants for the hydrocarbons were similar to each other and almost 2.5 times higher than the non-normalized concentration rates (Figure 3.5).

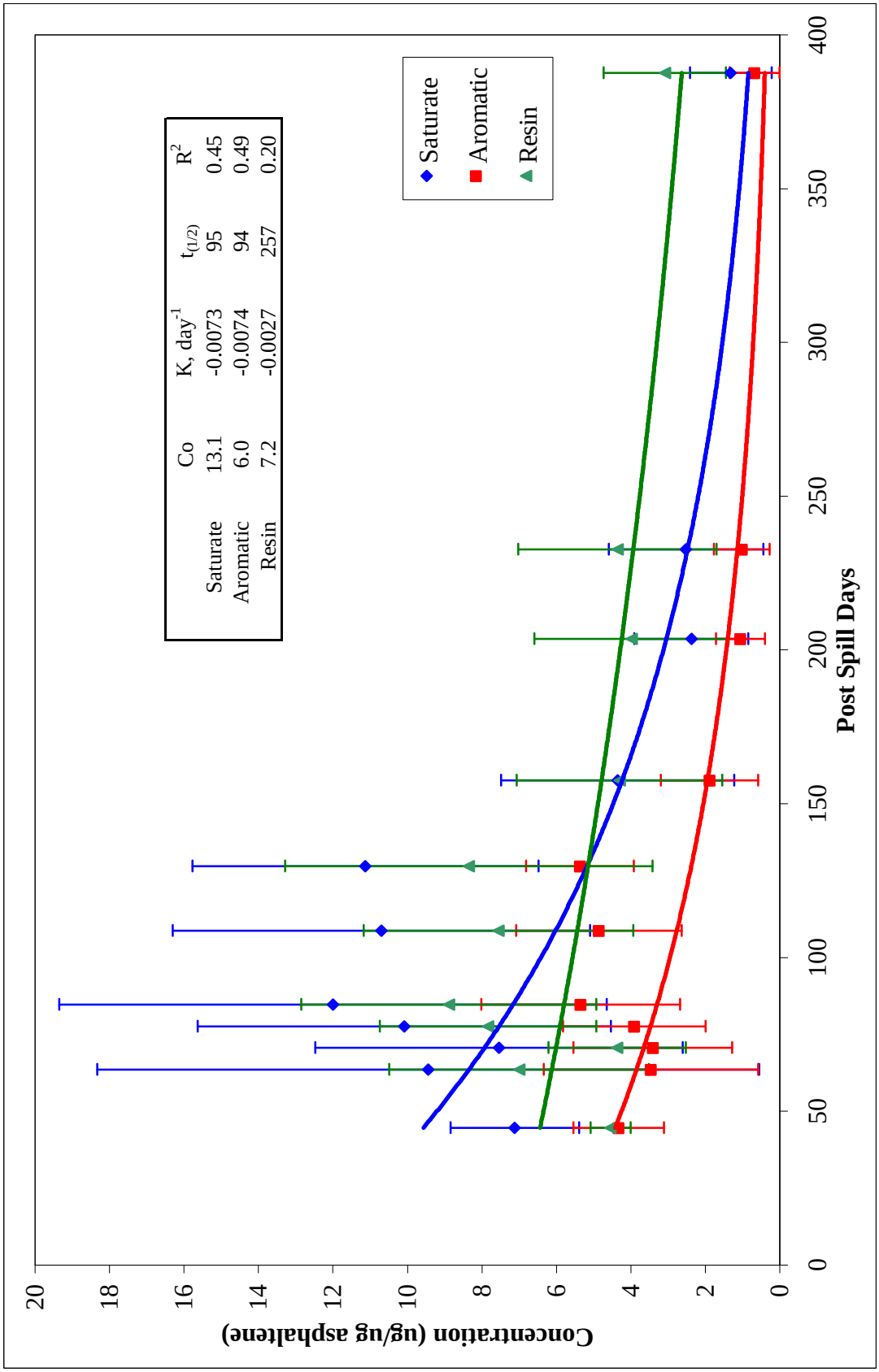

Figure 3.7 Phase I Asphaltene Normalized Fraction Concentration TLC-FID Data. Shows the gross temporal variations of the saturate, aromatic, and resin fractions. The data points represent the respective average values and the lines represent the respective models. Error bars represent one standard deviation.

The rate constants and the half-lives determined for the two hydrocarbon fractions were almost equal, supporting the conclusion suggested by the non-normalized results; i.e., there was no preferential degradation of either hydrocarbon fraction.

Unlike the hopane-normalized models of the polar fraction, the asphaltene-normalized data indicate the reduction of the resin fraction. This is an erroneous observation due to normalizing the data with the non-conservative asphaltene compound. Rather this trend indicates that the resin concentration varied at a slower rate than the asphaltene concentration.

It was hypothesized that decreased degradation rates, increased $t_{1/2}$, and increased R^2 coefficients would be observed in the asphaltene normalized data. The hypothesis is not supported as only higher R^2 coefficients were observed but, temporal rates were higher and half-lives shorter than the non-normalized results.

The model of asphaltene-normalized data improves the hydrocarbon R^2 coefficients, suggesting a better model fit to the data. However, from the TLC-FID non-normalized data it is evident that the asphaltene fraction does not meet the conditions of a conservative biomarker like hopane. Therefore, the conclusions of significant biodegradation cannot be supported by this method of analysis.

Phase II Bioremediation Study

The Phase II data are presented in a format that allows the comparison of the different treatments with respect to each petroleum fraction. Each figure presents a different petroleum fraction (saturate, aromatic, resin, asphaltene) for each of the three oil treatments, oiled control (O-C), oiled nutrient (O-N), and oiled nutrient plus alternate electron acceptor (nitrate) (O-NN). A statistical analysis of the models was performed to determine significant differences between the amended treatments and the oiled control as an indication of relative treatment performance. In addition, data for unoiled control (UO-C) plots are also presented on the figures. For the Phase II field study they are presented in Figures 3.8 through 3.25.

Each datum point represents the mean of the sample replicates, with error bars

indicating one standard deviation. The curves represent the first-order regression models (eq-3.1) for each respective component fraction. The Co values represent the predicted initial fraction concentration at Day 0 for both Phase I and Phase II; the k value represents the model rate constants. The $t_{1/2}$ values represent the predicted half-lives of the fraction concentrations. The correlation coefficients (R^2) represent a measure of the model fit; an R^2 of 1.0 indicates a perfect fit of the model to the data. An R^2 value greater than 0.65 was considered a "good fit" for the field data first order models.

Phase II Fraction Percents

The TLC-FID fraction percent data for all four petroleum fractions is presented in Figures 3.8, 3.9, 3.10, and 3.11. The data indicates that on Day 0 (four days after petroleum application), the Arabian light crude oil can be characterized as 44% saturates, 32% aromatics, 16% resins, and 7% asphaltenes. By experimental end (Day 140), the residual oil had changed significantly and was made up of mostly polar components (10% saturates, 19% aromatics, 48% resins, and 23% asphaltenes).

In general, these data shows an average 61% reduction of the hydrocarbon fractions and an average 68% increase of the polar fractions, irrespective of oil treatment. This trend represents the systematic reduction of the hydrocarbon fractions, allowing the recalcitrant polars to make up a greater percentage of the total sample mass. As with the Phase I analysis, this increasing polar trend is more a reflection of the 100 percent data analysis than an indication of increasing polar concentrations. The R^2 results indicate a good fit for the saturate and resin fractions (Figures 3.8, 3.10), though not the aromatic and asphaltene fractions. For all treatments the rate constants for the saturates were 2 to 2.7 times greater than those of the aromatics. Comparing the beginning and end fraction characteristics, the saturates reduction averaged 76% and aromatics reduction averaged 46%. Over time, the polars increased 62% and 75% for the resin and asphaltene fractions, respectively.

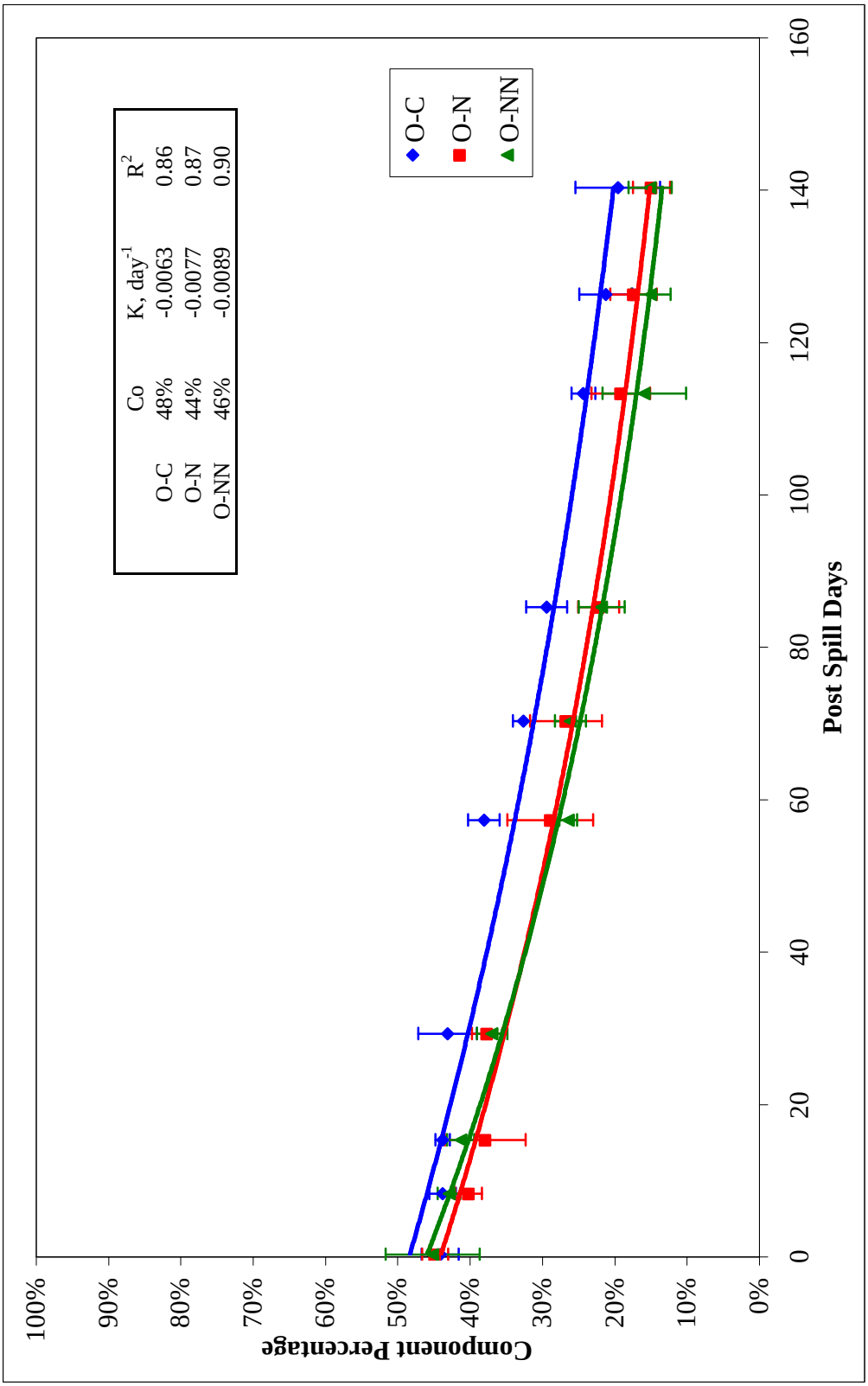

Figure 3.8 Phase II Fraction Percent TLC-FID Saturate Data. Shows the gross temporal variation of the saturate fractions for the three treatments and unoiled control; where O-C is oiled control, O-N is oiled with nutrients, and O-NN is oiled with nutrients plus nitrate as electron acceptor. Error bars represent one standard deviation.

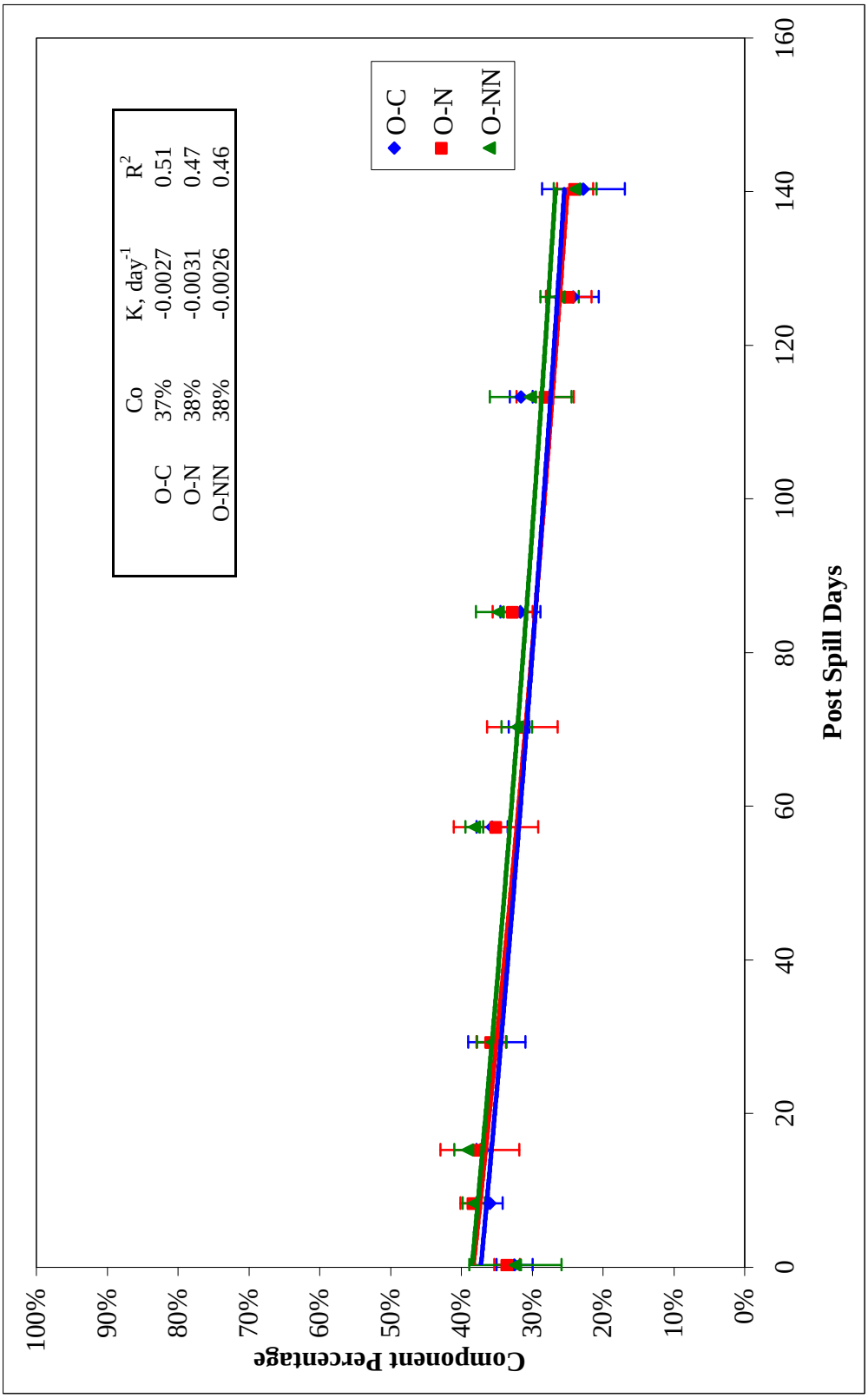

Figure 3.9 Phase II Fraction Percent TLC-FID Aromatic Data. Shows the gross temporal variation of the aromatic fractions for the three treatments and unoiled control; where O-C is oiled control, O-N is oiled with nutrients, and O-NN is oiled with nutrients plus nitrate as electron acceptor. Error bars represent one standard deviation.

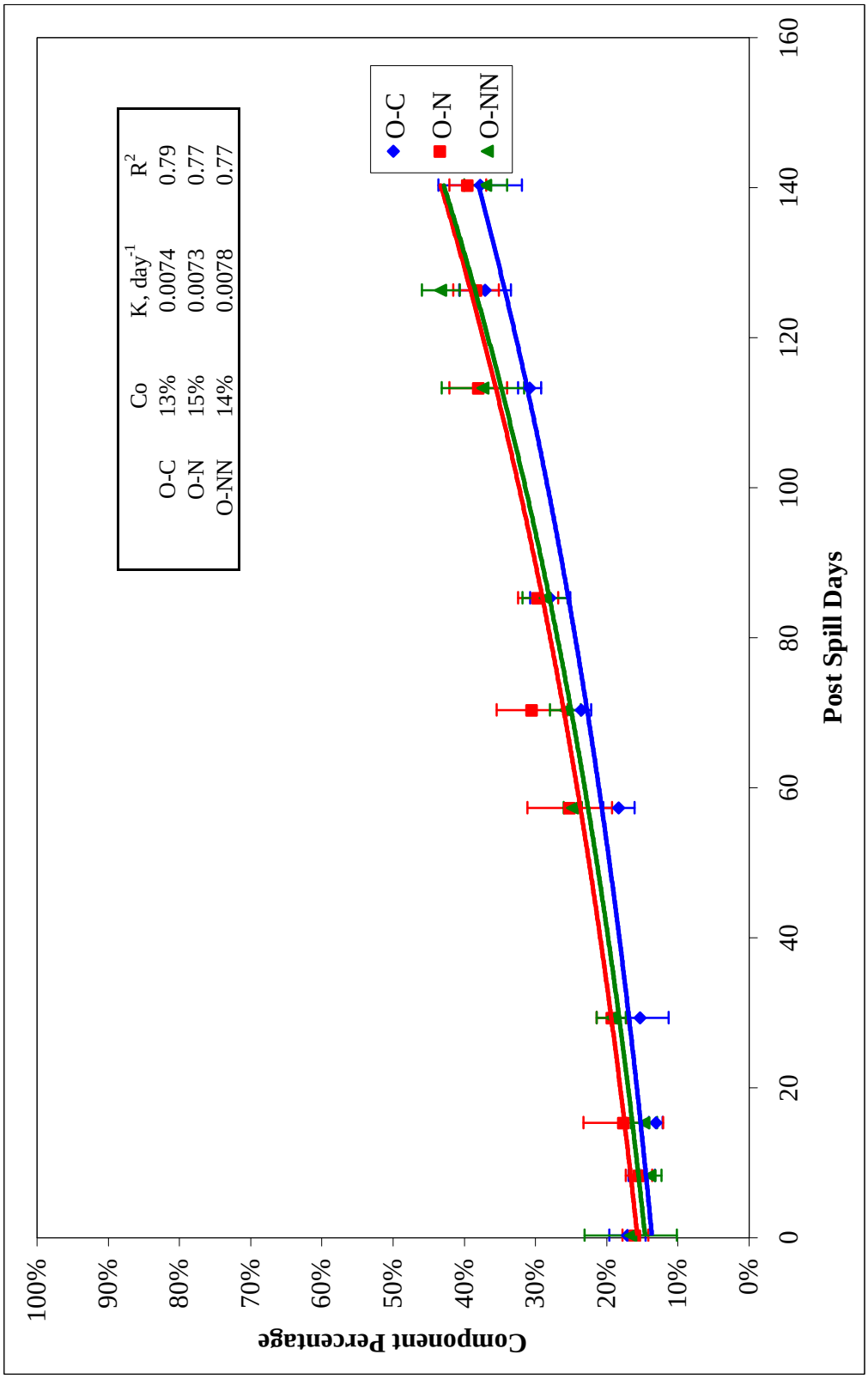

Figure 3.10 Phase II Fraction Percent TLC-FID Resin Data. Shows the gross temporal variation of the resin fractions for the three treatments and unoiled control; where O-C is oiled control, O-N is oiled with nutrients, and O-NN is oiled with nutrients plus nitrate as electron acceptor. Error bars represent one standard deviation.

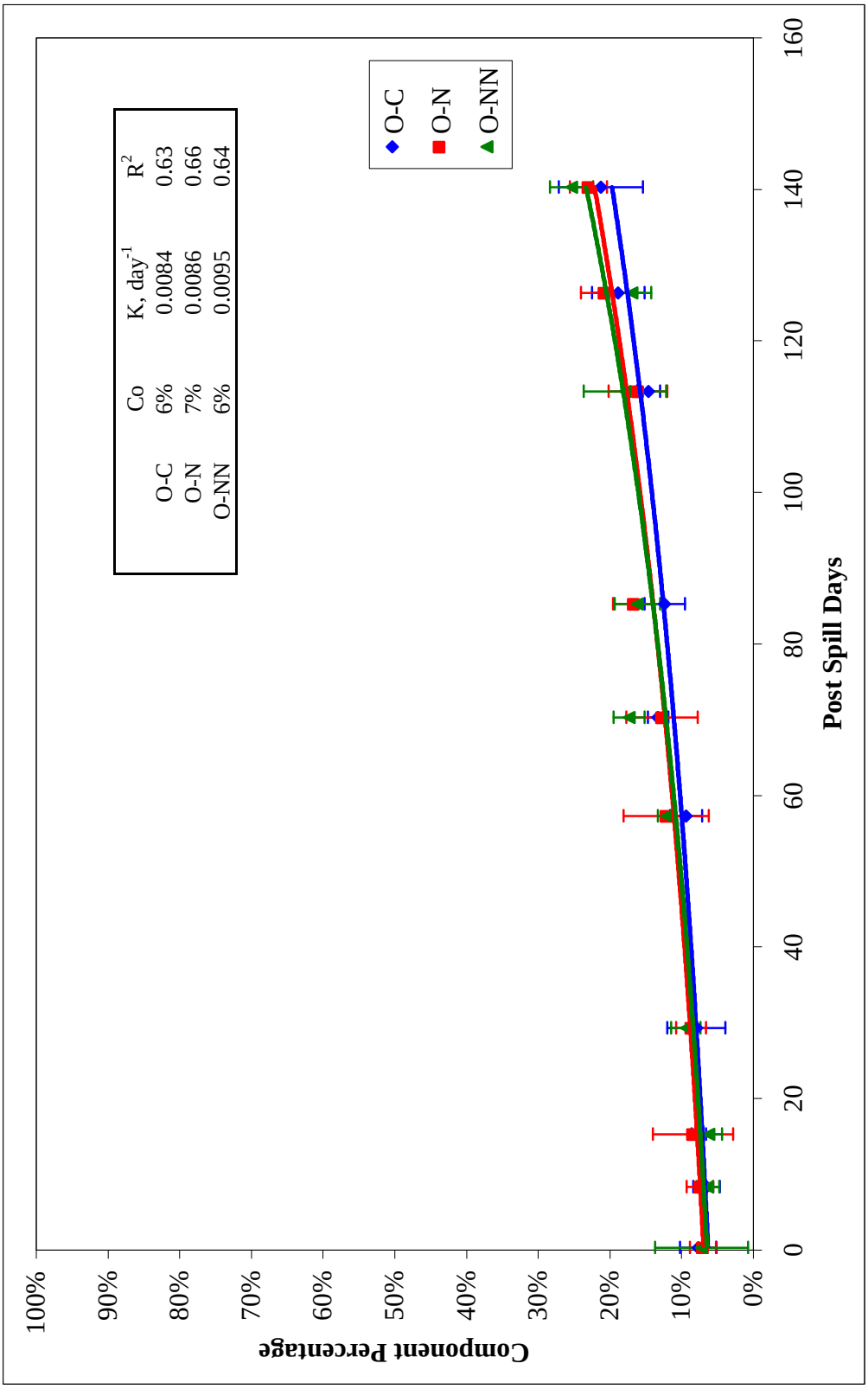

Figure 3.11 Phase II Fraction Percent TLC-FID Asphaltene Data. Shows the gross temporal variation of the asphaltene fractions for the three treatments and unoiled control; where O-C is oiled control, O-N is oiled with nutrients, and O-NN is oiled with nutrients plus nitrate as electron acceptor. Error bars represent one standard deviation.

The statistical comparison of the models indicated that there was a significant difference between the saturate fractions of both amended treatments (O-N and O-NN) as compared to the oiled control (O-C). There were no significant differences between the amended treatments and the control for the three other fractions. These results indicate that the amended treatments were more effective than the oiled control in reducing the susceptible saturate hydrocarbons, but were ineffective in enhancing the biodegradation of the aromatic and polar fractions.

An interesting detail revealed in the comparison of the models is the common rate coefficient determined for the degradation of the aromatic fraction by all three treatments. This trend suggests that the amendments had no greater or lesser effect on the degradation of the aromatic compounds. The GC-MS analysis of these samples by Mills et al. (2004) concluded that the aromatic target analyte degradation rates were not significantly different between the treatments. Similar in-vitro studies have demonstrated that while aromatic compounds were degraded, nitrogen and phosphorus amendments had no significant effect on the degradation rates of the aromatic fraction (Atlas and Bartha, 1972; Fedorak and Westlake, 1981).

Phase II TEM Concentrations

The Phase II TEM concentrations are presented on Figure 3.12 for all treatments as well as the unoiled control. By the end of the study TEM concentrations were reduced approximately 60%, which represents losses due to biotic activity and abiotic activity. ANOVA analysis of the TEM data indicated a significant difference between Day 0 and Day 140 concentrations for only the O-C and O-NN treatments. The R^2 coefficients indicate a poor fit of the models to the data.

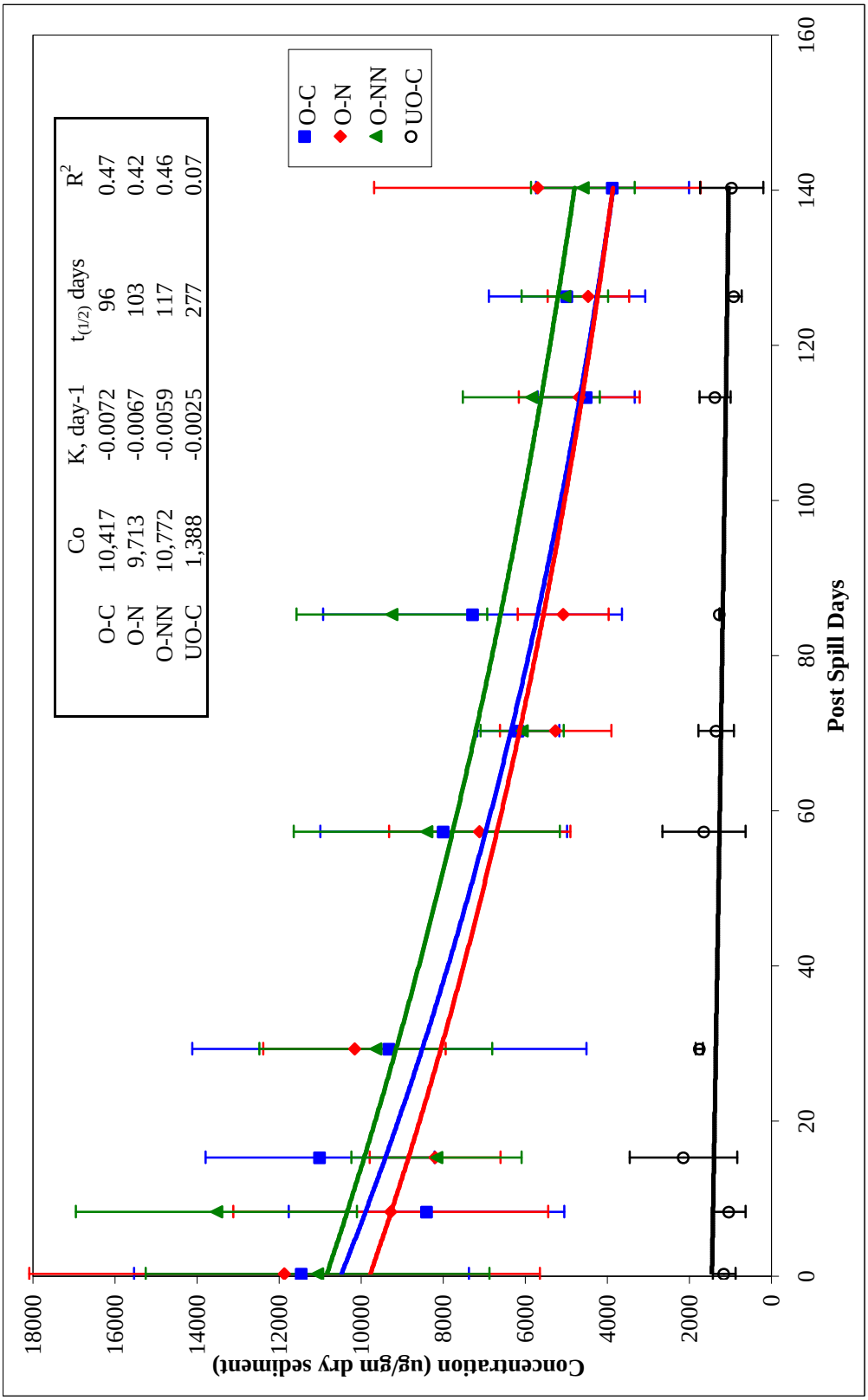

Figure 3.12 Phase II TEM Data. Shows the gross temporal variation of the TEM data for the three treatments and unoiled control; where O-C is oiled control, O-N is oiled with nutrients, O-NN is oiled with nutrients plus nitrate as electron acceptor, and UN-C is unoiled control. Error bars represent one standard deviation.

Phase II TLC-FID Fraction Concentrations

The fraction concentration data and modeling results are presented in Figures 3.13, 3.14, 3.15, and 3.16 for the four fractions. ANOVA analysis of the saturate fraction concentrations revealed a significant difference between Day 0 and Day 140 concentrations for all three remediation treatments (Figure 3.13) with R^2 values indicating a good fit. For all three treatments, there was an 89% - 92% temporal reduction, and similar rate constants. Although only the O-N amended treatment was statistically different than the oiled control, all three treatments had comparable half-lives.

ANOVA analysis of the aromatic fractions also revealed a significant difference between Day 0 and Day 140 concentrations for all treatments (Figure 3.14). For all treatments, there was a 76% - 80% temporal reduction of the aromatic concentrations and similar rate constants, though slightly lower than those of the saturates. There were no statistical differences determined between the treatments and control, suggesting no improved degradation performance by any treatment. The predicted half-lives were similar, though the R^2 values did not suggest particularly good fits of the models to the data.

For both the resin and asphaltene fractions, there were no significant differences between Day 0 and Day 140 concentrations for any of the treatments (Figures 3.15 and 3.16). This result is contrary to the Phase I data where significant differences were determined. Although not statistically significant, an increase in both of the polar fractions was observed for the O-NN treatment as the study progressed.

The regression models for the resin fraction indicated very low degradation rates for the O-C and O-N treatments. However, a positive, or enrichment rate, was observed for the O-NN treatment, which was three times greater in absolute value, compared to the other two treatments. The asphaltenes rate constants were positive enrichment rates, with the O-NN rate twice that of the other two treatments. Statistical differences were not determined for either polar fraction between the amended treatments and the control. The R^2 value for both polar fractions indicated a very poor fit of the model to the data.

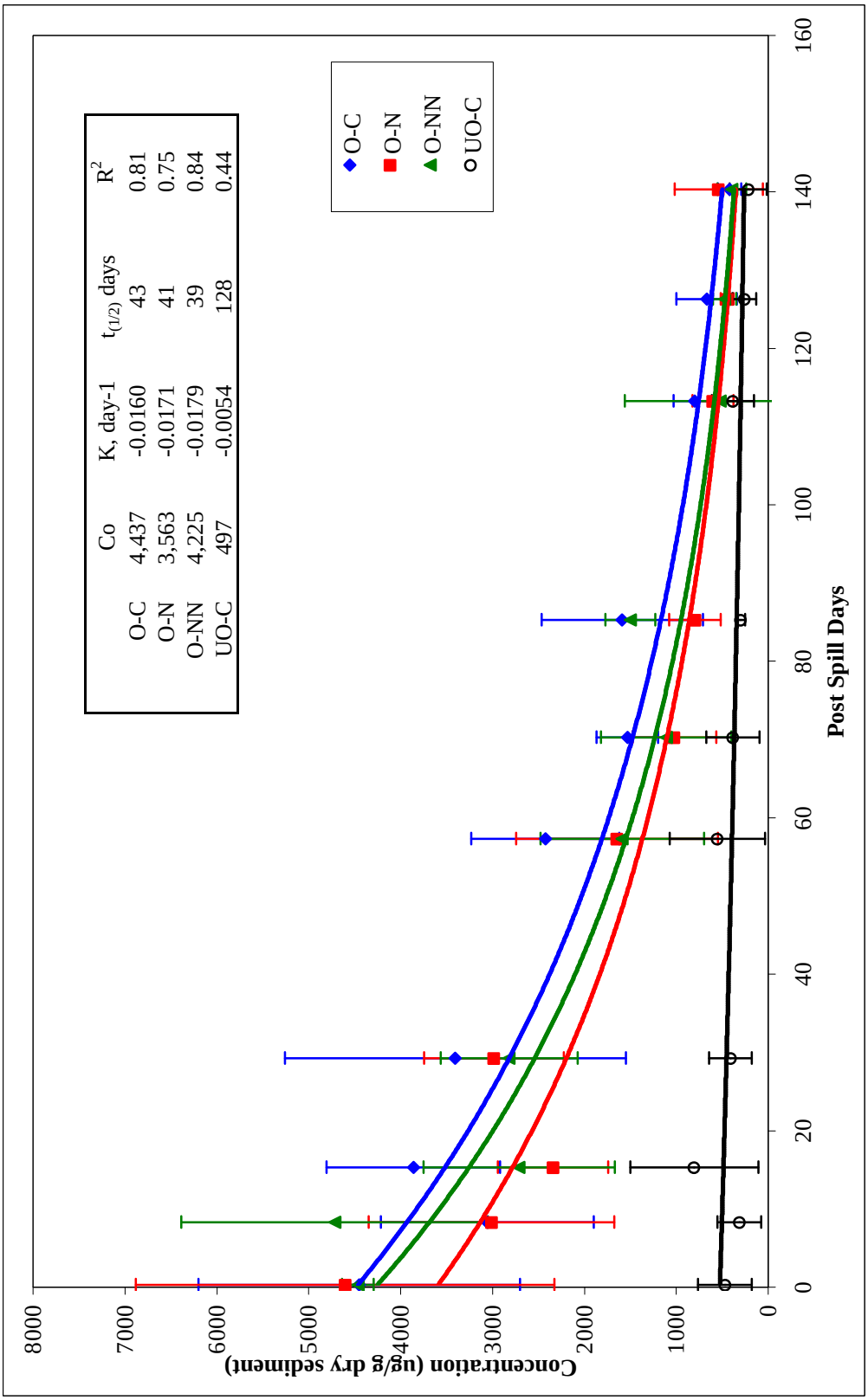

Figure 3.13 Phase II Fraction Concentration TLC-FID Saturate Data. Shows the gross temporal variation of the saturate fractions for the three treatments and unoiled control; where O-C is oiled control, O-N is oiled with nutrients, O-NN is oiled with nutrients plus nitrate as electron acceptor, and UN-C is unoiled control. Error bars represent one standard deviation.

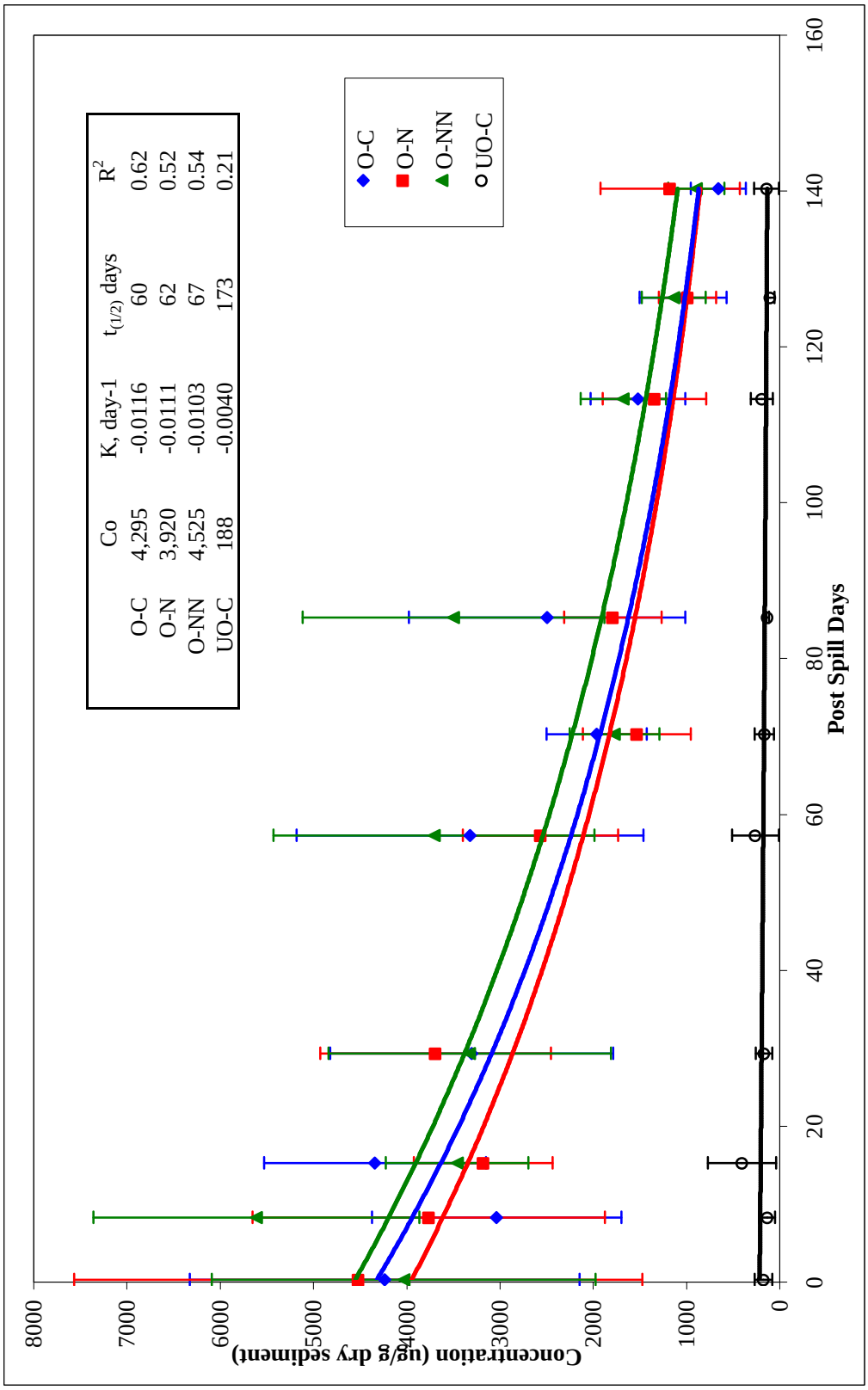

Figure 3.14 Phase II Fraction Concentration TLC-FID Aromatic Data. Shows the gross temporal variation of the aromatic fractions for the three treatments and unoiled control; where O-C is oiled control, O-N is oiled with nutrients, O-NN is oiled with nutrients plus nitrate as electron acceptor, and UN-C is unoiled control. Error bars represent one standard deviation.

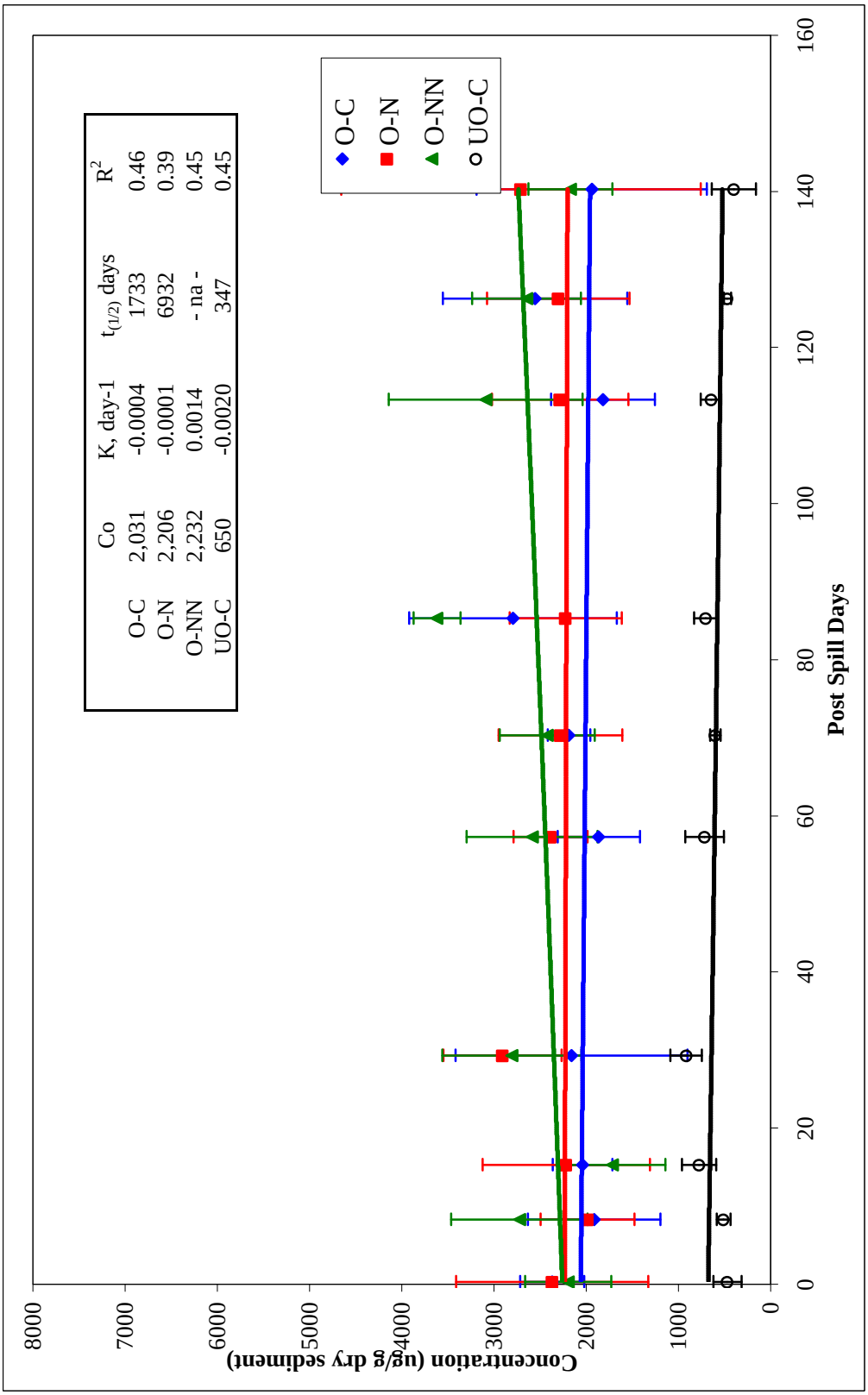

Figure 3.15 Phase II Fraction Concentration TLC-FID Resin Data. Shows the gross temporal variation of the resin fractions for the three treatments and unoiled control; where O-C is oiled control, O-N is oiled with nutrients, O-NN is oiled with nutrients plus nitrate as electron acceptor, and UN-C is unoiled control. Error bars represent one standard deviation.

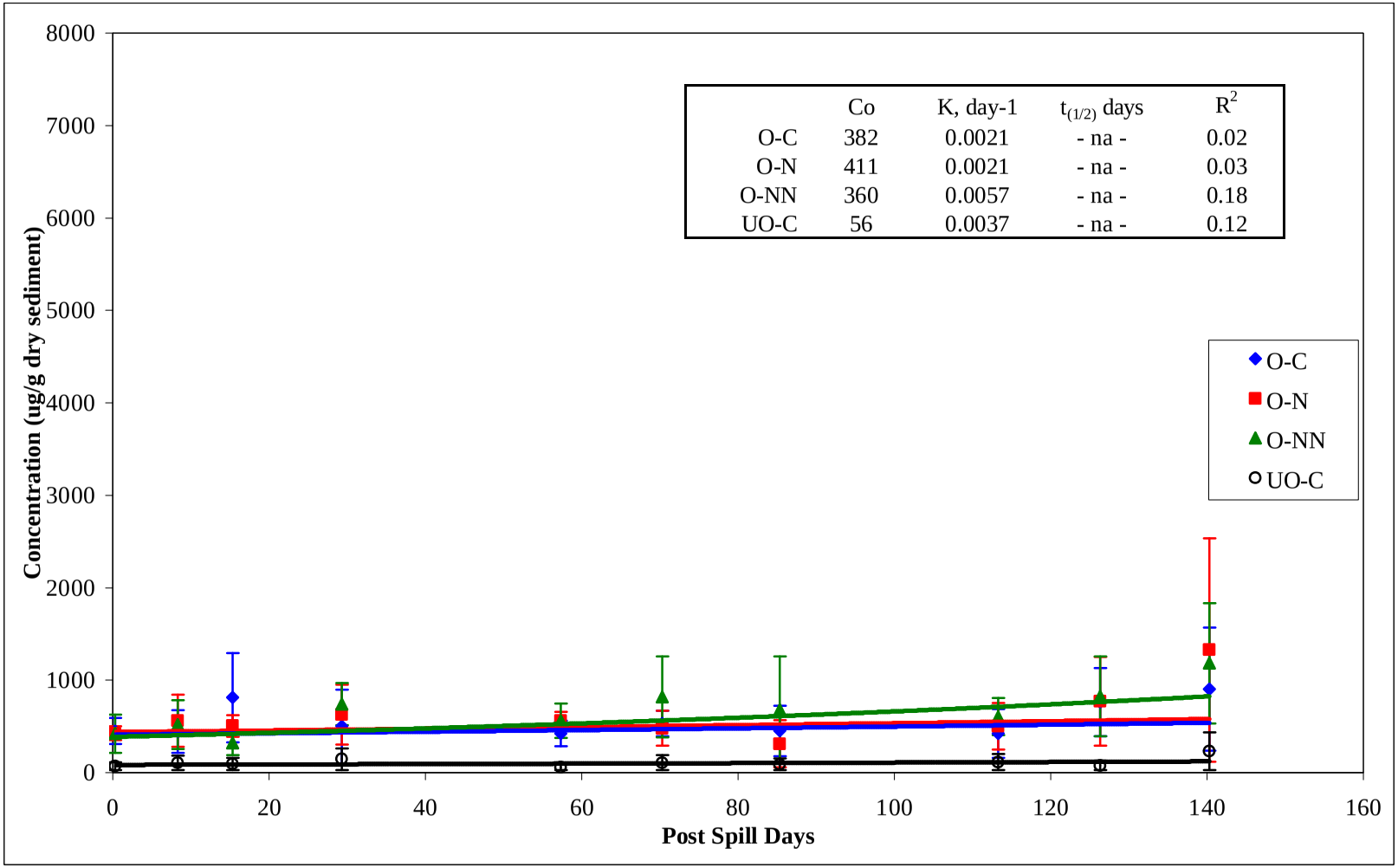

Figure 3.16 Phase II Fraction Concentration TLC-FID Asphaltene Data. Shows the gross temporal variation of the asphaltene fractions for the three treatments and unoiled control; where O-C is oiled control, O-N is oiled with nutrients, O-NN is oiled with nutrients plus nitrate as electron acceptor, and UN-C is unoiled control. Error bars represent one standard deviation.

The qualitative comparison of the data over the experimental timeframe shows that saturate hydrocarbons were almost completely degraded to background levels, but the aromatic, resin, and asphaltene fractions did not exhibit the same trend. These trends were expected as many studies have demonstrated that complex PAHs and polar compounds are recalcitrant compounds in the environment (Prince, 1993). The results indicate that the O-N treatment was more effective degrading saturate hydrocarbons but no more effective than the other treatments for the aromatics. The results also suggest that the O-NN amendment had an effect on the enrichment of the resin fraction, which may be an indication of an alternate degradation pathway. However, the poor R^2 value of the polars model suggests that these conclusions are not reliable.

Phase II Hopane Normalized Fraction Concentrations

As concluded in Mills et al. (2004), the hopane-normalized GC-MS analysis indicated significant differences in biodegradation rate constants for "total target saturate hydrocarbon" analytes for both amended treatments as compared to oiled control. For the "total target aromatic analytes" the GC-MS analysis showed a significant difference in biodegradation rate constants for the O-N amendment (though not the O-NN amendment) when compared to the oiled control. The GC-MS results for this research are fully discussed elsewhere (Mills et al., 2004).

The TLC-FID hopane-normalized fraction concentrations for the three treatments are presented in Figures 3.17 - 3.20 for the four petroleum fractions. For the saturate fraction, there were significant differences between Day 0 and Day 140 for all three treatments. The R^2 coefficients for the saturate fractions indicate a good fit. For all three treatments there was an average 83% to 87% temporal reduction of the saturate fractions. The reduction rate constants were similar for the O-C and O-N treatment, while the O-NN rate was slightly higher. The statistical comparison of the treatments indicated that both amended treatments were significantly different from the O-C.

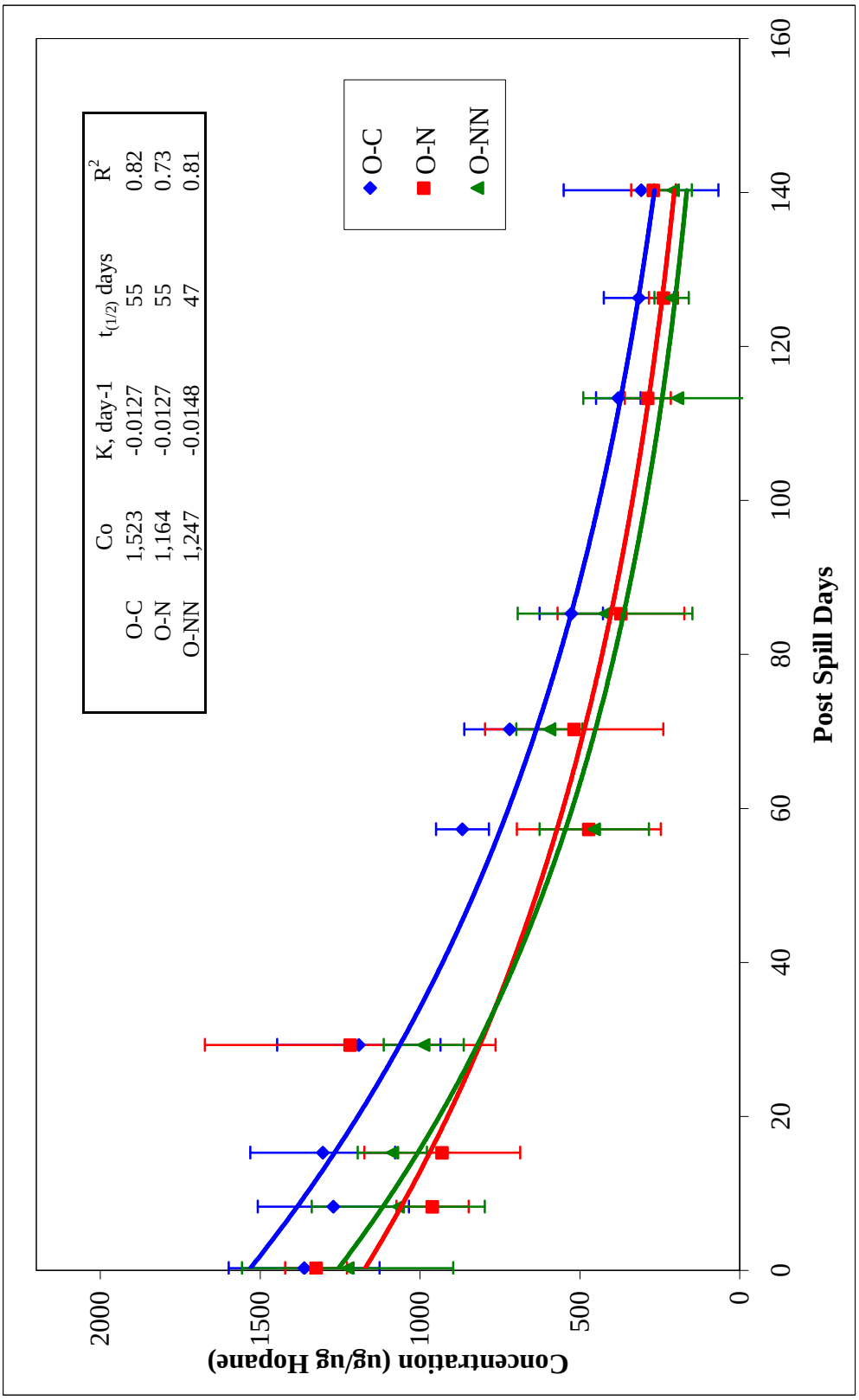

Figure 3.17 Phase II Hopane Normalized TLC-FID Saturate Data. Shows the gross temporal variation of the saturate fractions for the three treatments and unoiled control; where O-C is oiled control, O-N is oiled with nutrients, and O-NN is oiled with nutrients plus nitrate as electron acceptor. Error bars represent one standard deviation.

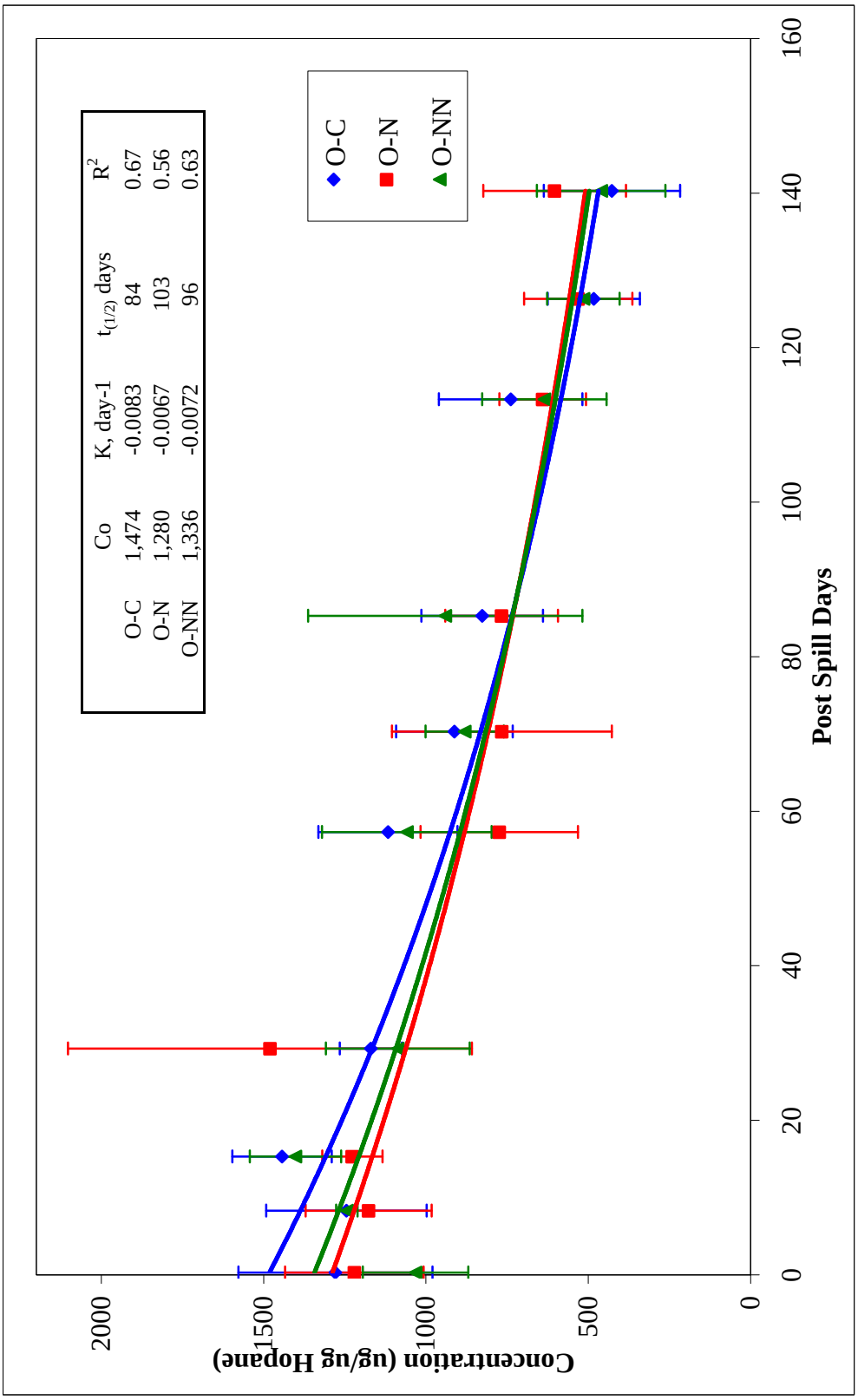

Figure 3.18 Phase II Hopane Normalized TLC-FID Aromatic Data. Shows the gross temporal variation of the aromatic fractions for the three treatments and unoiled control; where O-C is oiled control, O-N is oiled with nutrients, and O-NN is oiled with nutrients plus nitrate as electron acceptor. Error bars represent one standard deviation.

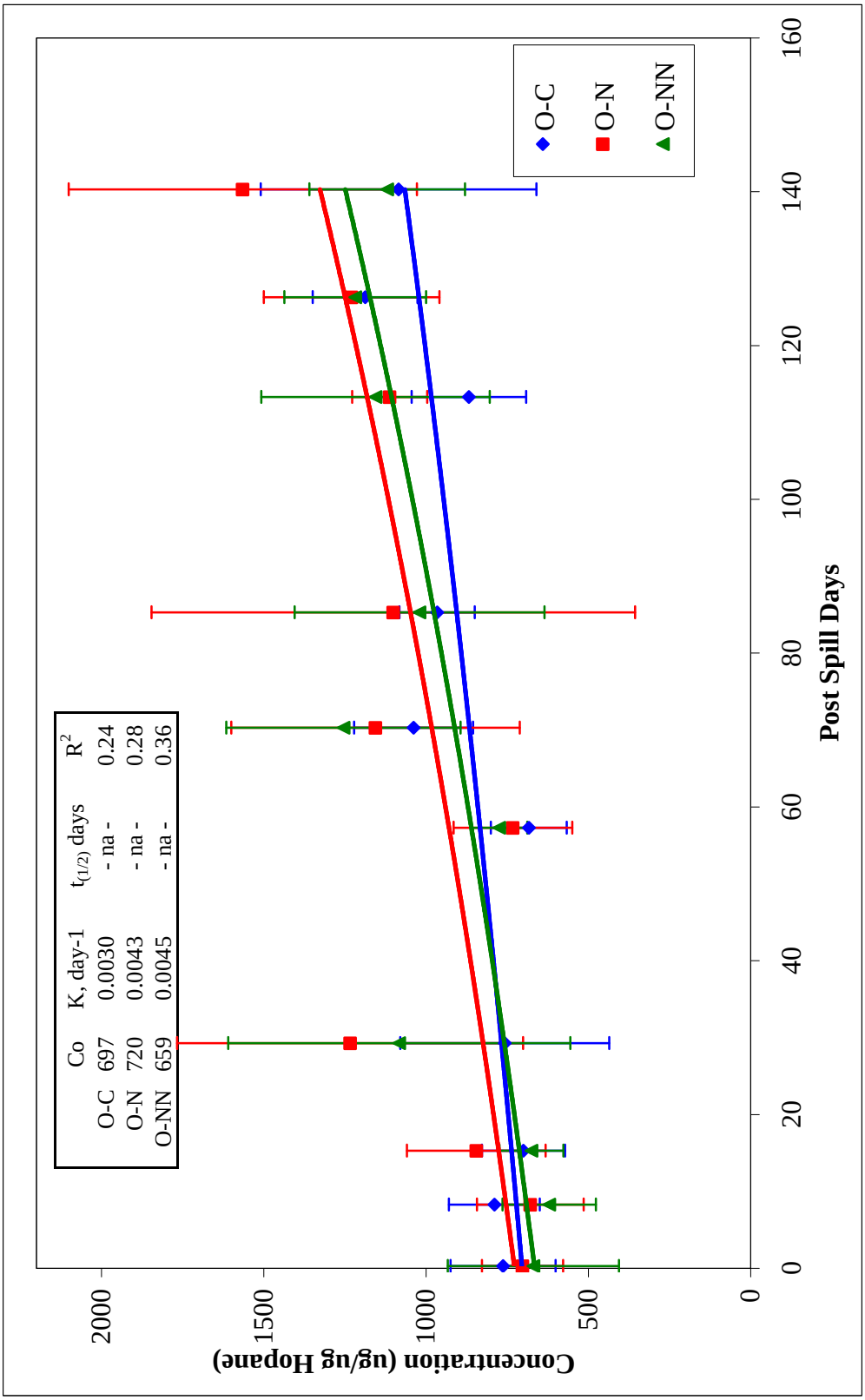

Figure 3.19 Phase II Hopane Normalized TLC-FID Resin Data. Shows the gross temporal variation of the resin fractions for the three treatments and unoiled control; where O-C is oiled control, O-N is oiled with nutrients, and O-NN is oiled with nutrients plus nitrate as electron acceptor. Error bars represent one standard deviation.

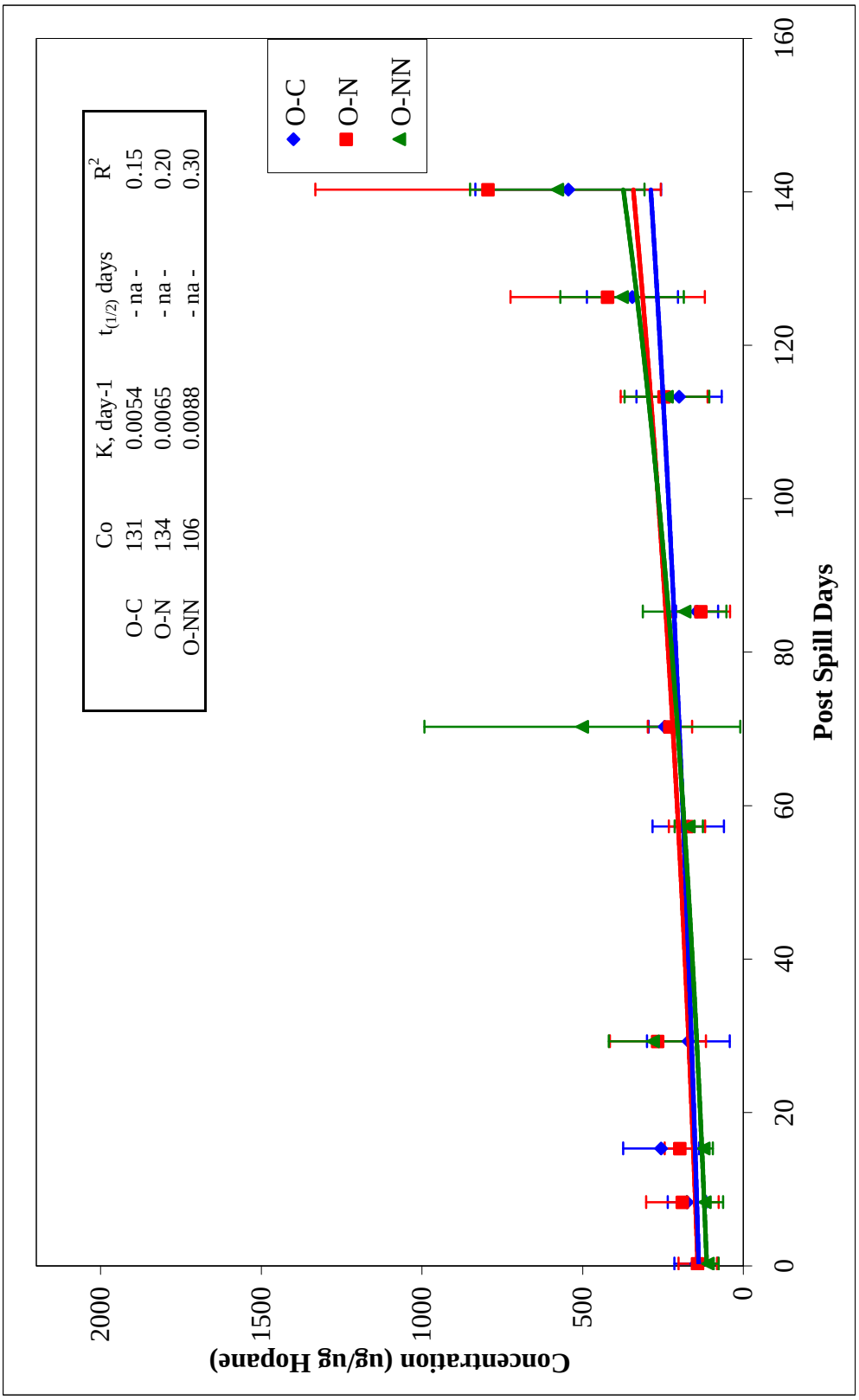

Figure 3.20 Phase II Hopane Normalized TLC-FID Asphaltene Data. Shows the gross temporal variation of the asphalten fractions for the three treatments and unoiled control; where O-C is oiled control, O-N is oiled with nutrients, and O-NN is oiled with nutrients plus nitrate as electron acceptor. Error bars represent one standard deviation.

Although the O-C and the O-N exhibit the same reduction rate and half-lives, the data sets are statistically different. Taking these results into consideration, the normalized data suggest that the O-N amended treatment did not improve degradation performance, whereas the O-NN did improve performance.

ANOVA analysis of the aromatic fractions revealed a significant difference between Day 0 and Day 140 normalized concentrations for all three treatments (Figure 3.18). For all three treatments there was an average 61% to 69% temporal reduction of the aromatic fractions. The R^2 coefficient for the aromatic fraction does not indicate as good a fit as the saturate models. The rate constants were similar for the O-N and O-NN treatment, while the O-C rate was slightly higher. The statistical comparison of the treatments indicated that only the O-N treatment was significantly different from the O-C. Unlike the saturate fractions, the O-C demonstrated a higher reduction rate and shorter half-life than the amended treatments, suggesting that the O-C demonstrated better degradation performance than the amended treatments.

ANOVA analysis of both of the polar fractions revealed a significant difference between Day 0 and Day 140 normalized concentrations for all three treatments (Figures 3.19 and 3.20), where the differences were due to enrichments of both polar fractions. The resin fraction of the O-C treatment showed the lowest enrichment of 34%, and the amended treatments showed similar enrichments of 46%. The enrichment rates of both amended treatments were 1.5 times higher than the O-C treatment. For the asphaltenes, the O-N treatment showed a higher enrichment (71%) as compared to the O-C and O-N treatments (56%). The O-NN rate constant was 1.5 times higher than those of the O-C and O-N treatments. For both the resins and the asphaltenes, the R^2 coefficients were low, indicating poor correlations between the models and the data.

The hopane-normalized results indicate that only the O-NN amendment was significantly more effective at saturate biodegradation than the O-C control. Unexpectedly, the O-C was more effective than the amended treatments degrading aromatics. The hopane normalized rate constants for the TLC-FID data were lower than non-normalized rates, which follows the trends observed in the GC-MS hopane analysis

(Mills et al., 2004). However, the TLC-FID hopane-normalized degradation rate constants are much lower and the half-lives are much longer than those observed in the GC-MS analysis. The hypothesis that hopane-normalization of the TLC-FID data does improve the evaluation of biodegradation is supported as moderately higher R^2 coefficients were observed, degradation rates were reduced, and predicted half-lives were longer than the non-normalized results.

However, the trends observed in the polar fraction hopane-normalized data cannot be supported by the results presented in Mills et al. (2004). The hopane-normalized data for the polar fractions indicates that there is a biological enrichment of these compounds. These increases represent a relatively small change in the fraction concentrations over time, 264 and 705 (ug/gm dry sediment) for the resin and asphaltene fractions respectively. These increases are negligible compared to the fraction concentration reductions of the hydrocarbons, 4055 and 3352 (ug/gm dry sediment) for the saturate and aromatic fractions respectively. As discussed in the Phase I results, research has demonstrated that this type of enrichment is plausible and can occur from the accumulation of refractory hydrocarbon molecules (dead-end metabolites) that are generated from the co-metabolization of less biologically susceptible hydrocarbons (Atlas and Cerniglia, 1995; Dutta and Harayama, 2000; Lee and Levy, 1991; Westlake et. al., 1974).

Phase II Asphaltene Normalized Fraction Concentrations

Hopane normalization to evaluate petroleum biodegradation is based on the assumption that hopane is non-biodegradable (over the time frame of the experiment). A similar assumption can be argued for the asphaltene fraction. As such, the asphaltene-normalized fraction concentration results are presented in Figure 3.21, 3.22, and 3.23.

Analysis of the saturate fractions indicated statistical differences between Day 0 and Day 140 normalized concentrations for all three treatments. All three treatments showed an average 92% - 96% temporal reduction of the saturate fractions. The rate constants were similar for the O-C and O-N treatment, while the O-NN rate was almost

1.5 times higher. The statistical analysis of the data indicated that only the O-N amended treatment was different from the O-C. Although the O-C and the O-N exhibit similar reduction rates and half-lives, the data sets are statistically different. Taking these results into consideration, the normalized data suggests that neither amended treatment improves degradation performance. The R^2 coefficient for the saturate fractions indicated a good fit of the data to the model.

Analysis of the aromatic fractions revealed statistical differences between Day 0 and Day 140 normalized concentrations for all three treatments (Figure 3.22). All three treatments showed an average 84% - 89% temporal reduction of the aromatic fractions. The rate constants were similar for the O-C and O-N treatment, while the O-NN rate was slightly higher. The statistical comparison of the treatments indicated no differences between the amended treatments and the control. The asphaltene-normalized data suggests that neither amended treatment improves degradation performance. The R^2 coefficient for the aromatic fractions indicates a weak fit.

As in the Phase I asphaltene normalized analysis (Figure 3.6), the resin fraction rate constant reflected a reduction over time (Figure 3.23). This observed trend is an indication that the resin fraction was enriched at a slower rate than the asphaltene fraction and is an erroneous observation.

The asphaltene-normalized half-lives for the hydrocarbon fractions were shorter than the non-normalized half-lives. The half-lives for all the treatments were similar for the O-C and the O-N, but noticeably different for the O-NN amendment. The hypothesis of asphaltene-normalization is not supported as only higher R^2 coefficients were observed but, temporal rates were higher and half-lives shorter than the non-normalized results. Given that the asphaltene TEM concentration does not appear to be conservative, the conclusions of significant petroleum biodegradation cannot be supported by this method of analysis.

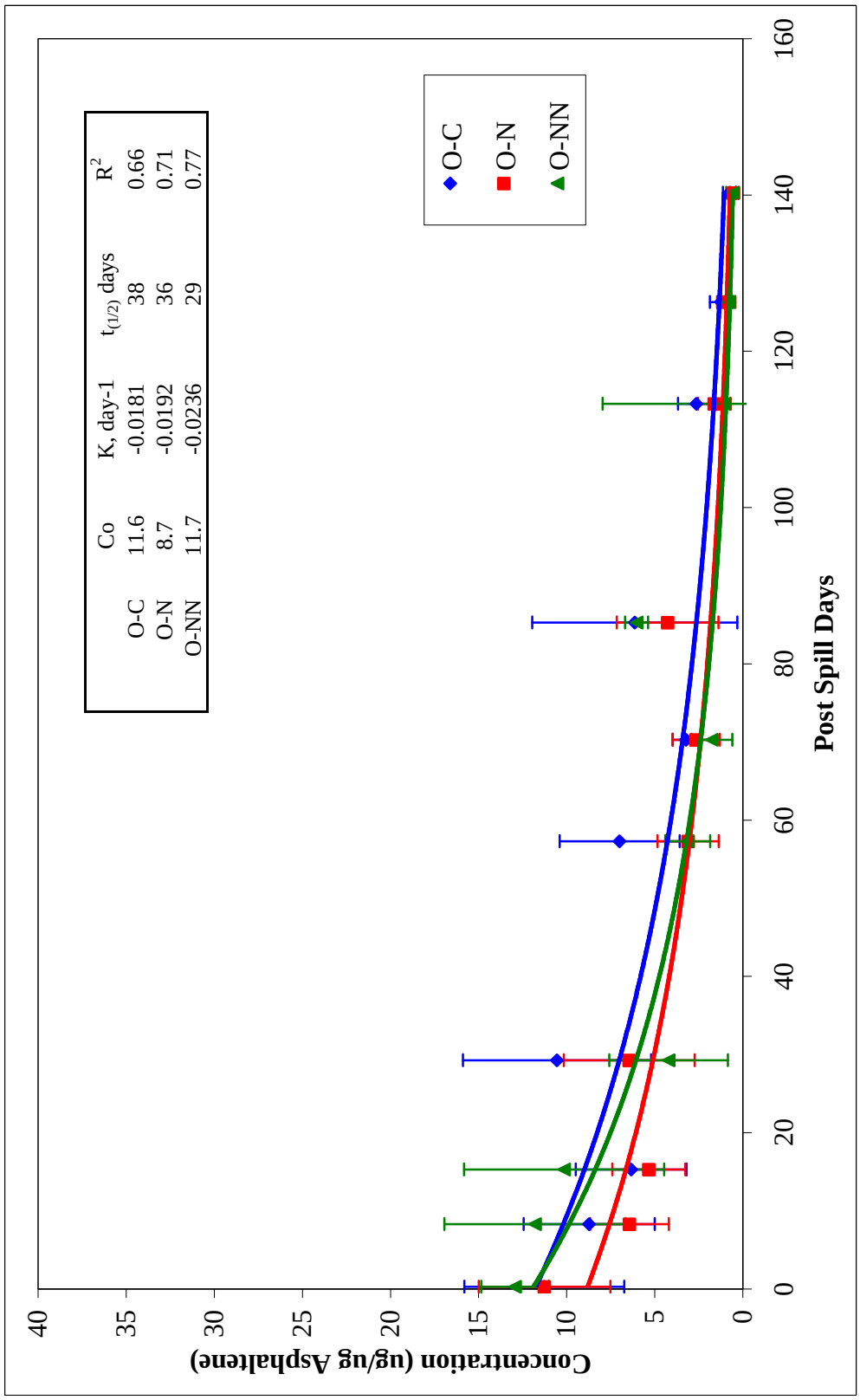

Figure 3.21 Phase II Asphaltene Normalized TLC-FID Saturate Data. Shows the gross temporal variation of the saturate fractions for the three treatments; where O-C is oiled control, O-N is oiled with nutrients, and O-NN is oiled with nutrients plus nitrate as electron acceptor. Error bars represent one standard deviation.

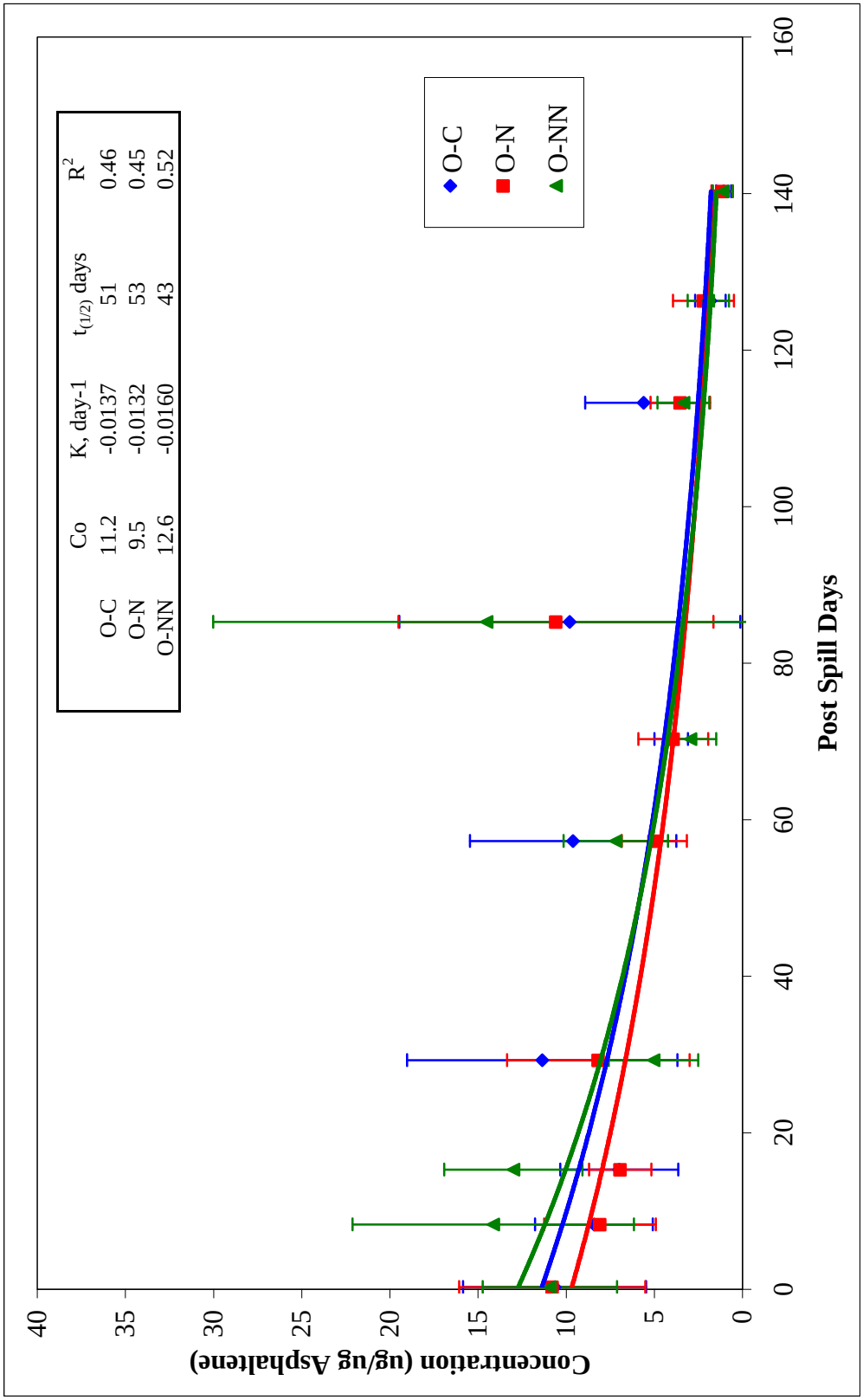

Figure 3.22 Phase II Asphaltene Normalized TLC-FID Aromatic Data. Shows the gross temporal variation of the aromatic fractions for the three treatments; where O-C is oiled control, O-N is oiled with nutrients, and O-NN is oiled with nutrients plus nitrate as electron acceptor. Error bars represent one standard deviation.

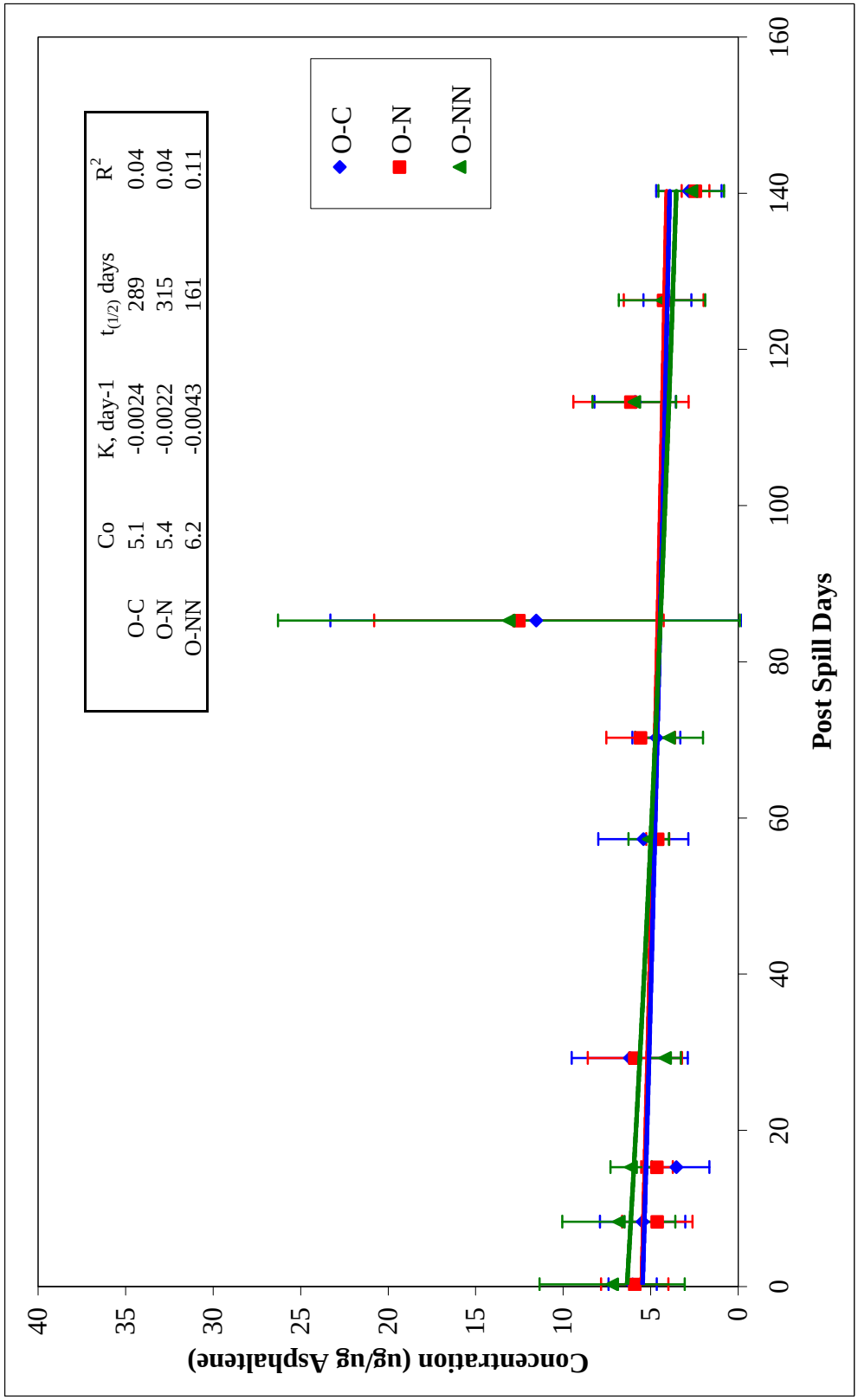

Figure 3.23 Phase II Asphaltene Normalized TLC-FID Resin Data. Shows the gross temporal variation of the resin fractions for the three treatments; where O-C is oiled control, O-N is oiled with nutrients, and O-NN is oiled with nutrients plus nitrate as electron acceptor. Error bars represent one standard deviation.

CONCLUSIONS

For the research presented in this chapter, the TLC-FID analysis was applied to monitor the temporal degradation of Arabian Light crude oil in two *in-situ* field studies of petroleum biodegradation in an estuarine wetland. In both bioremediation studies the TLC-FID analysis was able to distinguish temporal fraction changes of petroleum. The variability of the TLC-FID non-normalized concentrations highlights the importance of normalizing the data results to a conservative reference. Normalizing the TLC-FID data with the conservative biomarker hopane increased the degradation rates of the two hydrocarbon fractions, shortened the half-lives, and modestly increased the R^2 coefficients. However, these conclusions do not meet the criteria hypothesized for characterizing biotic activity versus abiotic activity. Normalizing the TLC-FID data with the asphaltene fraction was promising in that it reduced the half-lives and increased the R^2 coefficients. However these data were rejected as useful data as it appeared that the asphaltene concentration was not conservative.

The TLC-FID temporal fraction trends observed in both studies supports the GC-MS conclusions that bioremediation was the major form of petroleum reduction. The observed patterns of simultaneous hydrocarbon fraction reduction and relative polar fraction increase are indicative of the biotic losses associated with biodegradation (Atlas and Bartha, 1972; Leahy and Colwell, 1990; Westlake et al., 1974). In addition the TLC-FID concentration analysis was sensitive enough to quantify the effects of the different remedial amendments. This sensitivity was especially evident where it was determined that the O-N amendment improved the degradation performance of the saturate fraction, whereas none of the treatments had an effect on the aromatic fractions.

Of considerable interest is the quantification of the polar fractions of the petroleum. For this type of temporal field study with large sample sets, the quantification of polar compounds is not easily accomplished with other petroleum characterization techniques, as they can be tedious and time consuming. The enrichment trends observed in the polars concentration data were unanticipated. The hopane-normalized data suggests that the polars enrichment was a result of biological

enrichment. While these enrichments are not clearly understood, research indicates that these enrichments are plausible.

One possibility is that the observed polars enrichments are due to the accumulation of refractory hydrocarbon molecules (dead-end metabolites) that are generated from the co-metabolization of less biologically susceptible hydrocarbons (Atlas and Cerniglia, 1995; Dutta and Harayama, 2000; Lee and Levy, 1991; Westlake et. al., 1974). These unique degradation intermediary compounds cannot be quantified with the TLC-FID analysis; however, the data does suggest that the gross enrichment due to these intermediaries can be quantified.

Another explanation may be the TLC-FID chromatography method itself. Pollard et al., (1992) suggest that as compounds are exposed to degradation activities, significant changes can occur in the chemical polarities of the compounds (enrichment with oxygen molecules). Because the TLC separation is based on component polarities, these component changes could shift these compounds into more polar fractions (Pollard et al., 1992). It is not clear from these results if the observed polar enrichment trends are a direct effect of the TLC-FID analysis or a byproduct of degradation.

In addition, while a GC-MS analysis may demonstrate that the hydrocarbon compounds have been degraded to background conditions and declare that the remaining compounds are recalcitrant residuals, research has indicated that the resin and asphaltene fractions of oil can be biodegraded (Bertrand et al., 1983; Rontani et al., 1985; Venkateswaran et al., 1995). The TLC-FID analysis demonstrates that while there are hydrocarbon reductions, the polar fractions remain a significant concentration in the wetland. If the research indicating biodegradation of polar compounds is true, then the residual polar concentrations quantified by the TLC-FID analysis are a contaminant ‘sink’ and bioavailable.

The degradation constants reported for the TLC-FID are generally an order of magnitude or lower than those reported for the GC-MS analyses of the Phase I and Phase II data in Mills et al. (2003), and Mills et al. (2004). These differences in degradation rate constants are attributed to the different range of compounds that the two methods analyze. The GC-MS analysis quantifies the degradation rates for target analytes. These analytes are considered key priority pollutants, not only for their toxicity, but for their bioavailability. Hence theses analytes are more susceptible to microbial degradation, exhibiting higher degradation rate constants. The TLC-FID analysis quantifies the overall degradation rates for many compounds in each of the four fractions, some more bioavailable than others.

Effective evaluation of different remediation amendments is key to successful bioremediation research. The TLC-FID research presented here demonstrated the effectiveness and appropriateness of the TLC-FID as a tool to identify petroleum biodegradation and to evaluate petroleum bioremediation amendments in the field. As a tool the TLC-FID technique is very applicable to large sample sets and rapid analysis. While the GC-MS analysis is appropriate for quantitative analysis of bioremediation and the removal of target analytes, it lacks the capability to quantify the gross petroleum degradation activity and the overall petroleum removal. In conjunction with the TLC-FID analysis, a complete understanding and evaluation of the effectiveness of remediation treatments can be achieved.

CHAPTER IV
SUMMARY AND CONCLUSIONS

The TLC-FID is a gross petroleum analysis that was used to characterize petroleum biodegradation in two large scale field studies. The TLC-FID method analysis presented here was evaluated, modified, and successfully applied to the analysis of these field sample extracts. The TLC-FID ability to analyze ten samples at a time is a significant laboratory advantage that provides the flexibility to analyze large sample sets relatively quickly and concurrently with QA-QC standards. Several types of potential errors and means to monitor them were also successfully identified. In addition to using two representative laboratory control standards, this research presented the means to use real-time field sample extracts as part of the QA-QC monitoring. Together the QA-QC results presented here demonstrate that with effective protocols in place, the TLC-FID analysis is suitable for large field sample set analyses.

The TLC-FID analysis was also compared to the HPLC-SARA and TPH analyses, two accepted methods of gross petroleum characterization. The results of the petroleum analytical methods comparison demonstrate that the HPLC-SARA and TLC-FID analysis had similar characterizations. The open-column-chromatography TPH analysis did not demonstrate a similar characterization as the TLC-FID. While these two analyses have limitations, the differences presented here are more indicative of the different analytical procedures.

In the Phase I study all four data analyses indicated the same conclusion for the hydrocarbon fractions; neither the saturate and aromatic fractions were preferentially degraded within the period of the study. Overall, the Phase I TLC-FID analyses indicated that the impacted estuarine wetlands were not overly inundated with petroleum from the catastrophic oil spill, and as such, the wetlands recovered naturally without bioremediation amendments. In the Phase II analysis the TLC-FID was able to differentiate bioremediation treatment effectiveness. While biotic and abiotic activity could not be clearly quantified, the trends observed in TLC-FID data strongly support

the conclusions that petroleum biodegradation was the main petroleum removal mechanism.

Although these results concur with the GC-MS analysis performed by Mills et al. (2003) the evaluation of wetland recovery differs between the TLC-FID and GC-MS methods. The GC-MS analysis is not able to quantify temporal polar concentration changes and thus the Phase I and Phase II GC-MS results suggest that the wetland petroleum concentrations had returned to expected background conditions by the end of the study period. However, the TLC-FID data indicates that the overall petroleum reductions were not as significant as the GC-MS analysis may have implied. While the hydrocarbons concentrations were significantly reduced in both study phases, the TLC-FID results indicate that the non-hydrocarbon (polar) concentrations in the wetland were not significantly reduced. Research literature suggests that these residual materials are biologically inert; however, biodegradation of these compounds has been observed and quantified, which suggest that these residuals are a contaminant 'sink' and bioavailable (Bertrand et al., 1983; Prince, 1993; Rontani et al., 1985; Venkateswaran et al., 1995).

The observed trends in the TLC-FID analysis support the findings of bioremediation and suggest that the results are sufficient to draw conclusions and evaluate *in-situ* petroleum bioremediation. Although *in-situ* petroleum biodegradation conclusions are often largely supported by GC-MS target analyte analyses, the research presented here demonstrates how these results may be incomplete. The TLC-FID analysis can complement a GC-MS analysis to expand the knowledge of petroleum bioremediation and remediation strategies. Further investigation is required to determine the capability of the TLC-FID analysis to differentiate biotic activity from abiotic activity.

REFERENCES

Ackman, R.G., 1981. Methods Enzymol 72, 205.

Atlas, R.M., 1981. Microbiology Review 45, 180.

Atlas, R.M., 1995. Bioremediation 73(14), 32.

Atlas, R.M., Bartha, R., 1972. Biotechnology and Bioengineering 14, 309.

Atlas, R.M., Cerniglia, C.E., 1995. Bioscience 45, 332.

Bertrand, J.C., Rambeloarisoa, E., Rontani, J.F., Guisti, G., Mattei, G., 1983. Biotechnology 5, 567.

Bharati, S., Rostum, G.A., Loberg, R., 1993. Organic Geochemistry 22, 835.

Bizzell, C.J., Autenrieth, R.L., Townsend, T., Bonner, J.S., 1999. In: Leeson, A., Alleman, B.C., (Eds.), International In situ and On-Site Bioremediation Symposium, Phytoremediation and Innovative Strategies for Specialized Remedial Applications, Battelle Press, Columbus, OH.

Bowden, W.B., 1986. Ecology 67, 88.

Bragg, J.R., Prince, R.C., Harner, E.J., Atlas, R.M., 1994. Nature 368, 413.

Butler, E.L., Douglas, S.D., Steinhauer, W.G., 1991. In: Hinchee, R.E.,Offenbuttel, R.F., (Eds.), International In situ and On-Site Bioremediation Symposium, On-Site Bioreclamation: Process for Xenobiotic and Hydrocarbon Treatment, Butterworth-Heinemann, Boston, MA.

Cavanagh, J.E., Juhasz, A.L., Nichols, P.D., Franzmann, P.D., McMeekin, T. A., 1995. Journal of Microbiological Methods 22, 119.

Cebolla, V.L., Vela, J., Membrado, L., Ferrando, A.C., 1998. Journal of Chromatographic Science 36, 479.

Cerniglia, C.E., 1984. In: Bartha, R.M. (Ed.), Petroleum Microbiology. Macmillan Publishing Company, New York.

DeLuane, R.D., Gambrel, R.P., Pardue, J.H., Patrick Jr., W.H., 1990. Estuaries 13, 72.

Douglas, G.S., McCarthy, K.J. Dahlen, D.T., Seavey, J.A., Steinhauer, W.G., Prince, R.C. Elmendor, D.L., 1991. In: Kostecki, P.T., Calabrese, E.J. (Eds.), Contaminated Soils: Diesel Fuel Contamination. Lewis Publishers, Boca Raton, FL.

Dutta, T.K., Harayama, S., 2000. Environmental Science and Technology 34, 1500.

Fedorak, P.M., Westlake, D.W.S., 1981. Canadian Journal of Microbiology 27, 423.

Goto, M., Kato, M., Asaumi, M., Shirai, K., Venkateswaran, K., 1994. Journal of Marine Biotechnology 2, 45.

Harris, B.C., Bonner, J.S., Autentieth, R.L., 1999. Environmental Technology 20, 785.

Iatron Laboratories, Inc., 1995. Instruction Manual for Iatroscan MK-5 TLC-FID Analyser, Iatron Laboratories, Tokyo, Japan, 65.

Ishihara, M., Sugiura, K., Asaumi, M., Goto, M., Sasaki, E., Harayama, S. 1995. In: Hinchee, R.E. (Ed.), International In situ and On-Site Bioremediation Symposium, Microbial Processes for Bioremediation, Battelle Press, Columbus, OH.

Jobson, A., Cook, F.D., Westlake, D.W.S., 1974. Applied Microbiology 27, 1082.

Karlsen, D.A., Larter, S.R., 1991. Organic Geochemistry 17(5), 603.

LaRiviere D., Autenrieth, R.L., Bonner, J.S., 2003. Water Research 37, 3307.

Leahy, Joseph G., Rita R. Colwell, 1990. Microbiological Reviews 54(3), 305.

Lee, K., De Mora, S., 1999. Environmental Technology 20, 783.

Lee, K., Levy, E.M., 1991. In: Proceedings of the 1991 International Oil Spill Conference, American Petroleum Institute, Washington DC, pp. 541.

Mills, M.A., Bonner, J.S., McDonald, T.J., Page, C.A. and Autenrieth, R.L., 2003. Marine Pollution Bulletin 46(7), 887.

Mills, M.A., Bonner, J.S., Page, C.A., Autenrieth, R.L., 2004. Marine Pollution Bulletin, in press.

Mills M.A., McDonald, T.J., Bonner, J.S., Simon, M.A., Autenrieth, R.L., 1999. Chemosphere. 39(14), 2563.

Mueller, D.C., Bonner, J.S., McDonald, S.J., Autenrieth, R.L., 1999. Environmental Technology, 20: 875.

Mueller, D.C., Bonner, J.S., McDonald, S. J., Autenrieth, R.L., Donnelly, K.C., Lee, K., Doe, K., Anderson, J., 2003. Environmental Toxicology and Chemistry 22, 1945.

National Research Council (NRC), 2003. Oil in the Sea III: Inputs, Fates, and Effects. National Academy Press, Washington, D.C..

Page, C.A., Bonner, J.S., McDonald, T.J., Autenrieth, R.L., 2002. Water Research, 36(15), 3821.

Payne, J.R., McNabb Jr., G.D., 1984. MTS Journal, 18(3), 24.

Pollard, S.J., Hrudey, S.E., Fuhr, B.J., 1992. Environmental Science and Technology 26(12), 2528.

Prince, R.C., 1993. Critical Reviews in Microbiology 19(4), 217.

Prince, R.C., Varadaraj, R., Fiocco, R.J., Lessard, R.R., 1999. Environmental Technology 20, 891.

Pritchard, P.H.; Mueller, J.G.; Rogers, J.C.; Kremer, F.V.; Glaser, J.A., 1992. Biodegradation 3, 315.

Ray, J.E., Oliver, K.M., Wainwright, J.C., 1981. In: Proceedings of the 1981 Petroanalysis IP Symposium, London, UK, 361.

Rontani, J.F., Bosser-Joulak, F., Rambeloarisoa, E., Bertrand, J.C., Giusti, G., Faure, R., 1985. Chemosphere 14, 1413.

Selucky, M.L., Hafermann, P., Lacchelli, A., Manske, T., 1985. Liquid Fuels Technology 3(1), 15.

Simon, M.A., Bonner, J.S., McDonald, T.J., Autenrieth, R.L., 1999. Polycyclic Aromatic Compounds, 14-15, 231.

Snyder, W.S., 1996. Master of Science Thesis, University of Houston Press, Houston, TX.

Swanell, R.P.J., Mitchell, D.J., Jones, D.M., Willis, A., Lee, K., Lepo, J., 1997. In: Leeson, A., Alleman, B.C., (Eds.), International In situ and On-Site Bioremediation Symposium, Battelle Press, Columbus, OH.

Swanell, R.P.J., Mitchell, D., Lethridge, G., Jones, D., Heath, D., Hafley, M., Jones, M., Petch, S., Milne, R., Croxford, R., Lee, K., 1999. Environmental Technology 20, 863.

Townsend, R.T., Bonner, J.S., Autenrieth, R.L., 2000. Bioremediation Journal 4(3), 203.

Vela, J., Membrado, L. Cebolla, V.L., Ferrando, A.C., 1998. Journal of Chromatographic Science 36, 487.

Venkateswaran, K., Hoaki, T., Kato, M., Maruyama, T., 1995. Canadian Journal of Microbiology 41, 418.

Venosa, A.D., Suidan, M.T., Wrenn, B.A., Strohmeier, K.L., Haines, J.R., Eberhart, B.L., King, D., Holder, E., 1996. Environmental Science and Technology 30, 1764.

Wang, Z., Fingas, M., 1995. LC-GC 13(12), 950.

Westlake, D.W.S., Jobson, A., Phillippe, R., Cook, F.D., 1974. Canadian Journal of Microbiology 20, 915.

Wood, T.M., Lehman, R.L., Bonner, J.S. 1997. In: Proceedings of the 1997 International Oil Spill Conference, American Petroleum Institute, Washington DC, pp. 415.

APPENDIX A

SHEWHART CONTROL CHARTS

Shewhart control charts were used to identify any significant deviations from the average results. Deviations were identified as results that exceeded warning and action limits, set at 2 and 3 standard deviations respectively, above and below each average condition. When an LCS exceeded the action limits once, sample analysis continued, but efforts were made to minimize all forms of errors. When an LCS exceeded the action limits consecutively, then sample analysis stopped and analysis conditions were reevaluated before more samples were analyzed. For all action limit exceedances the associated LCSs and sample data were reviewed and compared and if deemed necessary, the sample results were discarded and reanalyzed. The Shewhart control charts used for this research are presented here.

APPENDIX A LIST OF FIGURES

Figure A1: Shewhart Control Chart, Phase I, LCS-S, Saturate Fraction 83
Figure A2: Shewhart Control Chart, Phase I, LCS-S, L-Aromatic Fraction 84
Figure A3: Shewhart Control Chart, Phase I, LCS-S, H-Aromatic Fraction 85
Figure A4: Shewhart Control Chart, Phase I, LCS-S, Resin Fraction 86
Figure A5: Shewhart Control Chart, Phase II, LCS-S, Saturate Fraction.....87
Figure A6: Shewhart Control Chart, Phase II, LCS-S, L-Aromatic Fraction.....88
Figure A7: Shewhart Control Chart, Phase II, LCS-S, H-Aromatic Fraction.....89
Figure A8: Shewhart Control Chart, Phase II, LCS-S, Resin Fraction.....90
Figure A9: Shewhart Control Chart, Phase I, LCS-P, Saturate Fraction 91
Figure A10: Shewhart Control Chart, Phase I, LCS-P, Aromatic Fraction 92
Figure A11: Shewhart Control Chart, Phase I, LCS-P, Resin Fraction 93
Figure A12: Shewhart Control Chart, Phase I, LCS-P, Asphaltene Fraction 94
Figure A13: Shewhart Control Chart, Phase II, LCS-P, Saturate Fraction.....95
Figure A14: Shewhart Control Chart, Phase II, LCS-P, Aromatic Fraction.....96
Figure A15: Shewhart Control Chart, Phase II, LCS-P, Resin Fraction.....97
Figure A16: Shewhart Control Chart, Phase II, LCS-P, Asphaltene Fraction.....98
Figure A17: Shewhart Control Chart, Phase I, Replicates, Saturate Fraction 99
Figure A18: Shewhart Control Chart, Phase I, Replicates, Aromatic Fraction 100
Figure A19: Shewhart Control Chart, Phase I, Replicates, Resin Fraction 101
Figure A20: Shewhart Control Chart, Phase I, Replicates, Asphaltene Fraction.....102
Figure A21: Shewhart Control Chart, Phase II, Replicates, Saturate Fraction 103
Figure A22: Shewhart Control Chart, Phase II, Replicates, Aromatic Fraction 104
Figure A23: Shewhart Control Chart, Phase II, Replicates, Resin Fraction 105
Figure A24: Shewhart Control Chart, Phase II, Replicates, Asphaltene Fraction 106

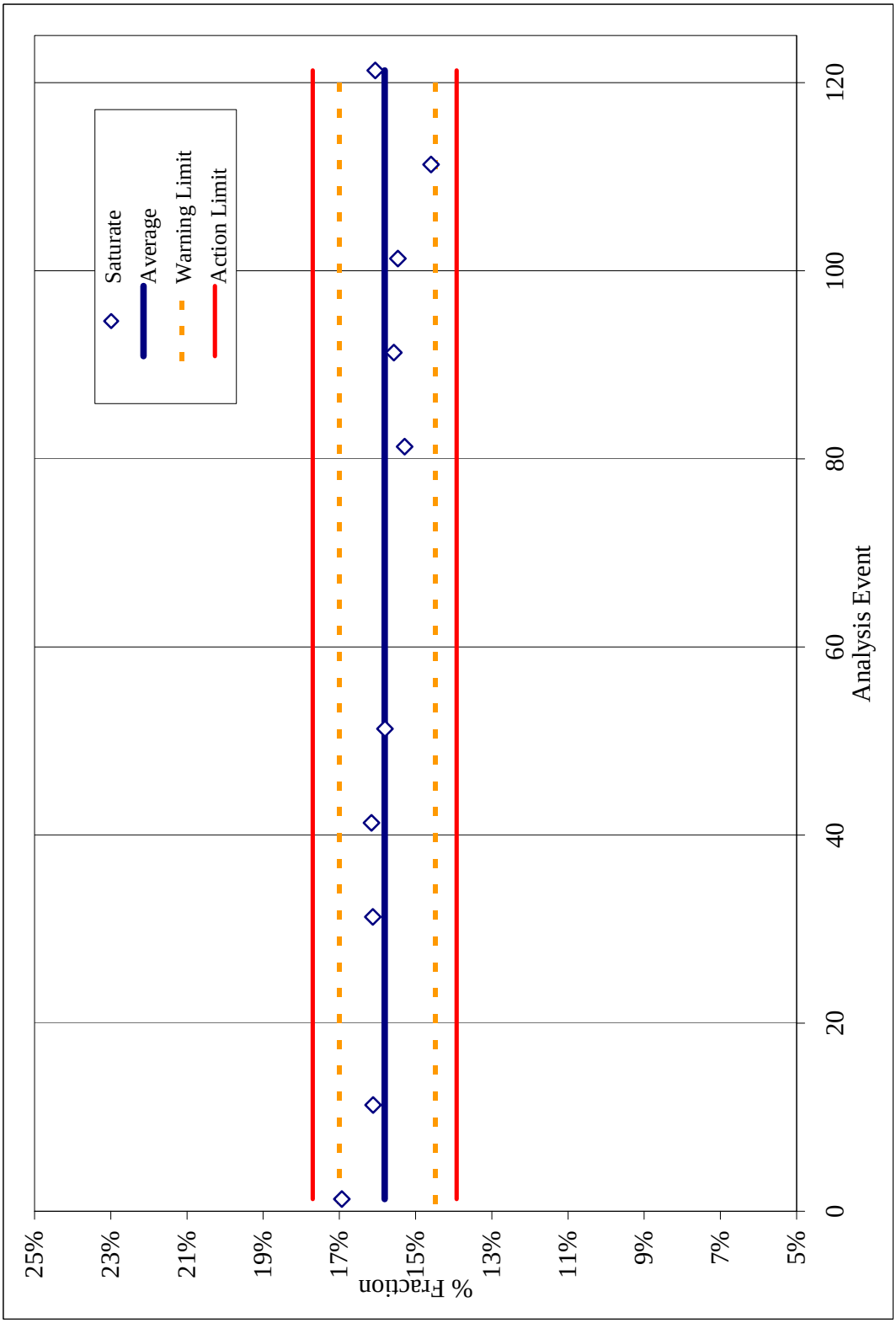

FIGURE A1: Phase I Synthetic LCS, Saturate Fraction, Shewhart Control Chart. Shows the saturate fraction for the LCS-S replicates with the average and 2 and 3 standard deviation warning and action limits shown respectively. The data points on the graph represent the respective LCS-S fraction results for each tray of ten chromarods.

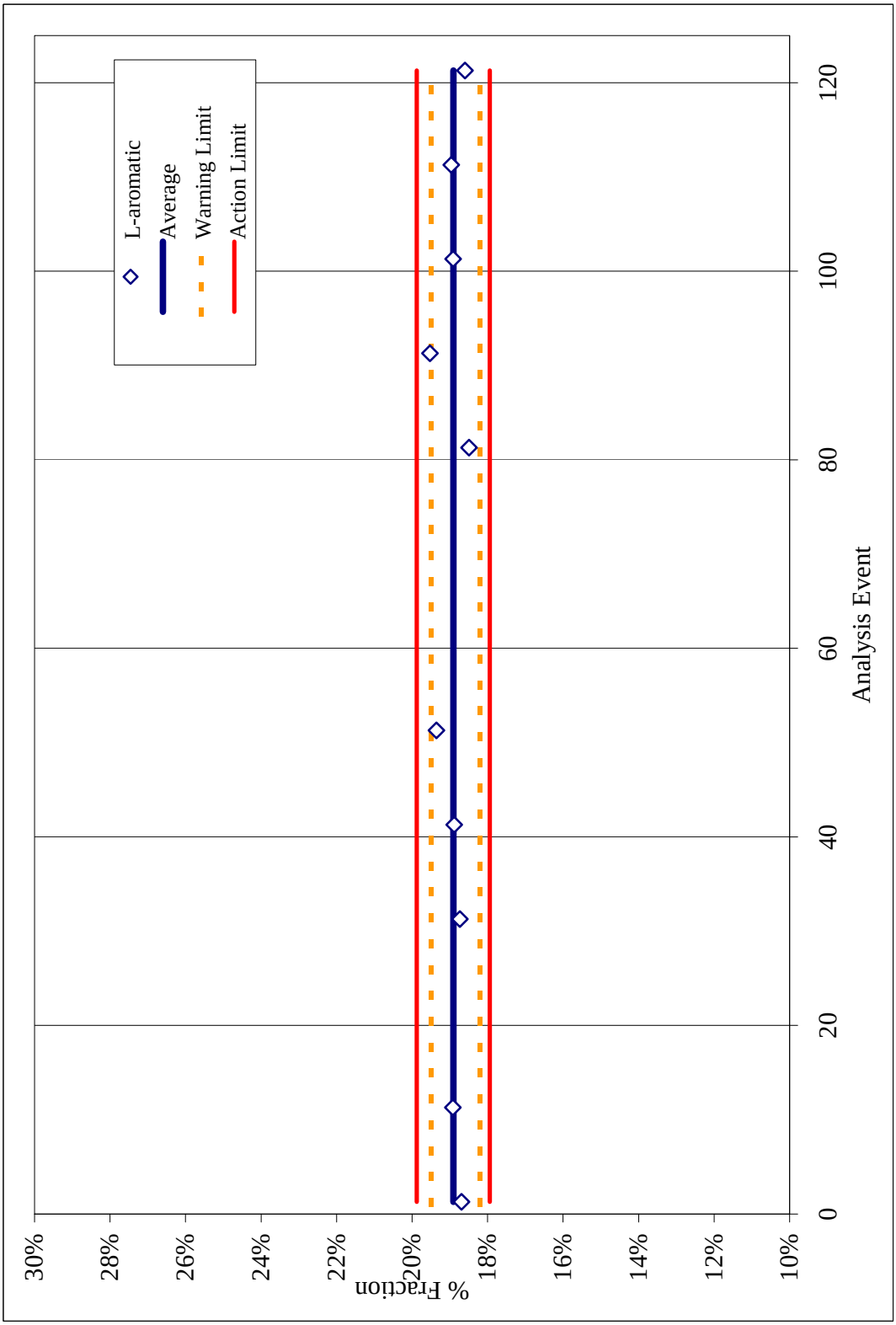

FIGURE A2: Phase I Synthetic LCS, Light Aromatic Fraction, Shewhart Control Chart. Shows the light aromatic fraction for the LCS-S replicates with the average and 2 and 3 standard deviation warning and action limits shown respectively. The data points on the graph represent the respective LCS-S fraction results for each tray of ten chromarods.

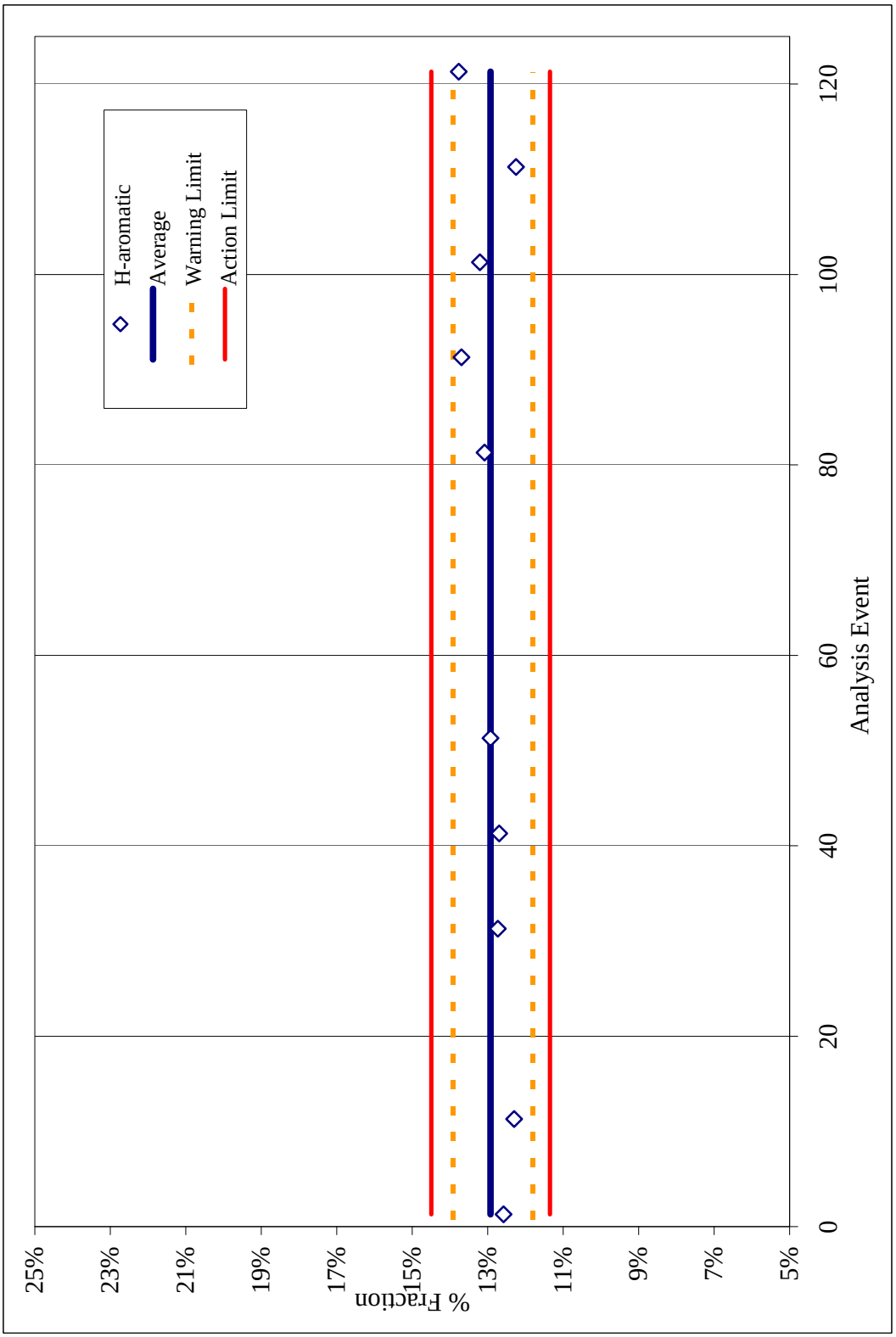

FIGURE A3: Phase I Synthetic LCS, Heavy Aromatic Fraction, Shewhart Control Chart. Shows the heavy aromatic fraction for the LCS-S replicates with the average and 2 and 3 standard deviation warning and action limits shown respectively. The data points on the graph represent the respective LCS-S fraction results for each tray of ten chromarods.

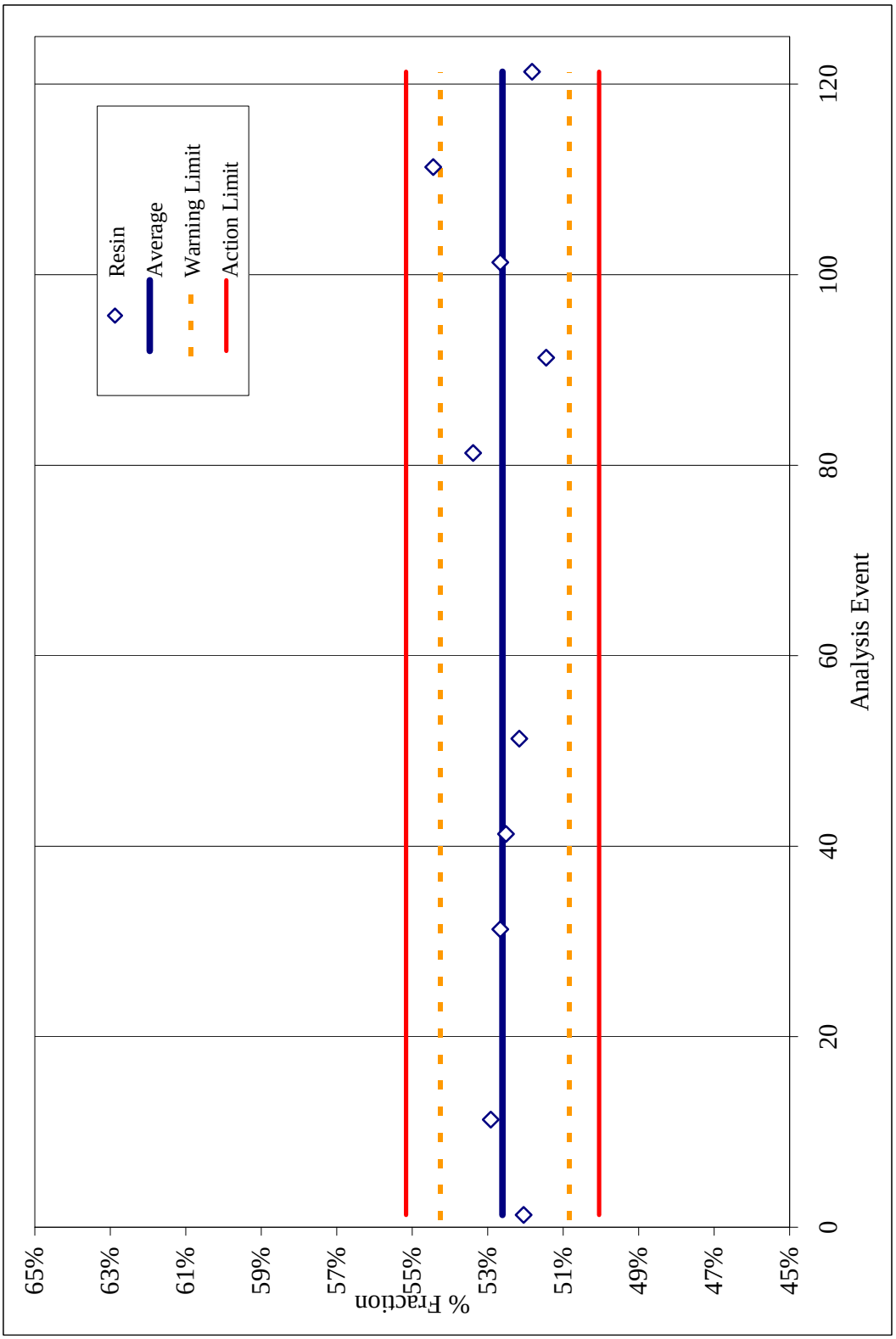

FIGURE A4: Phase I Synthetic LCS, Resin Fraction, Shewhart Control Chart. Shows the resin fraction for the LCS-S replicates with the average and 2 and 3 standard deviation warning and action limits shown respectively. The data points on the graph represent the respective LCS-S fraction results for each tray of ten chromarods.

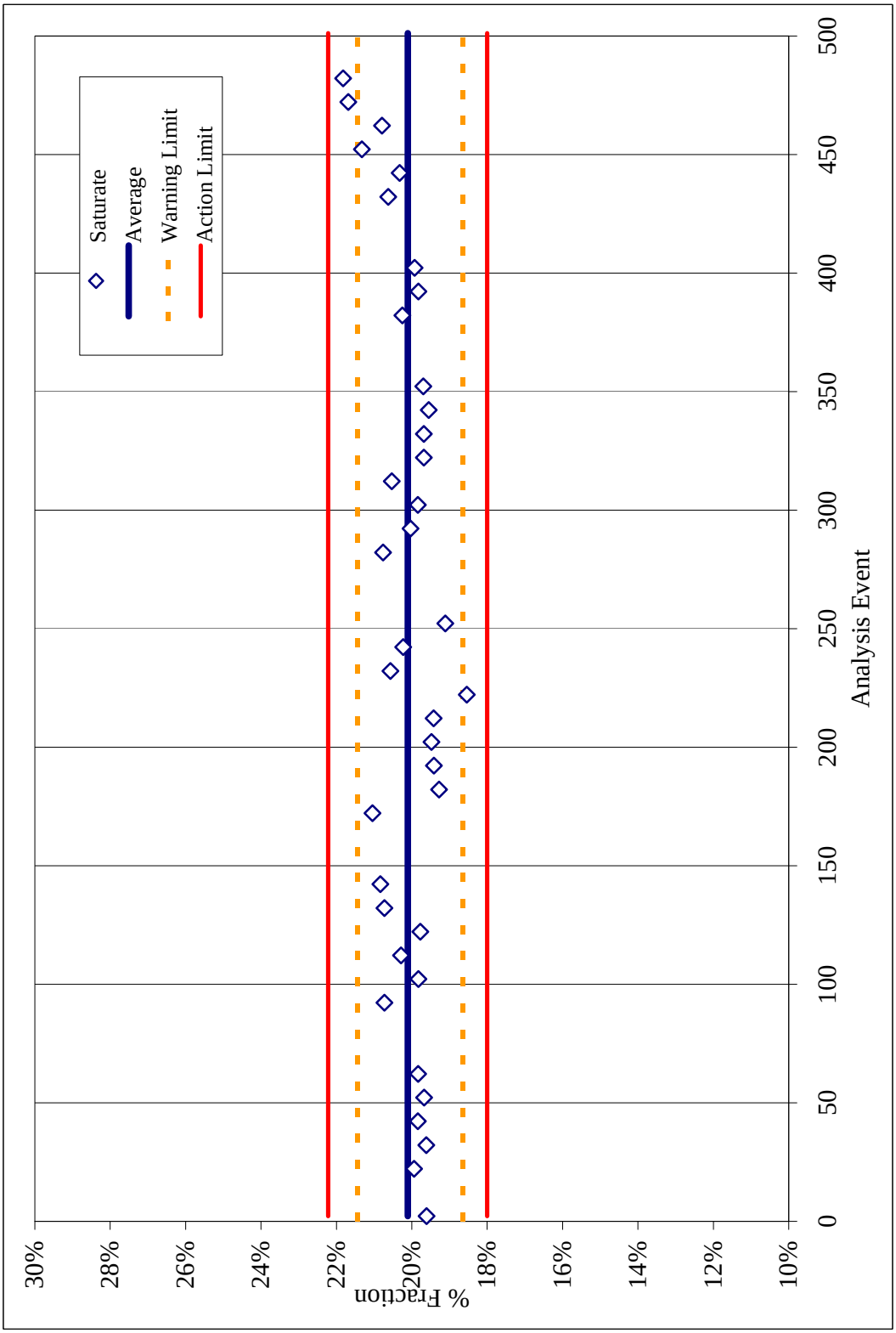

FIGURE A5: Phase II Synthetic LCS, Saturate Fraction, Shewhart Control Chart. Shows the saturate fraction for the LCS-S replicates with the average and 2 and 3 standard deviation warning and action limits shown respectively. The data points on the graph represent the respective LCS-S fraction results for each tray of ten chromarods.

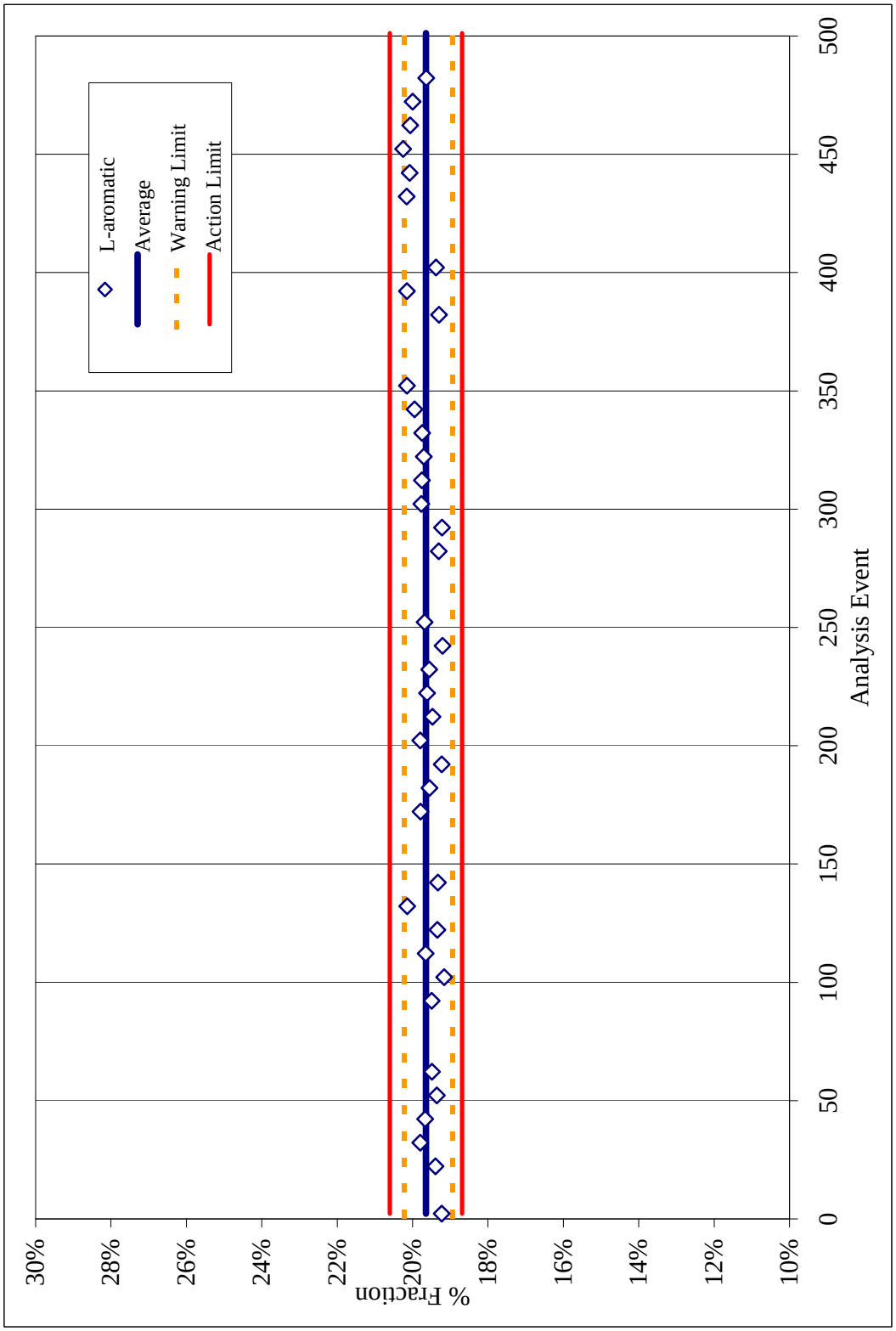

FIGURE A6: Phase II Synthetic LCS, Light Aromatic Fraction, Shewhart Control Chart. Shows the light aromatic fraction for the LCS-S replicates with the average and 2 and 3 standard deviation warning and action limits shown respectively. The data points on the graph represent the respective LCS-S fraction results for each tray of ten chromarods.

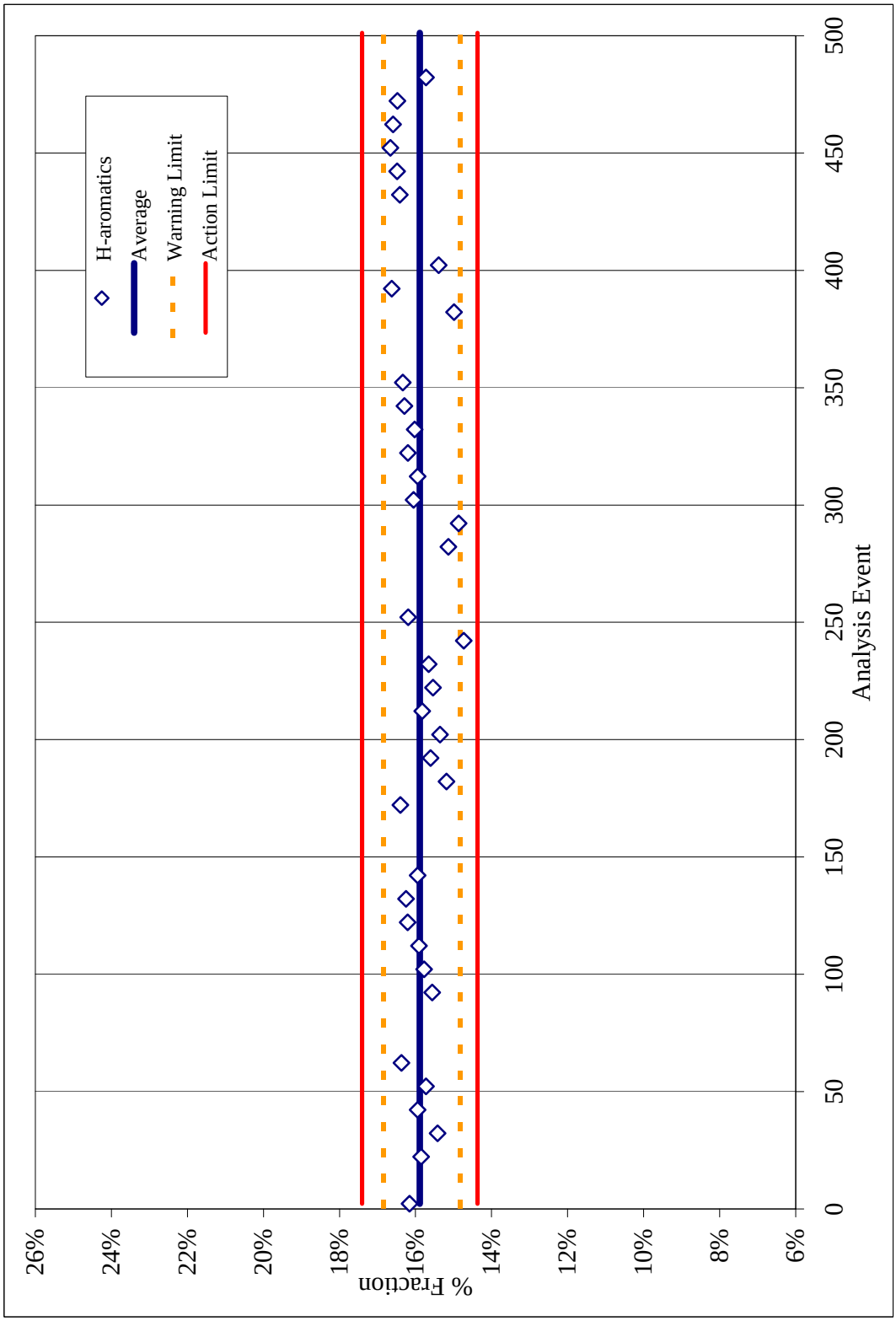

FIGURE A7: Phase II Synthetic LCS, Heavy Aromatic Fraction, Shewhart Control Chart. Shows the heavy aromatic fraction for the LCS-S replicates with the average and 2 and 3 standard deviation warning and action limits shown respectively. The data points on the graph represent the respective LCS-S fraction results for each tray of ten chromarods.

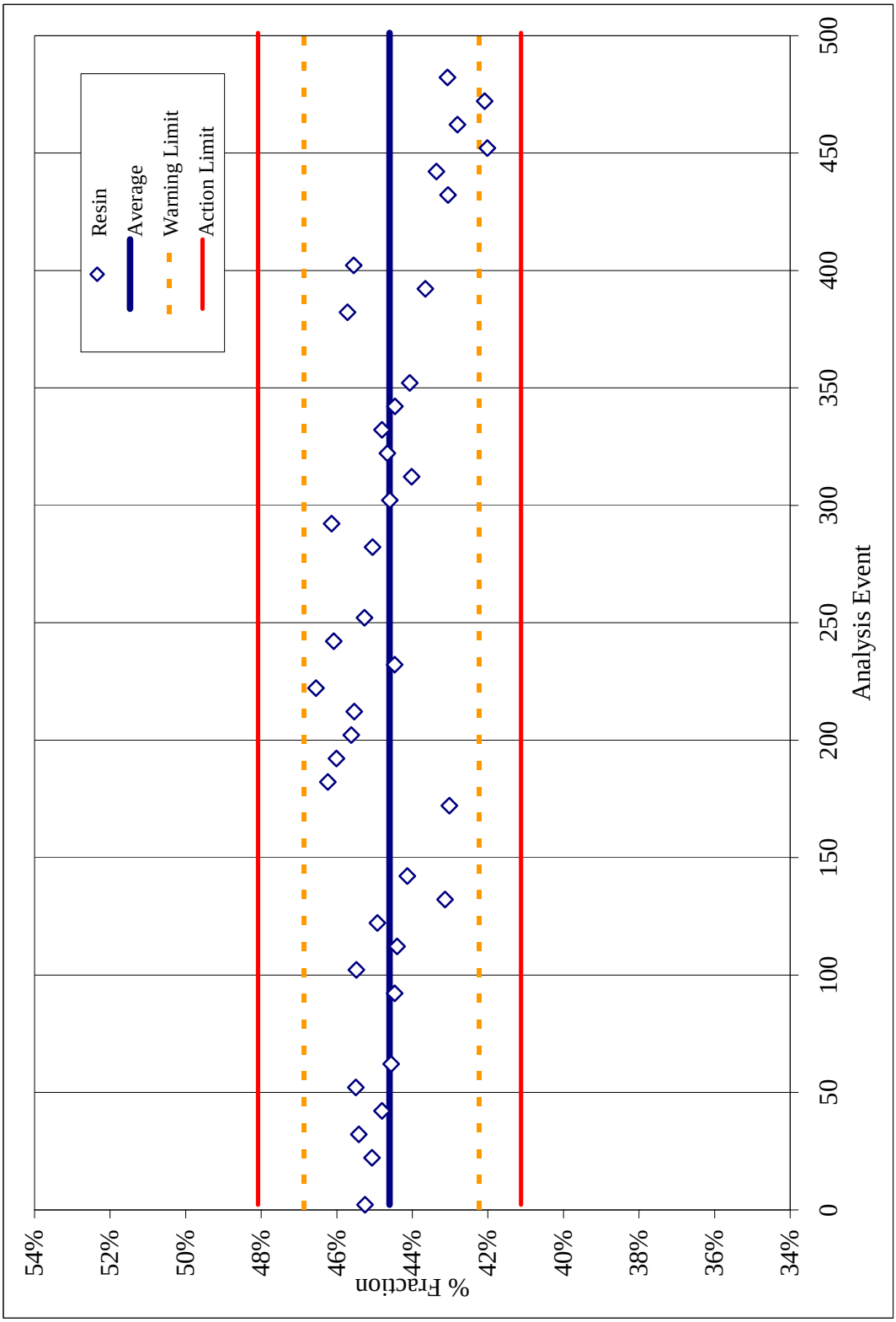

FIGURE A8: Phase II Synthetic LCS, Resin Fraction, Shewhart Control Chart. Shows the resin fraction for the LCS-S replicates with the average and 2 and 3 standard deviation warning and action limits shown respectively. The data points on the graph represent the respective LCS-S fraction results for each tray of ten chromarods.

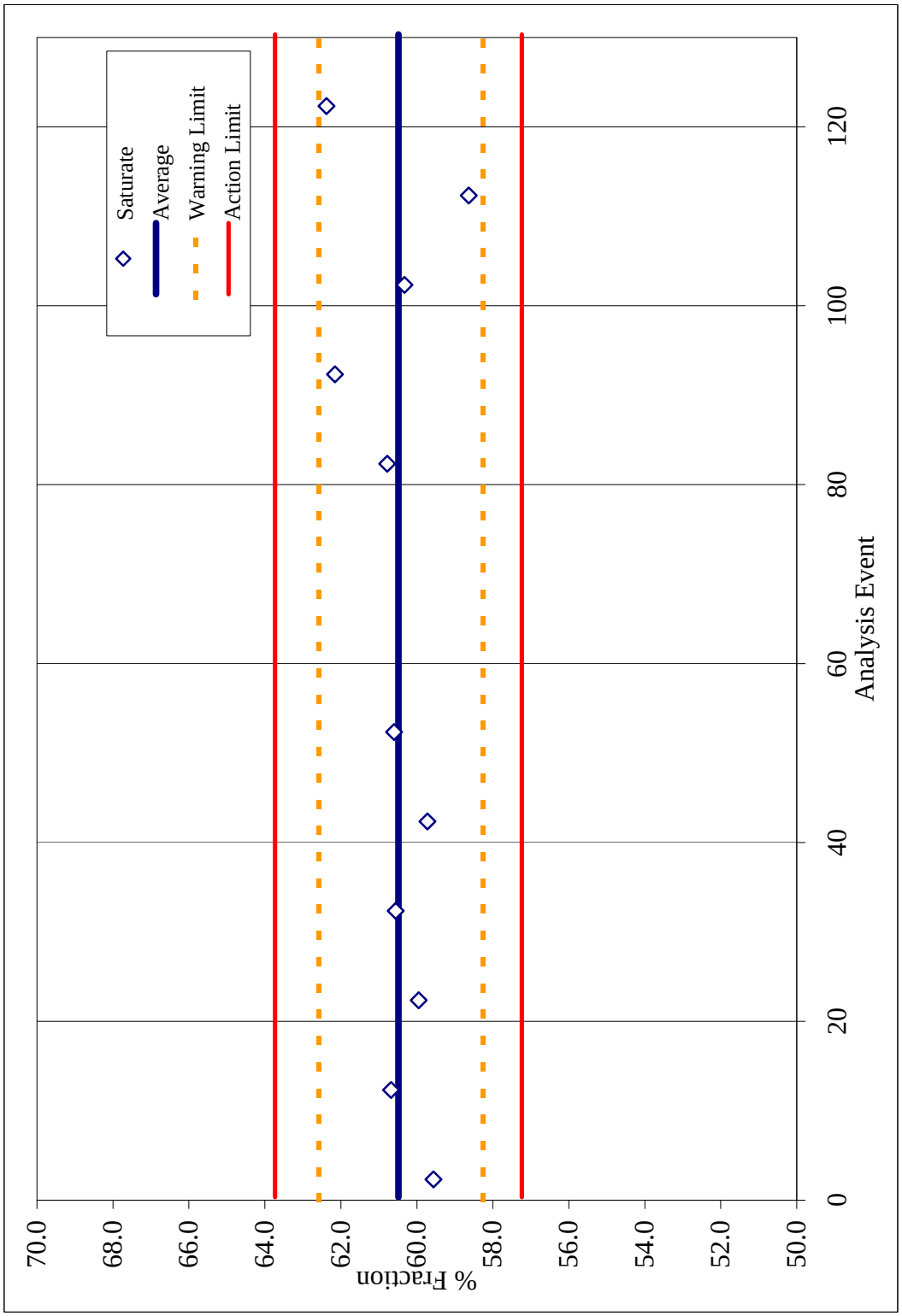

FIGURE A9: Phase I Bonny Light LCS-P, Saturate Fraction, Shewhart Control Chart. Shows the saturate fraction for the LCS-P replicates with the average and 2 and 3 standard deviation warning and action limits shown respectively. The data points on the graph represent the respective LCS-P fraction results for each tray of ten chromarods.

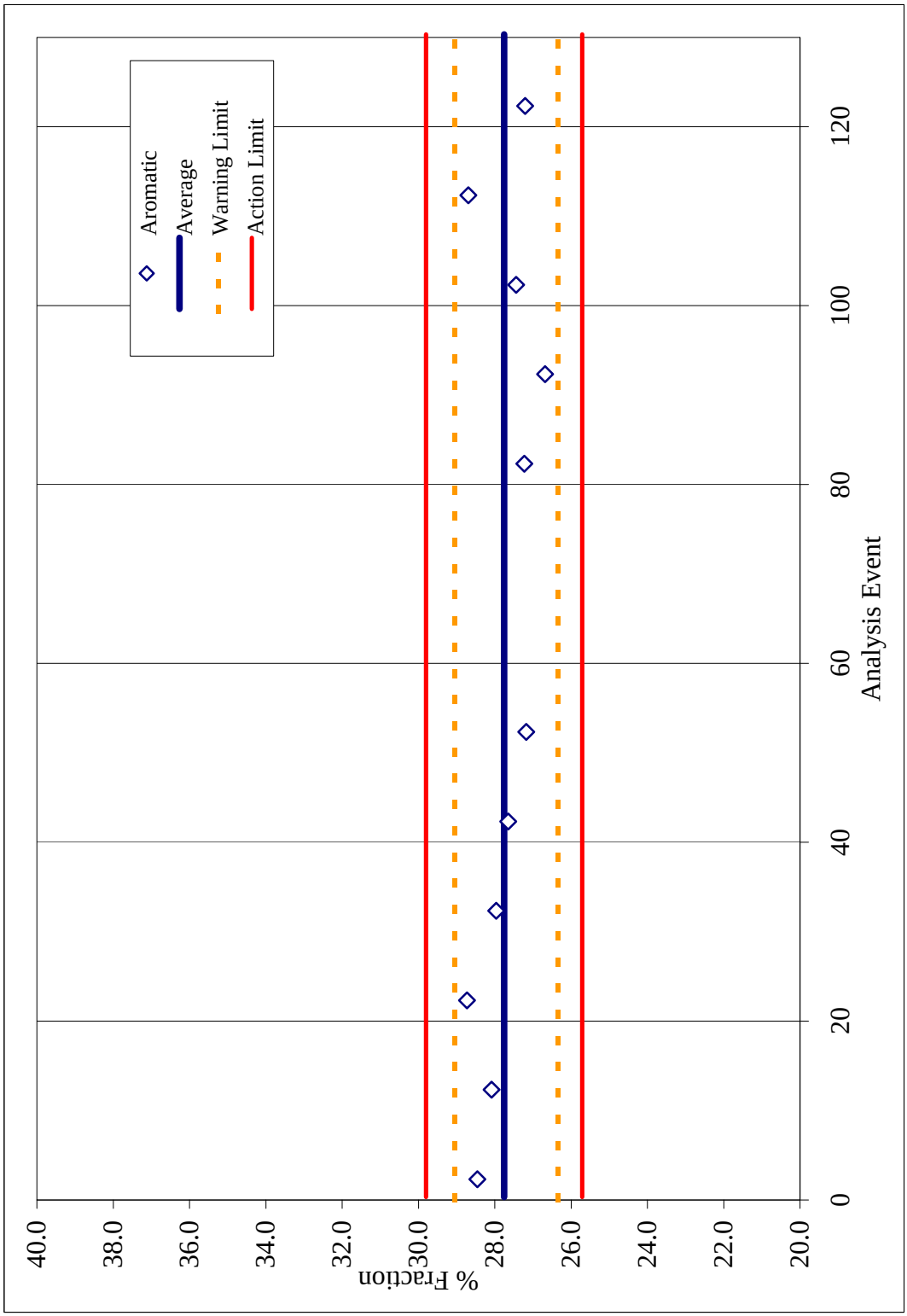

FIGURE A10: Phase I Bonny Light LCS-P, Aromatic Fraction, Shewhart Control Chart. Shows the Aromatic fraction for the LCS-P replicates with the average and 2 and 3 standard deviation warning and action limits shown respectively. The data points on the graph represent the respective LCS-P fraction results for each tray of ten chromarods.

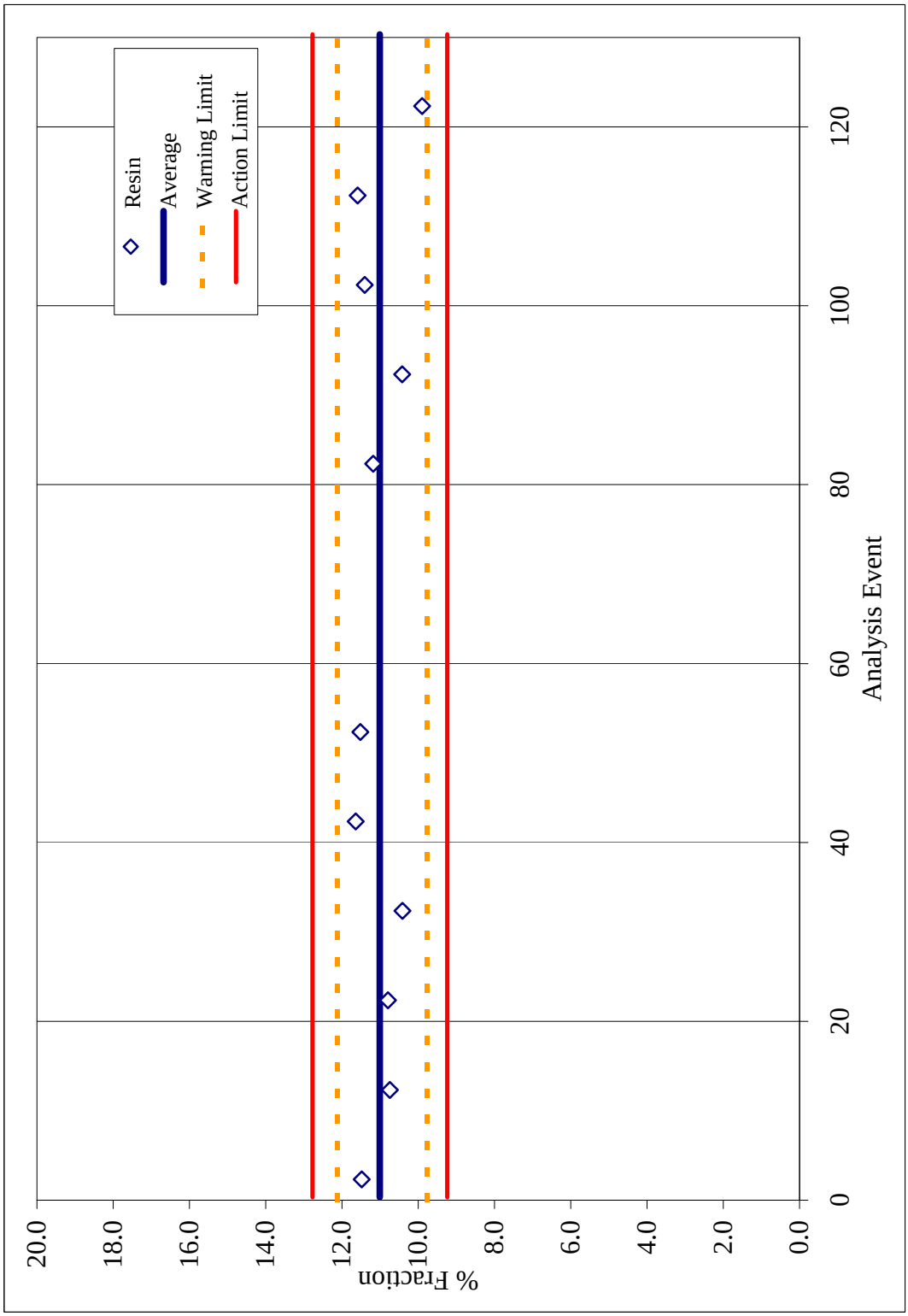

FIGURE A11: Phase I Bonny Light LCS-P, Resin Fraction, Shewhart Control Chart. Shows the resin fraction for the LCS-P replicates with the average and 2 and 3 standard deviation warning and action limits shown respectively. The data points on the graph represent the respective LCS-P fraction results for each tray of ten chromarods.

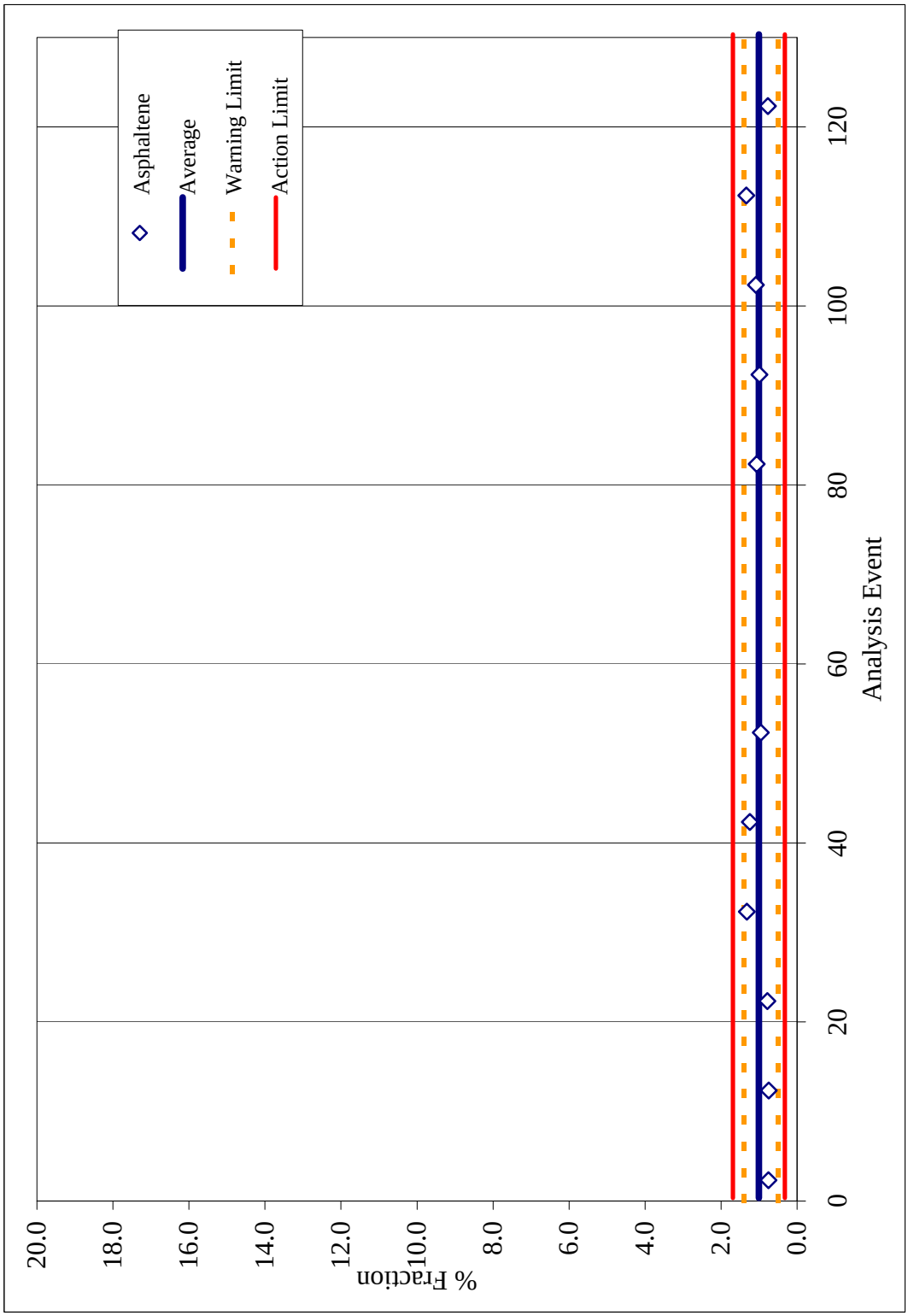

FIGURE A12: Phase I Bonny Light LCS-P, Asphaltene Fraction, Shewhart Control Chart. Shows the asphaltene fraction for the LCS-P replicates with the average and 2 and 3 standard deviation warning and action limits shown respectively. The data points on the graph represent the respective LCS-P fraction results for each tray of ten chromarods.

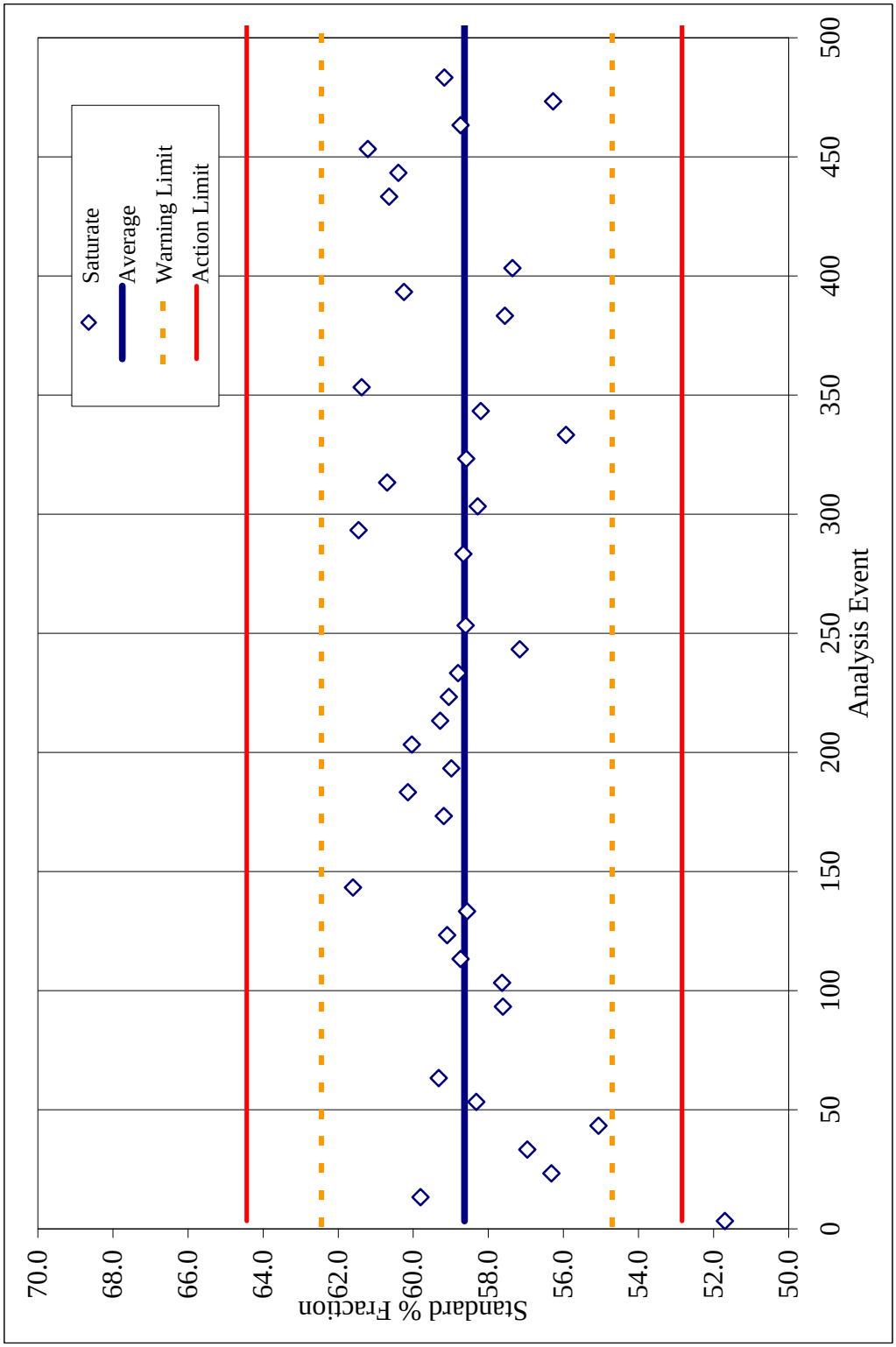

FIGURE A13: Phase II Bonny Light LCS-P, Saturate Fraction, Shewhart Control Chart. Shows the saturate fraction for the LCS-P replicates with the average and 2 and 3 standard deviation warning and action limits shown respectively. The data points on the graph represent the respective LCS-P fraction results for each tray of ten chromarods.

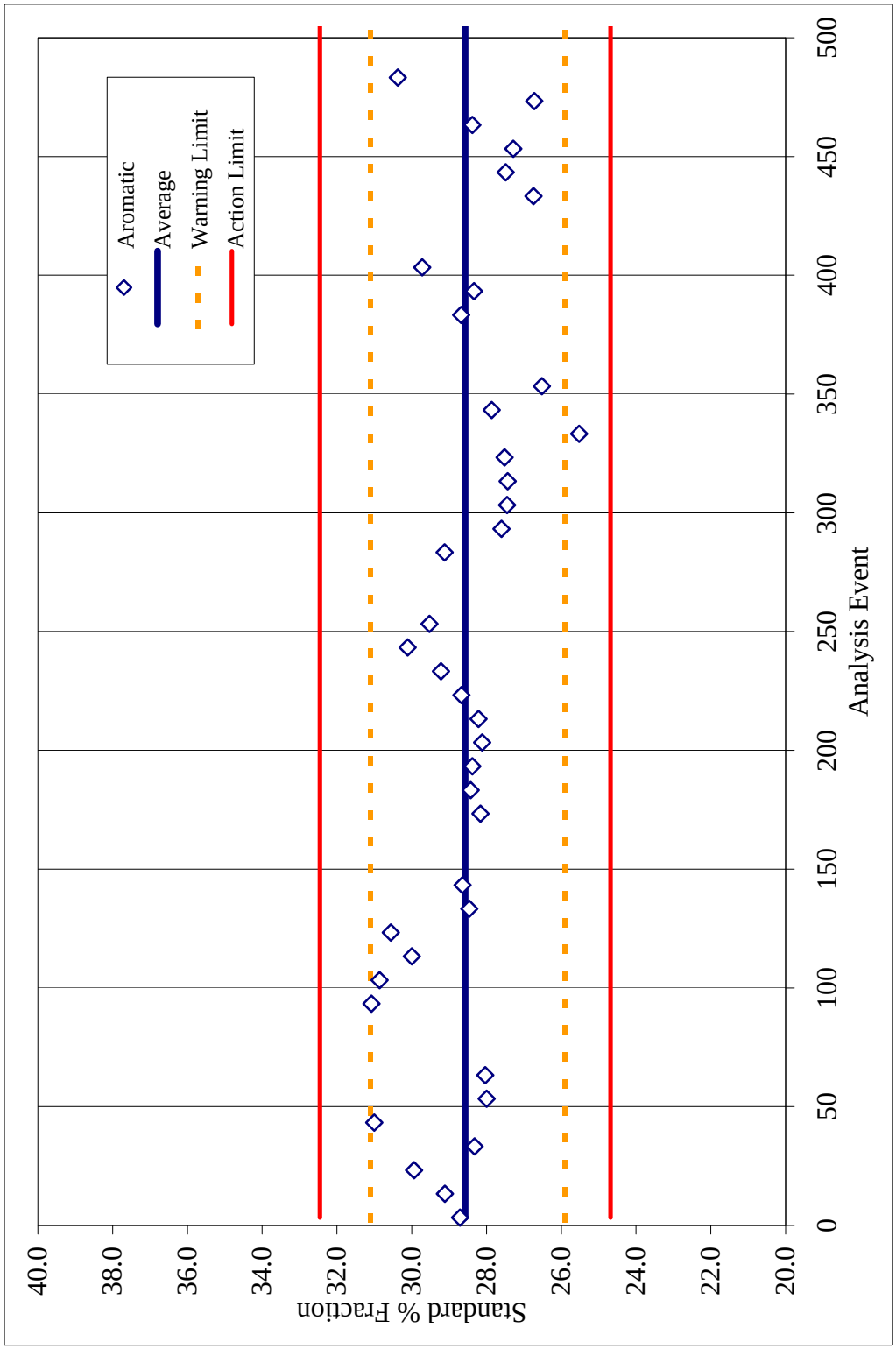

FIGURE A14: Phase II Bonny Light LCS-P, Aromatic Fraction, Shewhart Control Chart. Shows the aromatic fraction for the LCS-P replicates with the average and 2 and 3 standard deviation warning and action limits shown respectively. The data points on the graph represent the respective LCS-P fraction results for each tray of ten chromarods.

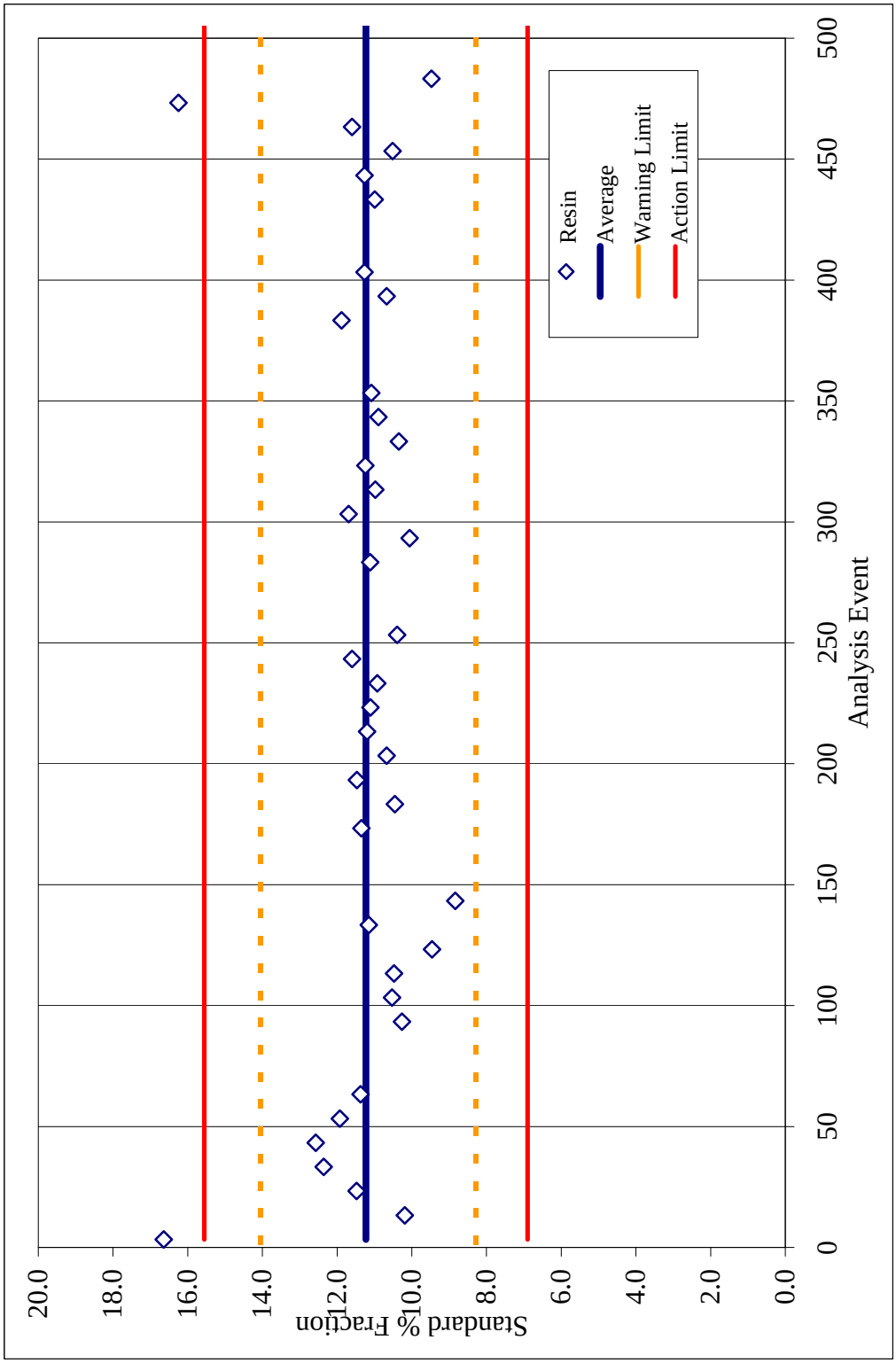

FIGURE A15: Phase II Bonny Light LCS-P, Resin Fraction, Shewhart Control Chart. Shows the resin fraction for the LCS-P replicates with the average and 2 and 3 standard deviation warning and action limits shown respectively. The data points on the graph represent the respective LCS-P fraction results for each tray of ten chromarods.

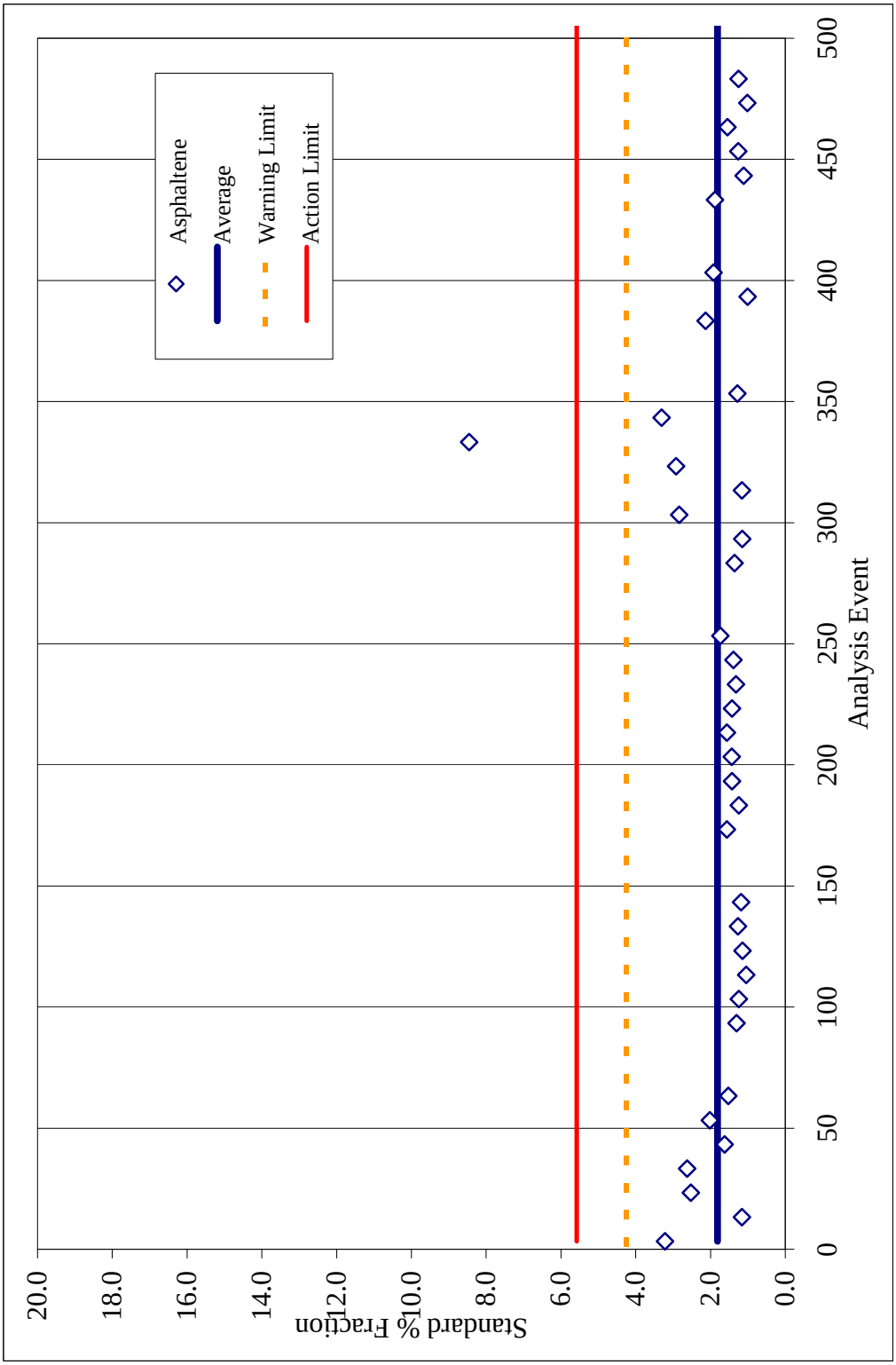

FIGURE A16: Phase II Bonny Light LCS-P, Asphaltene Fraction, Shewhart Control Chart. Shows the asphaltene fraction for the LCS-P replicates with the average and 2 and 3 standard deviation warning and action limits shown respectively. The data points on the graph represent the respective LCS-P fraction results for each tray of ten chromarods.

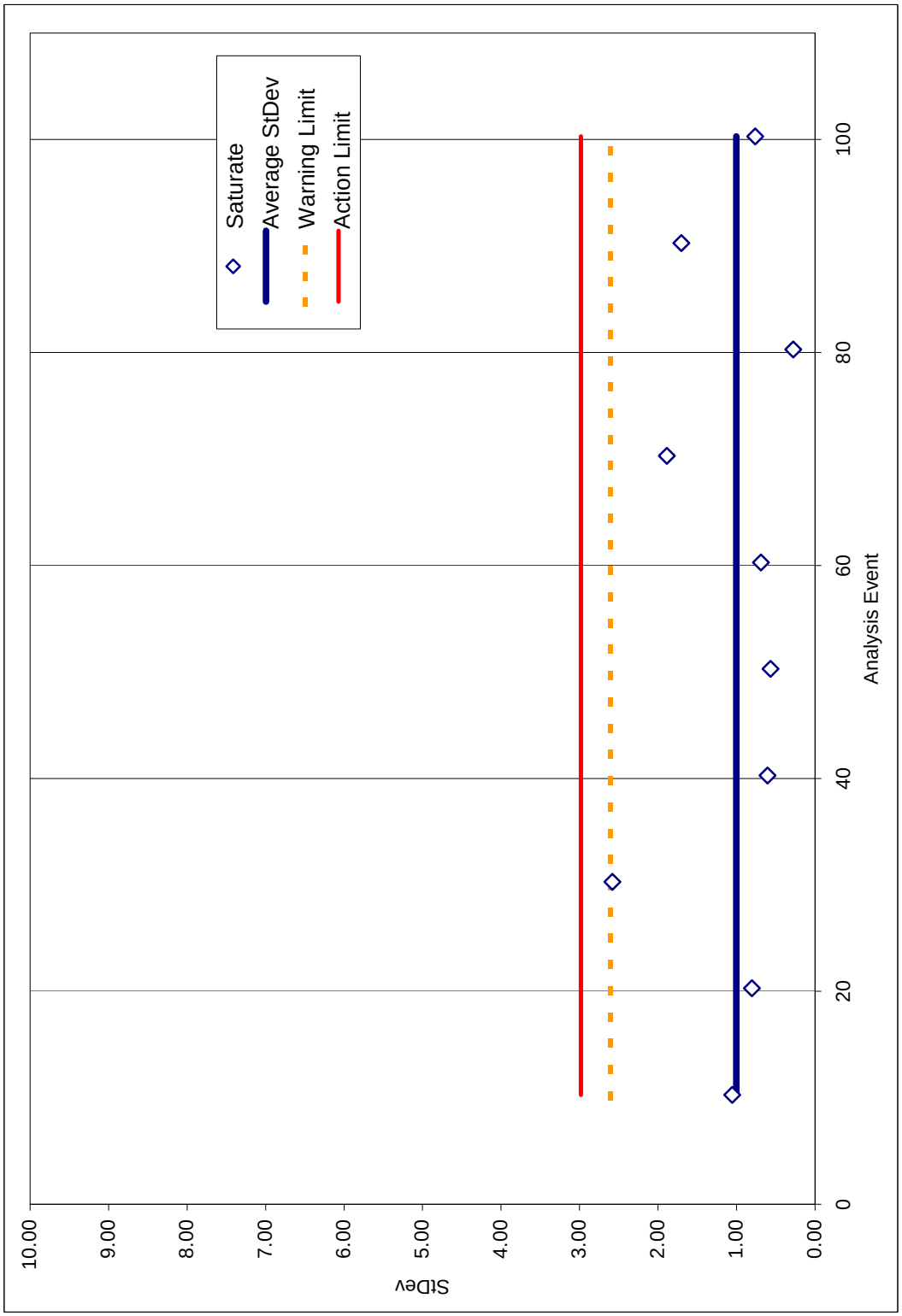

FIGURE A17: Phase I Sample Replicates, Saturate Fraction, Shewhart Control Chart. Shows the average standard deviation for the saturate fraction of the sample replicates with the average and 2 and 3 standard deviation warning and action limits shown respectively.

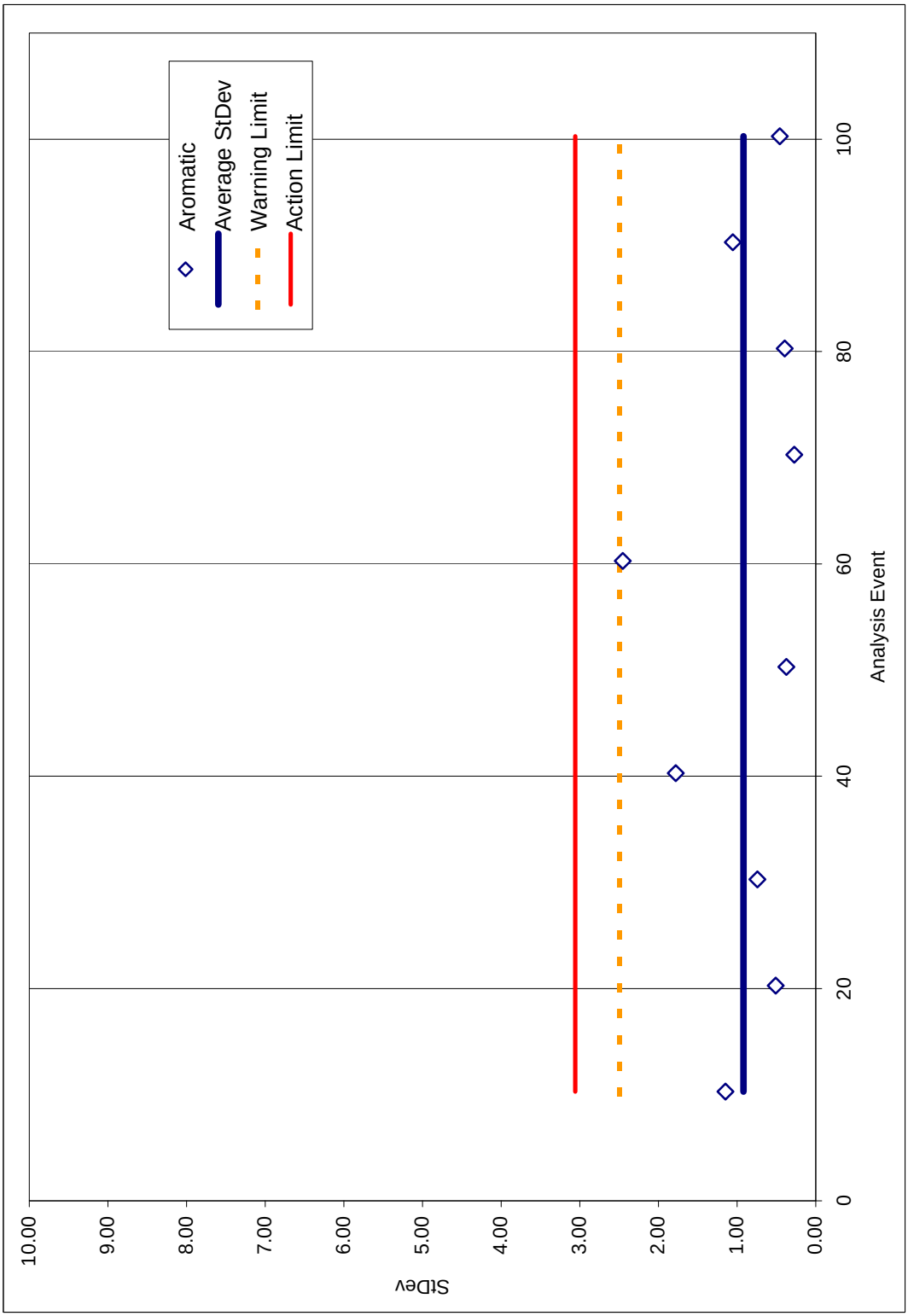

FIGURE A18: Phase I Sample Replicates, Aromatic Fraction, Shewhart Control Chart. Shows the average standard deviation for the aromatic fraction of the sample replicates with the average and 2 and 3 standard deviation warning and action limits shown respectively.

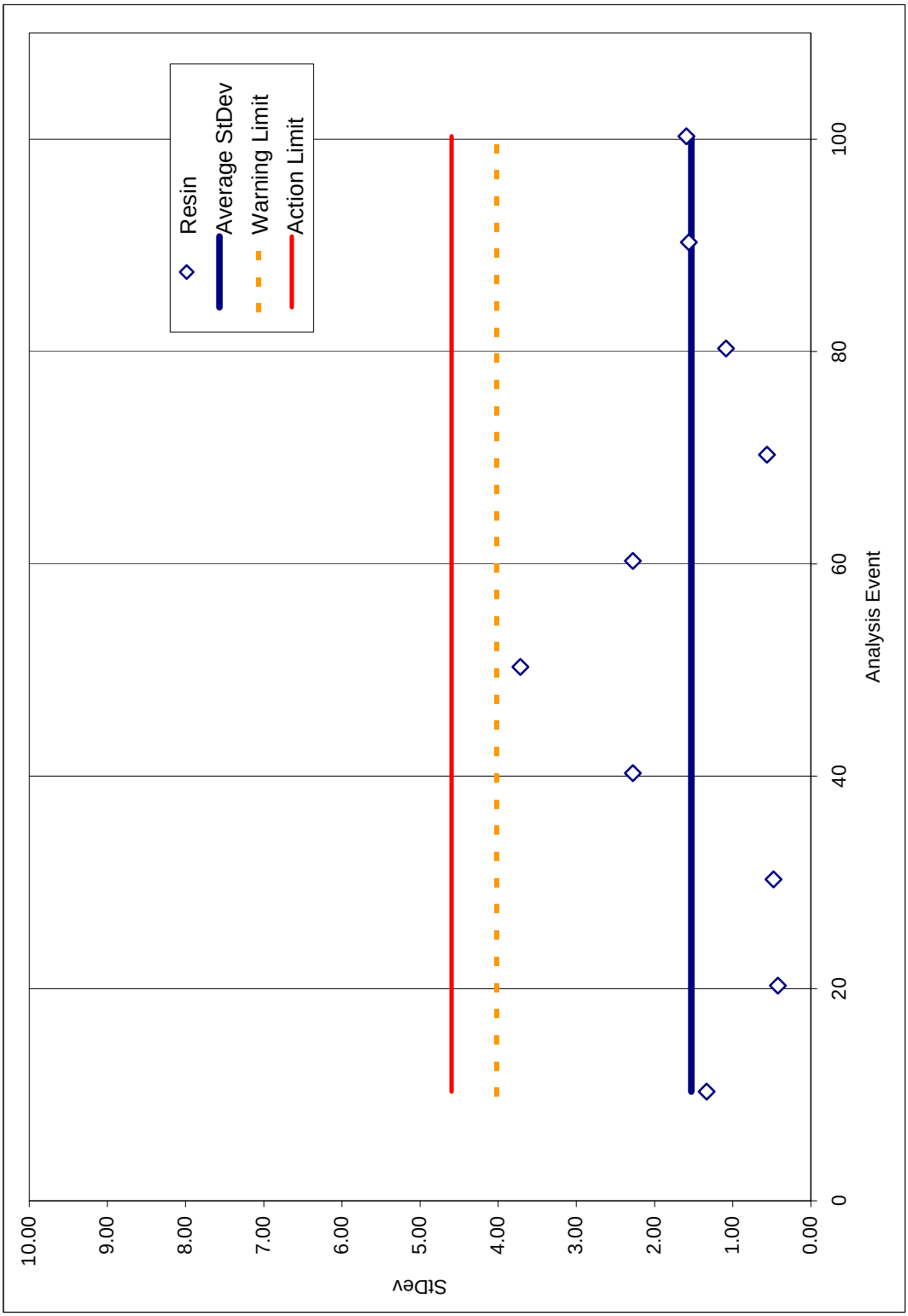

FIGURE A19: Phase I Sample Replicates, Resin Fraction, Shewhart Control Chart. Shows the average standard deviation for the resin fraction of the sample replicates with the average and 2 and 3 standard deviation warning and action limits shown respectively.

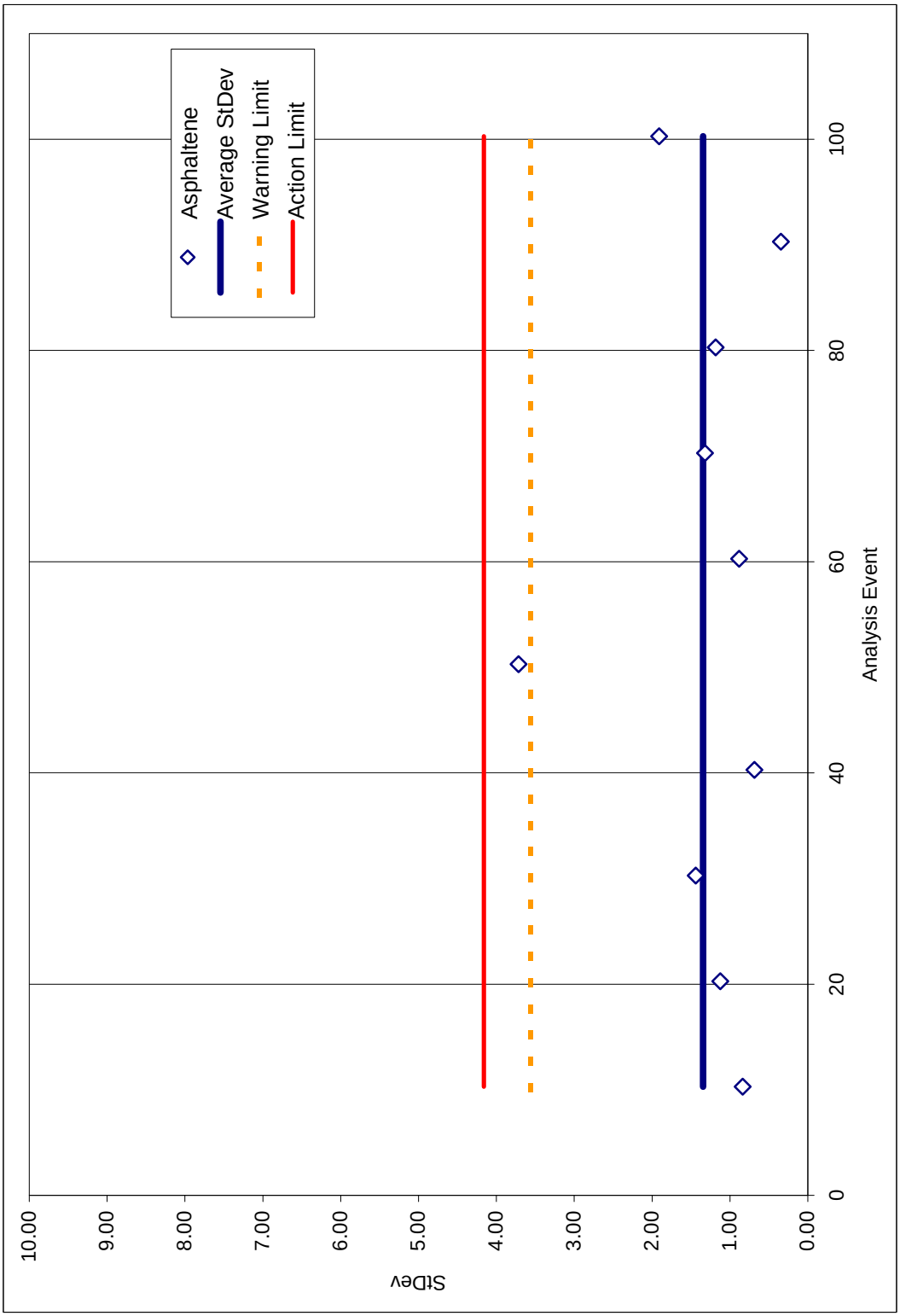

FIGURE A20: Phase I Sample Replicates, Asphaltene Fraction, Shewhart Control Chart. Shows the average standard deviation for the asphaltene fraction of the sample replicates with the average and 2 and 3 standard deviation warning and action limits shown respectively.

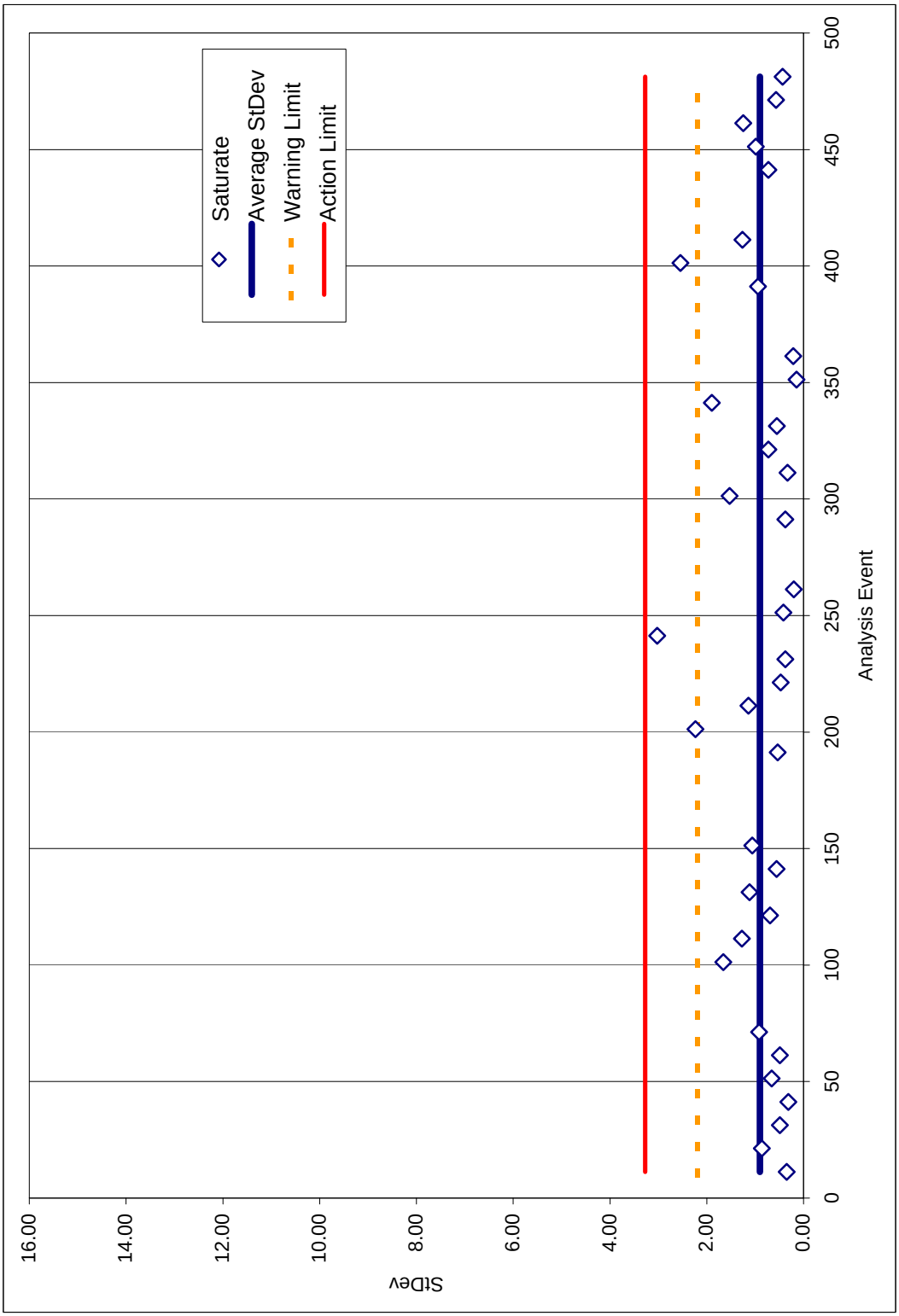

FIGURE A21: Phase II Sample Replicates, Saturate Fraction, Shewhart Control Chart. Shows the average standard deviation for the saturate fraction of the sample replicates with the average and 2 and 3 standard deviation warning and action limits shown respectively.

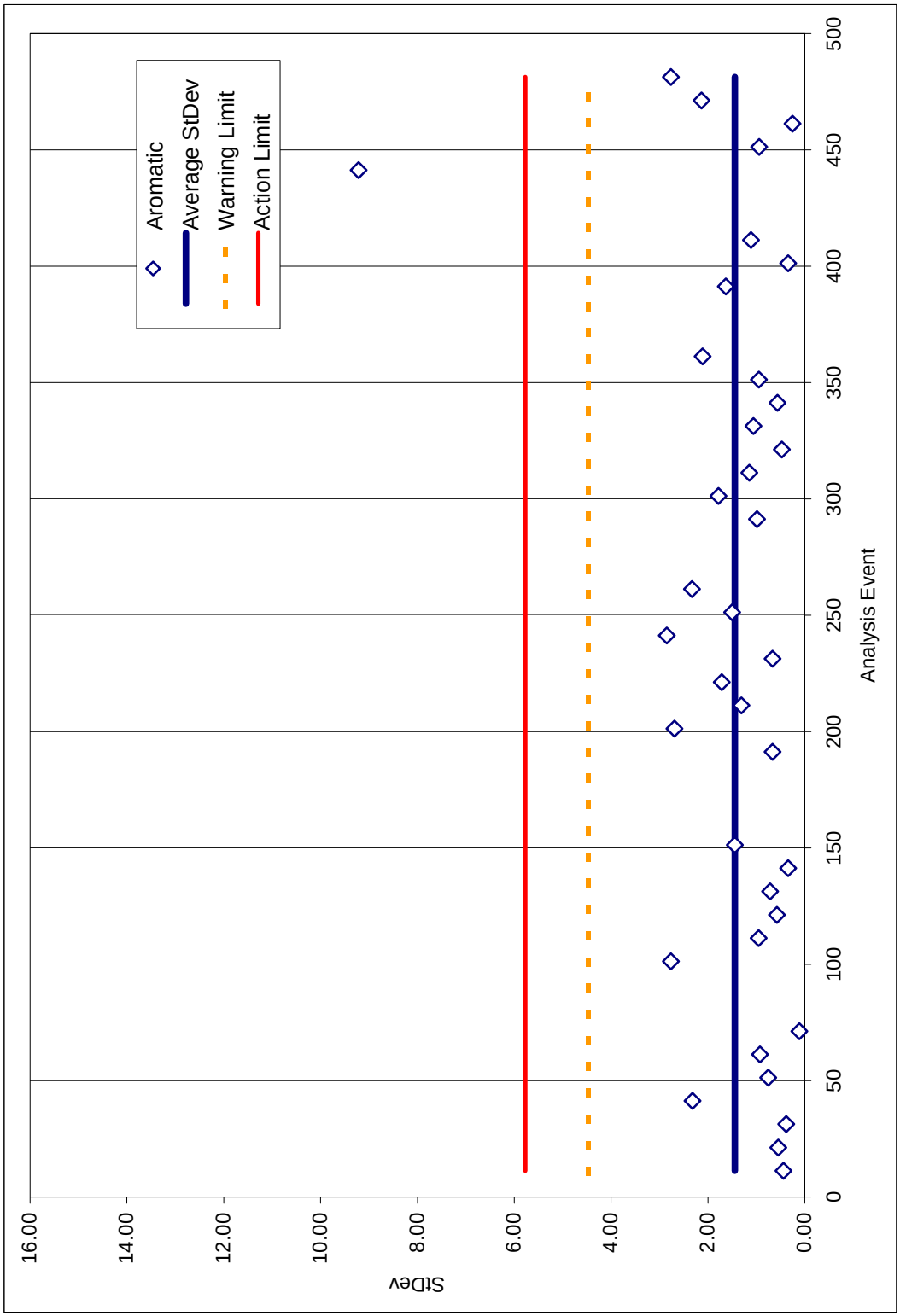

FIGURE A22: Phase II Sample Replicates, Aromatic Fraction, Shewhart Control Chart. Shows the average standard deviation for the aromatic fraction of the sample replicates with the average and 2 and 3 standard deviation warning and action limits shown respectively.

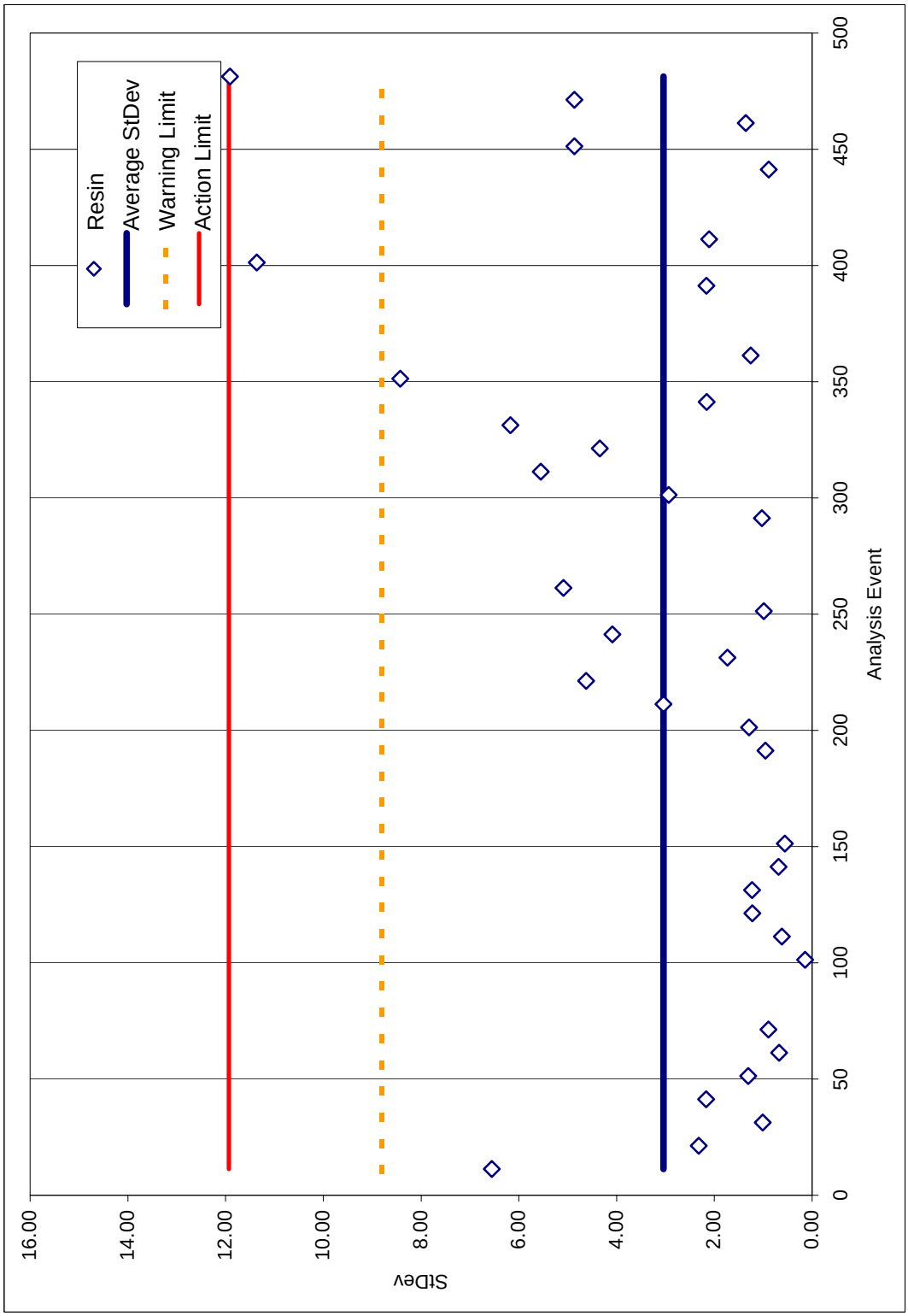

FIGURE A23: Phase II Sample Replicates, Resin Fraction, Shewhart Control Chart. Shows the average standard deviation for the resin fraction of the sample replicates with the average and 2 and 3 standard deviation warning and action limits shown respectively.

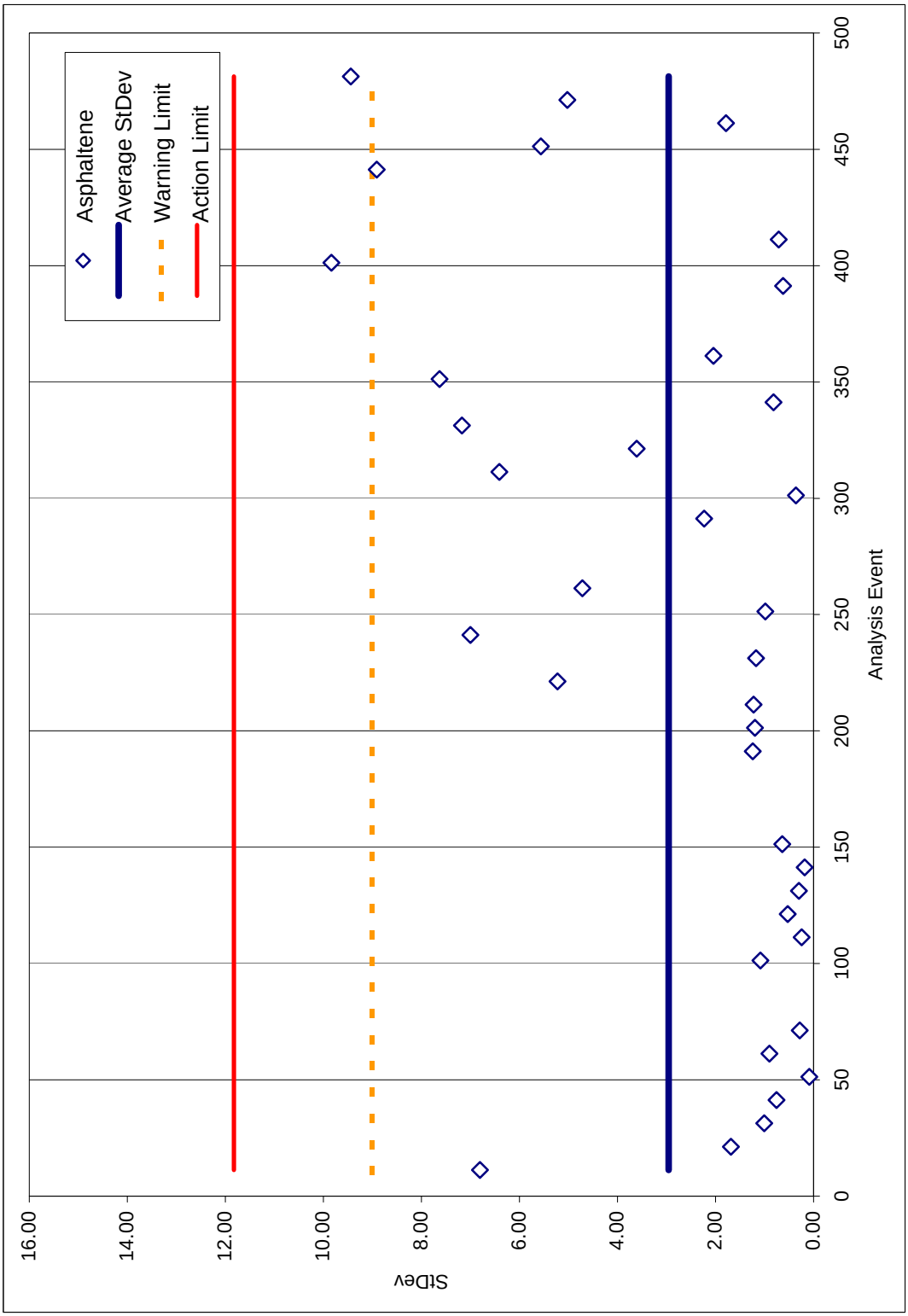

FIGURE A24: Phase II Sample Replicates, Asphaltene Fraction, Shewhart Control Chart. Shows the average standard deviation for the asphaltene fraction of the sample replicates with the average and 2 and 3 standard deviation warning and action limits shown respectively.

VITA

Name: Frank L. Stephens

Spouse: Danica C. Mueller

Address: 104 Corporate Park Drive
White Plains, NY 10602

Education: Bachelor of Science, 1995
Civil Engineering
Texas A&M University
College Station, TX 77843